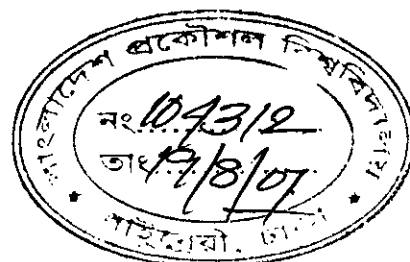


A New Model for Prediction of Tray Efficiency in Cross Flow Sieve Trays

By



Fatema Begum

**A THESIS
SUBMITTED TO THE DEPARTMENT OF
CHEMICAL ENGINEERING FOR PARTIAL FULFILMENT OF THE
REQUIREMENTS FOR THE DEGREE
OF
MASTER OF SCIENCE IN CHEMICAL ENGINEERING**

**DEPARTMENT OF CHEMICAL ENGINEERING
BANGLADESH UNIVERSITY OF ENGINEERING AND
TECHNOLOGY
AUGUST 06, 2007**

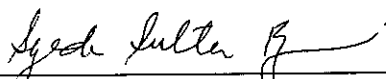


BANGLADESH UNIVERSITY OF ENGINEERING AND TECHNOLOGY

DEPARTMENT OF CHEMICAL ENGINEERING


CERTIFICATION OF THESIS WORK

We, the undersigned, certify that **Fatema Begum** candidate for the degree of Master of Engineering (Chemical) has presented her thesis on the subject "**A New Model for Prediction of Tray Efficiency in Cross Flow Sieve Trays**". The thesis is acceptable in form and content. The student demonstrated a satisfactory knowledge of the field covered by this thesis in an oral examination held on August 06, 2007.



Dr. Syeda Sultana Razia
Associate Professor
Dept. of Chemical Engineering
BUET, Dhaka.

Chairman



Dr. A.K.M. Abdul Quader
Professor
Dept. of Chemical Engineering
BUET, Dhaka.

Member



Dr. M. Sabder Ali
Professor & Head
Dept. of Chemical Engineering
Dean, Faculty of Engineering
BUET, Dhaka.

Member



Dr. M. Waliuzzaman
Former Chairman
Bangladesh Council of Scientific & Industrial Research (BCSIR)
48/4A BUET Staff Quarters, Dhaka.

External Member

CANDIDATE'S DECLARATION

I hereby declared that this thesis or any part of it has not been submitted elsewhere for the award of any degree or diploma.

Signature of the candidate

Fatema Begum

(Fatema Begum)

ACKNOWLEDGEMENT

I like to express my gratefulness to the almighty Allah for allowing me to complete this work.

I like to express my deep honor and sincere gratitude to Dr. Syeda Sultana Razia, Assistant Professor, Department of Chemical Engineering, BUET, for her valuable support, encouragement, and supervision throughout this work. It was not possible for me to complete this work without her proper guidance. I sincerely appreciate her patience in dealing with me.

ABSTRACT

A new simplified model for predicting mass transfer efficiency on a commercial scale sieve tray has been developed. The model is based on the analysis of tray hydrodynamics on a cross flow sieve tray. It considers the froth as a combination of small and large bubbles as well as gas jets. The small bubbles are considered to reach saturation in froth and thus have the efficiency of 100%. The model estimates the average efficiency of large bubbles as 40% and that of jets as 70%. The model requires estimation of only two parameters, namely, fraction of small bubble (F_{SB}), fraction of jetting (F_J), and is applicable to both froth and spray regime. The model has been confirmed by a large and diverse database. The model is applicable within pressure range 1.3-2758 kPa, liquid density range 380-949 kg/m³, gas density range 380-949 kg/m³, liquid viscosity range 0.05-1.56 mPa.s, gas viscosity range 0.007-0.013 mPa.s, and surface tension range 01-55 mN/m. The prediction is found to be within $\pm 25\%$. According to the model tray efficiency (E_{OG}) is calculated by following equation.

$$E_B = (0.4(1 - F_{SB}) + 1.0F_{SB})(1 - F_J) + 0.7F_J$$

Table of content

	Pages
Acknowledgement	ii
Abstract	iii
Table of Contents	iv
List of Tables	vi
List of Figures	xii
CHAPTER 1	
INTRODUCTION	1
1.1 Introduction	1
1.2 Sieve tray hydraulics	1
1.2.1 Contacting Characteristics on Cross-Flow Sieve Trays	3
1.2.2 Flow regimes on sieve trays	3
1.3 Tray Efficiency	3
1.4 Objectives	6
CHAPTER 2	
LITERATURE REVIEW	7
2.1 Sieve Tray Hydraulics	7
2.1.1 Regimes on Sieve Tray	8
2.1.2 Forth to Spray Transition	9
2.1.3 Bubbling Zone	9
2.1.3.1 Bubbles Formation at the Orifice	10
2.1.3.2 Bubbles Size Distribution	10
2.2 Tray Efficiency	11
2.2.1 Definitions	11
2.2.2 Point Efficiency Fundamentals	12
2.3 Models for the Prediction of Tray Efficiency	14
2.3.1 Empirical Methods	14
2.3.1.1 O'Connell Correlation (1946)	14
2.3.1.2 MacFarland, Sigmund, and Van Winkle Correlation (1972)	15
2.3.2 Theoretical or Semi-Empirical Models.	15
2.3.2.1 AIChE Model	16
2.3.2.2 Chan and Fair (1984)	17
2.3.2.3 Chen and Chuang (1993)	18
2.3.2.4 The Mechanistic Model of Prado and Fair (1990)	20
2.3.2.5 The Mechanistic Model of Garcia and Fair (2000)	20
2.3.2.6 Syeda et al. model (2000)	20
CHAPTER 3	
DATA BASE SELECTION	25
3.1 Introduction	
3.2 Tray Efficiency Sources	25
3.2.1 Jones and Pyle (1955)	28
3.2.2 Kastanck and Standart (1967)	28
3.2.3 Billet, Conrad and Grubb (1969)	28
3.2.4 Sakata and Yanagi (1979); Yanagi and Sakata (1982)	28
3.2.5 Korchinsky, Eashani and Plaka (1994)	29

3.1.6 Nutter and Perry (1995)	29
3.1.7 Early FRI Data	29
3.2 Conversion of Overall and Murphree Efficiencies to Point Efficiencies	29
CHAPTER 4	33
MODEL DEVELOPMENT	
4.1 Model structure	33
4.2 Determination of fraction of jetting	36
4.3 Determination of fraction of Small bubbles	37
4.4 Determination of efficiencies	37
CHAPTER 5	44
RESULT AND DISCUSSION	
CHAPTER 6	73
CONCLUSIONS	
CHAPTER 7	
SUGGESTIONS FOR FUTURE WORK	
REFERENCES	74
APPENDIX A	80
NOMENCLATURE	
APPENDIX B	84
DATA BANK FOR SIEVE TRAY EFFICIENCIES	
APPENDIX C	145
SAMPLE CALCULATION	

LIST OF TABLES

		Page
Table 3.1	Summary of tray efficiency data bank.	26
Table 3.2	Summary of physical properties and operating conditions of tray efficiency data bank.	27
Table 4.1	Determination of constants C_3 , C_4 , C_7 and C_8	41
Table 4.2	Steps and Equations Used in Proposed Model-3	42
Table 5.1	Range of operating pressure and physical properties used in model validation.	45
Table 5.2	Pressures, average schmidt numbers, characteristics of aqueous systems	46
Table 5.3	Pressures, average schmidt numbers, characteristics of hydrocarbon systems	46
Table 5.4	Comparison of Proposed Model-3 with Garcia-Fair and Chan-Fair Model.	47
Table B.1.1	Sieve tray efficiencies (experimental & calculated by present models). For acetic acid/water at atmospheric pressure. Source: Jones and Pyle, 1955.	85
Table B.1.2	Calculations for fraction of jetting (FJ) & fraction of small bubbles (FSB). For acetic acid/water at atmospheric pressure. Source: Jones and Pyle, 1955.	86
Table B.1.3	Efficiencies for large bubbles & jetting by present models. For acetic acid/water at atmospheric pressure. Source: Jones and Pyle, 1955.	87
Table B.2.1	Sieve tray efficiencies (experimental & calculated by present models). For isopropanol/water at 13.3 kPa operating pressure. Source: FRI, 1966a.	88
Table B.2.2	Calculations for fraction of jetting (FJ) & fraction of small bubbles (FSB) For isopropanol/water at 13.3 kPa operating pressure. Source: FRI, 1966a.	89
Table B.2.3	Efficiencies for large bubbles & jetting by present models. For isopropanol/water at 13.3 kPa operating pressure. Source: FRI, 1966a.	90

Table B.3.1	Sieve tray efficiencies (experimental & calculated by present models). For ortho/para xylenes at 2.13 kPa operating pressure. Source: FRI, 1966a.	91
Table B.3.2	Calculations for fraction of jetting (FJ) & fraction of small bubbles (FSB) For ortho/para xylenes at 2.13 kPa operating pressure. Source: FRI, 1966a.	92
Table B.3.3	Efficiencies for large bubbles & jetting by present models. For ortho/para xylenes at 2.13 kPa operating pressure. Source: FRI, 1966a.	93
Table B.4.1	Sieve tray efficiencies (experimental & calculated by present models): For ortho/para xylenes at 2.13 kPa operating pressure. Source: FRI, 1966b.	94
Table B.4.2	Calculations for fraction of jetting (FJ) & fraction of small bubbles (FSB). For ortho/para xylenes at 2.13 kPa operating pressure. Source: FRI, 1966b.	95
Table B.4.3	Efficiencies for large bubbles & jetting by present models. For ortho/para xylenes at 2.13 kPa operating pressure. Source: FRI, 1966b.	96
Table B.5.1	Sieve tray efficiencies (experimental & calculated by present models). For n-octanol/n-decanol at 1.3 kPa operating pressure. Source: FRI, 1966b.	97
Table B.5.2	Calculations for fraction of jetting (FJ) & fraction of small bubbles (FSB). For n-octanol/n-decanol at 1.3 kPa operating pressure. Source: FRI, 1966b.	98
Table B.5.3	Efficiencies for large bubbles & jetting by present models. For n-octanol/n-decanol at 1.3 kPa operating pressure. Source: FRI, 1966b.	99
Table B.6.1	Sieve tray efficiencies (experimental & calculated by present models). For n-octanol/n-decanol at 8.0 kPa operating pressure. Source: FRI, 1966b.	100
Table B.6.2	Calculations for fraction of jetting (FJ) & fraction of small bubbles (FSB). For n-octanol/n-decanol at 8.0 kPa operating pressure. Source: FRI, 1966b.	101
Table B.6.3	Efficiencies for large bubbles & jetting by present models. For n-octanol/n-decanol at 8.0 kPa operating pressure. Source: FRI, 1966b.	102

Table B.7.1	Sieve tray efficiencies (experimental & calculated by present models). For methanol/water at 101.4 kPa operating pressure. Source: Kastanek & Standart, 1967	103
Table B.7.2	Calculations for fraction of jetting (FJ) & fraction of small bubbles (FSB). For methanol/water at 101.4 kPa operating pressure. Source: Kastanek & Standart, 1967	104
Table B.7.3	Efficiencies for large bubbles & jetting by present models. For methanol/water at 101.4 kPa operating pressure. Source: Kastanek & Standart, 1967	105
Table B.8.1	Sieve tray efficiencies (experimental & calculated by present models). For ethylbenzenc/styrcne at 13.3 kPa operating pressure. Source: Billet et al., 1969.	106
Table B.8.2	Calculations for fraction of jetting (FJ) & fraction of small bubbles (FSB). For ethylbenzenc/styrcne at 13.3 kPa operating pressure. Source: Billet et al., 1969.	107
Table B.8.3	Efficiencies for large bubbles & jetting by present models. For ethylbenzenc/styrcne at 13.3 kPa operating pressure. Source: Billet et al., 1969	108
Table B.9.1	Sieve tray efficiencies (experimental & calculated by present models). For cyclohexane/n-heptane at 27.6 kPa operating pressure. Source: Sakata and Yanagi, 1979.	109
Table B.9.2	Calculations for fraction of jetting (FJ) & fraction of small bubbles (FSB). For cyclohexane/n-heptane at 27.6 kPa operating pressure. Source: Sakata and Yanagi, 1979.	110
Table B.9.3	Efficiencies for large bubbles & jetting by present models. For cyclohexanc/n-heptane at 27.6 kPa operating pressure. Source: Sakata and Yanagi, 1979	111
Table B.10.1	Sieve tray efficiencies (experimental & calculated by present models). For cyclohexane/n-heptan at 165 KPa pressure. Source: Sakata and Yanagi, 1979.	112
Table B.10.2	Calculations for fraction of jetting (FJ) & fraction of small bubbles (FSB). For cyclohexane/n-heptan at 165 Kpa pressure. Source: Sakata and Yanagi, 1979.	113
Table B.10.3	Efficiencies for large bubbles & jetting by present models. For cyclohexanc/n-heptan at 165 Kpa pressure. Source: Sakata and Yanagi, 1979.	114

Table B.11.1	Calculations for fraction of jetting (FJ) & fraction of small bubbles (FSB). For iso-butane/n-butane at 1138 kPa operating pressure. Source: Sakata and Yanagi, 1979.	115
Table B.11.2	Calculations for fraction of jetting (FJ) & fraction of small bubbles (FSB). For iso-butane/n-butane at 1138 kPa operating pressure. Source: Sakata and Yanagi, 1979	116
Table B.11.3	Efficiencies for large bubbles & jetting by present models. For iso-butane/n-butane at 1138 kPa operating pressure. Source: Sakata and Yanagi, 1979.	117
Table B.12.1	Sieve tray efficiencies (experimental & calculated by present models). For iso-butane/n-butane at 2068 kPa operating pressure. Source: Sakata and Yanagi, 1979.	118
Table B.12.2	Calculations for fraction of jetting (FJ) & fraction of small bubbles (FSB). For iso-butane/n-butane at 2068 kPa operating pressure. Source: Sakata and Yanagi, 1979.	119
Table B.12.3	Efficiencies for large bubbles & jetting by present models. For iso-butane/n-butane at 2068 kPa operating pressure. Source: Sakata and Yanagi, 1979.	120
Table B.13.1	Sieve tray efficiencies (experimental & calculated by present models). For iso-butane/n-butane at 2758 kPa operating pressure. Source: Sakata and Yanagi, 1979.	121
Table B.13.2	Calculations for fraction of jetting (FJ) & fraction of small bubble (FSB). For iso-butane/n-butane at 2758 kPa operating pressure. Source: Sakata and Yanagi, 1979.	122
Table B.13.3	Efficiencies for large bubble & jetting by present models. For iso-butane/n-butane at 2758 kPa operating pressure. Source: Sakata and Yanagi, 1979.	123
Table B.14. 1	Sieve tray efficiencies (experimental & calculated by present models). For cyclohexane/N-heptane 34 kPa pressure. Source:Yanagi and sakata, 1982.	124
Table B.14.2	Calculations for fraction of jetting (FJ) & fraction of small bubble (FSB). For cyclohexane/N-heptane 34 kPa pressure. Source:Yanagi and sakata, 1982.	125
Table B.14.3	Efficiencies for large bubble & jetting by present models. For cyclohexane/N-heptane 34 kPa pressure. Source:Yanagi and sakata, 1982.	126

Table B.15.1	Sieve tray efficiencies (experimental & calculated by present models). For cyclohexane/n-heptane at 165 kPa operating pressure. Source: Yanagi and Sakata, 1982.	127
Table B.15.2	Calculations for fraction of jetting (FJ) & fraction of small bubble (FSB). For cyclohexane/n-heptane at 165 kPa operating pressure. Source: Yanagi and Sakata, 1982.	128
Table B.15.3	Efficiencies for large bubble & jetting by present models. For cyclohexane/n-heptane at 165 kPa operating pressure. Source: Yanagi and Sakata, 1982.	129
Table B.16.1	Sieve tray efficiencies (experimental & calculated by present models). For iso-butane/n-butane at 1138 kPa operating pressure. Source: Yanagi and Sakata, 1982.	130
Table B.16.2	Calculations for fraction of jetting (FJ) & fraction of small bubble (FSB). For iso-butane/n-butane at 1138 kPa operating pressure. Source: Yanagi and Sakata, 1982.	131
Table B.16.3	Efficiencies for large bubble & jetting by present models. For iso-butane/n-butane at 1138 kPa operating pressure. Source: Yanagi and Sakata, 1982.	132
Table B.17.1	Sieve tray efficiencies (experimental & calculated by present models). For methanol/water at 101.4 kPa operating pressure. Source: Korchinsky et al., 1994	133
Table B.17.2	Calculations for fraction of jetting (FJ) & fraction of small bubble (FSB). For methanol/water at 101.4 kPa operating pressure. Source: Korchinsky et al., 1994.	134
Table B.17.3	Efficiencies for large bubble & jetting by present models. For methanol/water at 101.4 kPa operating pressure. Source: Korchinsky et al., 1994.	135
Table B.18.1	Sieve tray efficiencies (experimental & calculated by present models). For 1-propanol/water at 101.4 kPa operating pressure. Source: Korchinsky et al., 1994	136
Table B.18.2	Calculations for fraction of jetting (FJ) & fraction of small bubble (FSB). For 1-propanol/water at 101.4 kPa operating pressure. Source: Korchinsky et al., 1994.	137
Table B.18.3	Efficiencies for large bubble & jetting by present models. For 1-propanol/water at 101.4 kPa operating pressure. Source: Korchinsky et al., 1994.	138

Table B.19.1	Sieve tray efficiencies (experimental & calculated by present models). For methylcyclohexane/toluene at 101.4 kPa operating pressure. Source: Korchinsky et al., 1994	139
Table B.19.2	Calculations for fraction of jetting (FJ) & fraction of small bubble (FSB). For methylcyclohexane/toluene at 101.4 kPa operating pressure. Source: Korchinsky et al., 1994.	140
Table B.19.3	Efficiencies for large bubble & jetting by present models. For methylcyclohexane/toluene at 101.4 kPa operating pressure. Source: Korchinsky et al., 1994.	141
Table B.20.1	Sieve tray efficiencies (experimental & calculated by present models). For cyclohexane/n-heptane at 101.4 kPa operating pressure. Source: Nutter and Perry, 1995.	142
Table B.20.2	Calculations for fraction of jetting (FJ) & fraction of small bubble (FSB). For cyclohexane/n-heptane at 101.4 kPa operating pressure. Source: Nutter and Perry, 1995.	143
Table B.20.3	Efficiencies for large bubble & jetting by present models. For cyclohexane/n-heptane at 101.4 kPa operating pressure. Source: Nutter and Perry, 1995.	144

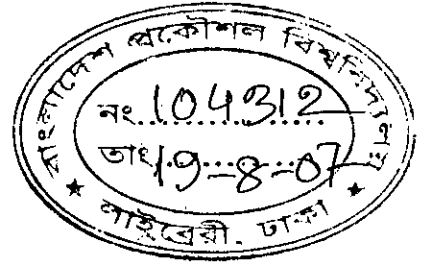
LIST OF FIGURES

		Page
Figure 1.1	Cross sectional view of cross-flow sieve tray	2
Figure 1.2	Cross-flow performance diagram	4
Figure 4.1	Schematic of the hydrodynamic model used by Prado and Fair, 1990.	33
Figure 4.2	Schematic of the two zone model adopted by Bennett et al. 1997.	34
Figure 4.3	Schematic of the forth structure model proposed by syeda et al. 2007.	35
Figure 5.1	Comparison of predicted and experimental point efficiencies acetic acid/water system at 101.4 kPa operating pressure	48
Figure 5.2	Comparison of predicted and experimental point efficiencies for the isopropanol/water system at 13.3 kPa operating pressure	49
Figure 5.3	Comparison of predicted and experimental point efficiencies for the ortho/para xylenes system at 101.1 kPa operating pressure	50
Figure 5.4	Comparison of predicted and experimental point efficiencies for the ortho/para xylcnes system at 101.4 kPa operating pressure	51
Figure 5.5	Comparison of predicted and experimental point efficiencies for the n-octanol/n-decanol system at 101.4 kPa operating pressure	52
Figure 5.6	Comparison of predicted and experimental point efficiencies for the n-octanol/n-decanol system at 2.13 kPa operating pressure	53
Figure 5.7	Comparison of predicted and experimental point efficiencies for the methanol/water system at 2.13 kPa operating pressure, h_w mm	54

Figure 5.8.1	Comparison of predicted and experimental point efficiencies for the ethylbenzene/styrene system at 13.3 kPa operating pressure, $h_w = 19$ mm	55
Figure 5.8.2	Comparison of predicted and experimental point efficiencies for the ethylbenzene/styrene system at 13.3 kPa operating pressure, $h_w = 38$ mm	56
Figure 5.9	Comparison of predicted and experimental point efficiencies for the cyclohexane/n-heptane system at 27.6 kPa operating pressure	57
Figure 5.10	Comparison of predicted and experimental point efficiencies for the cyclohexane/n-heptane system at 165 kPa operating pressure	58
Figure 5.11	Comparison of predicted and experimental point efficiencies for the i-butane/n-butane system at 34 kPa operating pressure	59
Figure 5.12	Comparison of predicted and experimental point efficiencies for the cyclohexane/n-heptane system at 165 kPa operating pressure	60
Figure 5.13.1	Comparison of predicted and experimental point efficiencies for the cyclohexane/n-heptane system at 101.4 kPa operating pressure	61
Figure 5.14.1	Comparison of predicted and experimental point efficiencies for the iso-butane/n-butane system at 2068 kPa operating pressure and 95% mole of iso-butane mixture	62
Figure 5.14.2	Comparison of predicted and experimental point efficiencies for the iso-butane/n-butane system at 2068 kPa operating pressure and 50% mole of iso-butane mixture	63
Figure 5.15.1	Comparison of predicted and experimental point efficiencies for the iso-butane/n-butane system at 2758 kPa operating pressure and 95% mole of iso-butane mixture	64
Figure 5.15.2	Comparison of predicted and experimental point efficiencies for the iso-butane/n-butane system at 2758 kPa operating pressure and 50% mole of iso-butane mixture	65

Figure 5.16	Comparison of predicted and experimental point efficiencies for the iso-butane/n-butane system at 1138 kPa operating pressure	66
Figure 5.17	Parity plot for the experimental and calculated point efficiency with Proposed Model-1	67
Figure 5.18	Parity plot for the experimental and calculated point efficiency with Proposed Model-2	68
Figure 5.19	Parity plot for the experimental and calculated point efficiency with Proposed Model-3	69

CHAPTER 1



INTRODUCTION

1.1 INTRODUCTION

Distillation is a dominant separation technology in the chemical process industries for separating a mixture into two or more products that have different boiling points, by preferentially boiling the more volatile components out of the mixture. When a liquid mixture of two volatile materials is boiled, the vapor that emerges has a higher concentration of the more volatile (i.e., lower boiling point) material than the liquid from which it was evolved. Conversely, if a vapor is cooled, the less volatile material (with the higher boiling point) has a tendency to condense more fully than the more volatile material. Stages are built in a vertical column to achieve desired separation. Actual stages in a vertical column are referred to as plates or trays. Bubble cap, sieve, valve trays etc. are used in distillation column. However, sieve trays are cheaper, more convenient and widely used in industries.

Worldwide, about 95% of all separations are made by distillation process. Without doubt distillation is the most important and most visible separation technology used in the process industries and is by far the best-developed method, The petroleum industry is the largest user of distillation technology and in 1991 had an annual primary distillation capacity of more than 3.36 billion tons (Darton, 1992). Today, this capacity has risen to more than 4.5 billion (Garcia and Fair, 2000) tons per year.

1.2 SIEVE TRAY HYDRAULICS

The cross-flow sieve tray is the most popular phase contacting device for commercial distillations. Its non-proprietary nature, simplicity of design, effectiveness of contacting are some of the factors that make this device attractive. Figure 1.1 illustrates a cross-flow sieve tray. Three parts can be distinguished: active (bubbling) area, entrance to the

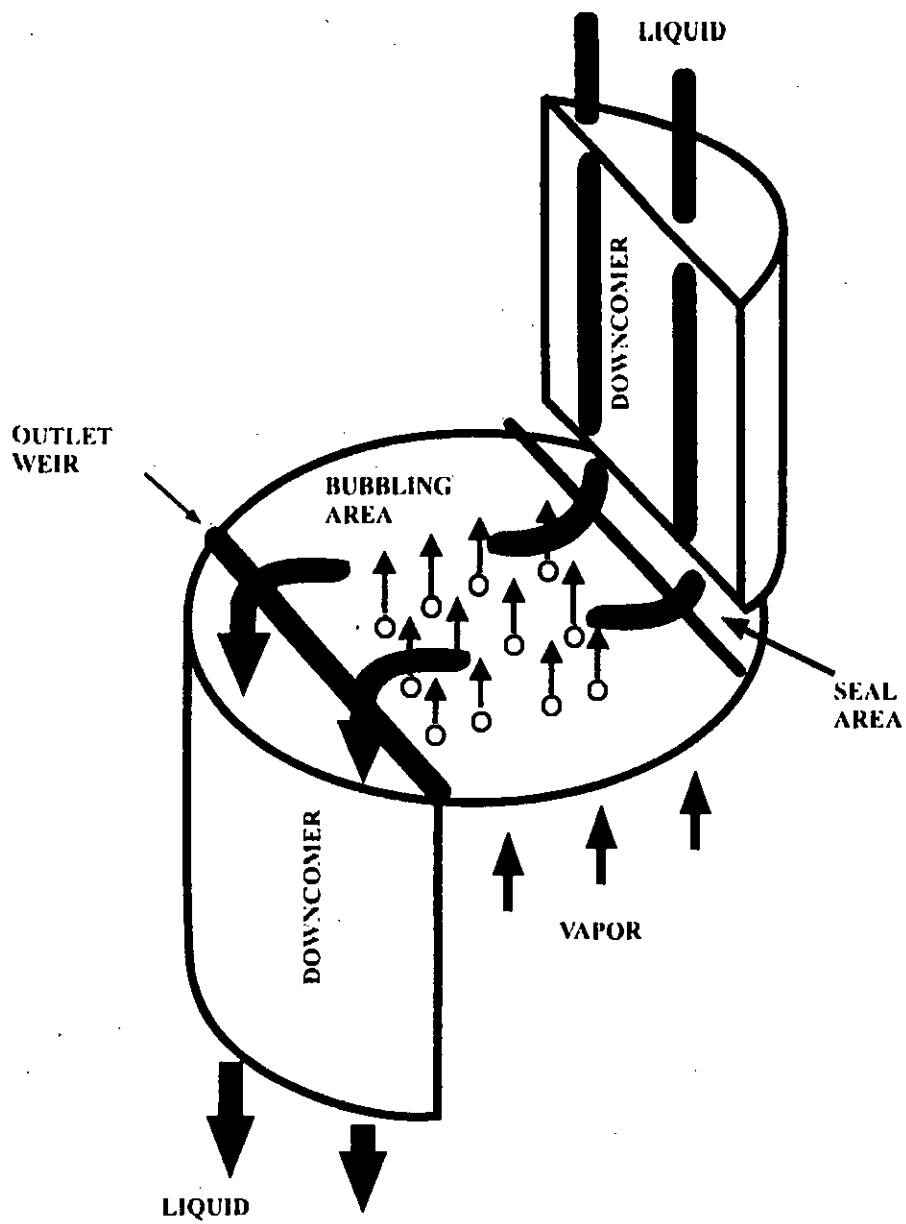


Figure 1.1. Cross-flow sieve tray

down comer that leads to the tray below, and the seal area for liquid coming from the tray above. The liquid enters the active area from the down comer after changing its direction at the seal area. In the active zone liquid and ascending vapor mix, forming a froth. The outlet weir, located on the downstream side of the bubbling area, maintains liquid inventory on the tray. Froth from the tray flows over the weir into the down comer, where the entrapped vapor is disengaged and the clarified liquid then flows to the tray below. The purpose of the vapor-liquid contacting is to create interfacial area for interphase mass transfer.

1.2.1 CONTACTING CHARACTERISTICS ON CROSS-FLOW SIEVE TRAYS

Different vapor and liquid flow rates through and across a sieve tray produce different types of vapor-liquid dispersions. The satisfactory performance of a tray is bounded by the limits of tray stability as shown in Figure 1.2. Entrainment flooding creates the upper capacity limit, where most of the liquid on the tray is in the form of drops and are carried upward with the vapor instead of flowing to the tray below. Down comer flooding occurs at high liquid loads where the frothy mixture cannot be transported to the tray below and instead builds up on the tray. The lower limit, dumping, is reached when the vapor rate is so low that essentially all of the liquid entering the tray passes through the holes instead of over the exit weir and into the down comer.

1.2.2 FLOW REGIMES ON SIEVE TRAYS

Experiments conducted in air/water simulators and in distillation columns, using gamma ray absorption techniques, have helped identify several flow regimes on sieve trays (Hofhuis and Zuiderweg, 1979). The regimes are spray, free bubbling, emulsified flow, and mixed froth. The two dominant regimes are froth and spray. The type of regime can strongly influence the hydraulic and mass transfer performance of the tray, and it is important for the tray designer to determine the type of regime which will predominate in terms of tray loading, tray geometry and system physical properties.

1.3 TRAY EFFICIENCY

Tray efficiency is a crucial factor in the analysis of sieve tray distillation columns, because in distillation tray efficiency is used to convert the number of theoretical plates to actual plates. While much effort has gone into the prediction of theoretical stages for

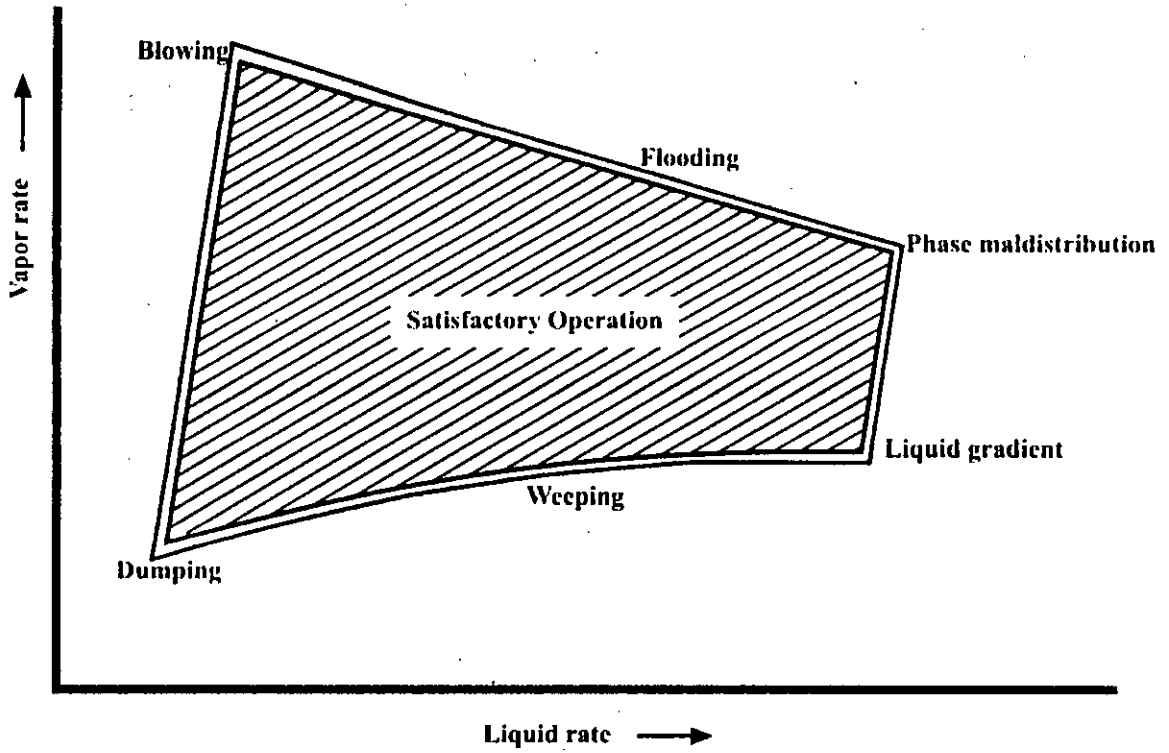


Figure 1.2. Sieve tray performance diagram

a given separation, relatively little attention has been given to the conversion to real stages, or plates. This problem has been termed the "last frontier" in the development of distillation technology (Fair, 1991).

Empirical and semi-empirical methods have been proposed for the determination of point efficiency. The first serious attempt to understand point efficiency was made in a special research program sponsored by the American Institute of Chemical Engineers (AIChE) and funded by contributions from industrial companies. This work took place in the late 1950s and is summarized two publications of the AIChE (1958a, 1958b). The experimental work was done with small bubble-cap plate simulators using the basic air-water system with transferring solutes. The AIChE work has served as a base for further studies.

Based on the definition of spray and froth regimes Zuiderweg (1982) and Stichlmair (1978) developed their efficiency model. They considered a sudden change in the nature of two-phase mixture in the transition zone of these two regimes. The FRI efficiency data for commercial sieve trays, on the other hand, show smooth transition of tray efficiency from the weeping to flooding point. This compelled many researchers to resort to a single efficiency model for both spray and froth regimes .AIChE, 1958; Chan and Fair, 1984; Chen and Chuang, 1993 are of this type. None of these models took into account two-phase mixture that is generated on the tray in different regimes. The single major step that considers the dispersion structure in the froth regime was made by Prado and Fair (1990) for air water system. Later, Garcia and Fair (2000) extended this model to other systems. However, too many adjustable parameters introduced at different stages of the model have made the model complicated and emphasized on its mechanistic nature. Finally Syeda et al. (2000) developed a single model for both froth and spray regimes that consider a simplified form of two phase mixture generated on the tray. This model used Zuiderweg's spray regime model for jetting zone which is limited for vapor density 1 to 80 kg/m³. All efficiency models based on tray hydrodynamics used complicated calculations which discourage researchers as well as industry people to adopt such models.

1.4 OBJECTIVES

The objectives of the project are:

- i. To develop a new user friendly model for prediction of tray efficiency on cross flow sieve trays in distillation, based on the analysis of tray hydrodynamics that will be applicable to both froth and spray regimes.
- ii. To validate the proposed model by a large bank of performance data on commercial scale columns reported in literature

CHAPTER 2

LITERATURE REVIEW

2.1 SIEVE TRAY HYDRAULICS

The manner in which the liquid and the vapor contact each other on a tray determines the interfacial area for mass transfer. The contacting is done in a vapor-liquid dispersion, the character of which can vary according to the relative flow rates of the phases as well as the physical properties of the phases. It is convenient to describe these dispersions in terms of two-phase regimes. The froth regime is the most common, especially in distillation, and is the principal focus of the present work. Other regimes include spray, free bubbling, and emulsified flow and will be described later. The froth regime is characterized by a liquid-continuous mixture with a variety of bubbles sizes that provide the interfacial area for mass transfer. The bubbles circulate rapidly and are of a wide range of non-uniform shapes and sizes.

Knowledge of disintegration of the bubbles is essential to the eventual understanding of the interfacial mechanisms. Breakup and coalescence rates are important factors in determining bubble size distribution, and hence the effectiveness of the interfacial transport of mass, momentum and energy. The bubble velocity determines the residence and contact time. This velocity depends on bubble dimensions as well as vapor flow rate and system physical properties. At higher vapor rates, chain bubbling and jetting can occur at the holes, the jets break up into bubbles, and in all cases the bubbles circulate rapidly throughout the froth.

The presence of the liquid may affect the way vapor flows through holes of the sieve tray. Thus affect the discharge coefficient. Some of the holes may be partially blocked by liquid, and variations in the local pressure head may cause local fluctuations in the vapor flow.

2.1.1 REGIMES ON SIEVE TRAY

There are two types of regimes that can be described for sieve trays: operating and two-phase. The latter deals with the type of dispersion on the tray. The former relates to operating conditions and its corresponding regimes may be described as follows:

- a) **Flooding:** This condition occurs at high vapor rates and which happens is caused either by excessive liquid entrainment or by excessive backup of liquid in the down comer
- b) **Blowing:** This condition occurs when vapor rates are very high and liquid rates very low, and prevents a stable liquid phase from forming near the holes. It causes atomization of much of the liquid, leading to entrainment.
- c) **Weeping:** This condition occurs when the vapor kinetic energy through the holes is low and the liquid potential energy above the holes is high. An imbalance in energies causes some liquid to drain through the holes.
- d) **Dumping:** This condition occurs when the vapor and liquid rates are both low, and essentially all of the liquid entering the tray is lost through the holes.

The two-phase regimes are of more importance in the present work and, as mentioned previously, the froth regime usually predominates. A useful dimensionless group for approximate prediction of the two-phase regimes is the flow parameter:

$$F_{LV} = \left(\frac{L}{G} \right) \left(\frac{\rho_V}{\rho_L} \right)^{1/2} \quad (2.1)$$

Where, L/G is the mass ratio of liquid to vapor. The parameter represents a ratio of liquid-to-vapor kinetic energies, A more complete description of the two-phase regimes (or "dispersions") follows.

- a) **Spray:** Characterized by vapor as the continuous phase and drops as dispersed phase. Usually occurs at high vapor-to-liquid volumetric ratios, as

experienced in high vacuum distillations. For the spray flow parameter has a value of 0.1 or less.

- b) **Free bubbling:** Characterized by simple bubbling of vapor through a continuous phase of liquid. It is represented by high values of the flow parameter and occurs in distillation conducted at higher pressures (e.g., 0.2 or greater). The relatively low kinetic energy of the vapor disturbs the liquid very little. Some investigators separate an emulsion regime for very low bubbling rates.
- c) **Froth:** This regime is intermediate to the spray and the free bubbling regimes, and sometimes is called the "mixed-froth" since it can contain some spray, although liquid-continuous contacting predominates. Flow parameter values are generally in the range of 0.01 to 0.2. This is the region that includes most distillations, and is the froth regime the one of emphasis in the present work.

Several investigators have attempted to generalize methods for predicting the flow regime (e.g., Loon, et al., 1973; Hofhuis and Zuiderweg, 1979). Prado et al. (1986) studied transitions between the regimes and did not observe discontinuities in such variables as pressure drop and liquid holdup.

2.1.2 FROTH TO SPRAY TRANSITION

In the late 1960s, papers began to appear with reports of attempts to study systematically the transition from froth to spray and to model and correlate the results. The transition from froth to spray occurs when a substantial proportion of vapor completely penetrates the dispersion as jets. The spray regime is favored by low clear liquid height and large hole diameters and vapor velocities.

2.1.3 BUBBLING ZONE

The hydraulics and rate processes, which govern bubble size in the froth regime, are very complex. First it is of importance to make clear the effects of various factors on the size and frequency of bubbles at their formation in the orifices. Usually, the size of the bubbles formed is different from the average size in the froth owing to bubble

coalescence and breakup. However, in some cases (c.g., in columns operated at a low hole velocities) the initial bubble size can determine the interfacial area and gas hold-up. For these cases, it is therefore of interest to determine the various parameters that can influence bubble formation size and frequency.

The dispersion produced by the agitation by the vapor is determined by the breakup and coalescence of bubbles. The equilibrium between these phenomena leads to a characteristic bubble size distribution. Bubble size-distributions have been correlated based on direct visual observations using photographic devices. The shape of the distributions was found to change with the physical properties of the system.

2.1.3.1 BUBBLE FORMATION AT THE ORIFICE

A considerable body of experimental and theoretical literature exists relating to the formation of gas or vapor bubbles issuing from orifices in quiescent liquids, taking into account that many factors affecting bubble formation, c.g., orifice diameter, gas flow rate, chamber volume beneath the orifice, and physical properties (Kumar and Kuloor, 1969; Tsuge and Hibino, 1983; Marshall, 1990, Tsuge et al., 1981a and Tsuge et al., 1992). The theory for single hole bubbling has been applied, to a limited extent, to a multi-orifice orifice system such as the sieve tray (Kupferberg and Jameson, 1969). However, most of the theoretical models are based on a two-stage spherical bubble growth model (Davison and Shuler, 1960; Wraith, 1971 and Tsuge et al., 1981b).

2.1.3.2 BUBBLE SIZE DISTRIBUTION

Several authors have reported bubble size distribution data for the air, water system, based on photographic techniques. It is widely accepted that bubble sizes in sieve tray froths for air-water can be represented by a bimodal distribution Hofer (1983) found that bubble distribution presented two peaks at bubble diameters of 5 and 25 mm at 100 kPa. Ashley and Haselden (1972) reported that in the continuous phase there existed small spherical bubbles with diameters ranging between 5 and 10 mm, and larger bubbles with diameters from 40 to 80 mm. The larger bubbles were referred to as "vapor voids". Kaltenbacher (1982), using small hole diameter sieve trays (2.5 and 1.5 mm, 8.76 and 5.14%, free area respectively) reported a bidisperse bubble size distribution with small bubble size close to 4 mm and large bubbles of 25 mm diameter. The volumetric portion

of gas going through the froth corresponding to small bubbles was found to be between 20-40% for the 1.5 mm holes and 0 to 20% for the 2.5 mm holes.

Bubble sizes in cellular foams and froths in 3.2 mm hole diameter trays were measured by Porter et al. (1967). The size of the bubbles formed at the hole was approximately 20 mm diameter as calculated by the bubble formation frequency and an overall mass balance. The reported bubble diameter in the froth was 5 mm.

Lockett et al. (1979), using a rectangular sieve tray, observed large (25 mm) bubbles that were continuously changing shape. Measurements from the photographs indicated that these large bubbles occupied about 65% of the froth volume. Small bubbles of about 5 mm diameter tended to be trapped in the liquid circulation patterns. The hole size of the tray appeared to have had no significant effect on the properties of the froth.

The concept of primary and secondary bubbles was introduced by Klugh and Vogelpohl (1983). Primary bubbles, usually larger than secondary bubbles, were produced at the orifice. The secondary bubbles were formed either due to the disintegration of the primary bubbles in the presence of a shear field or by the disintegration of a continuous jet in the jetting regime. They reported the existence of a unimodal secondary bubble size distribution when operating in the bubbling regime, while a bimodal secondary bubble size distribution was found in the jetting regime. Wilkinson and Dierendock (1990) determined the impact of gas density in the bubble size. An increase in gas density increased the gas hold-up as the result of the change in bubble size distribution.

2.2 TRAY EFFICIENCY

2.2.1 DEFINITIONS

Overall Column efficiency

The overall efficiency is the most commonly used for quick and rough calculations. It is defined as the ratio of the number theoretical stages required for a specified separation, at a specified reflux ratio, to the actual number of trays required for the separation at the same reflux ratio:

$$E_{oc} = \frac{N_t}{N_R} \quad (2.2)$$

This efficiency does not have a fundamental basis. The point and Murphree efficiency definitions below are expressed in term of vapor concentrations for convenience, and are equivalent to the alternative of using liquid concentrations.

Point efficiency, E_{OG}

The point efficiency is the ratio of the change of vapor composition at a point to the change that would occur if equilibrium were reached:

$$E_{OG} = \left(\frac{y_n - y_{n-1}}{y_n^* - y_{n-1}} \right)_{point} \quad (2.3)$$

Expressed as a fraction, this efficiency cannot exceed unity because the vapor composition change across the tray cannot exceed the thermodynamic equilibrium limit.

Murphree tray efficiency, E_{MV}

The Murphree tray efficiency is the ratio of the change of composition across the tray to the change that would occur on a theoretical stage.

$$E_{MV} = \left(\frac{y_n - y_{n-1}}{y_n^* - y_{n-1}} \right)_{tray} \quad (2.4)$$

By definition, the equilibrium vapor concentration y_n^* is based on the outlet liquid concentration, not the average liquid concentration. This makes possible E_{MV} values greater than 1.0 (100%), depending on the liquid concentration gradient across the tray.

2.2.2 POINT EFFICIENCY FUNDAMENTALS

The point efficiency concept is based on the two-film theory, and is usually expressed in terms of the molar rate of diffusion,

$$\begin{aligned} N &= k_G a_i \rho_{M,G} (y_i - y) = k_L a_i \rho_{M,L} (x - x_i) \\ &= K_{OG} a_i \rho_{M,G} (y^* - y_i) \end{aligned} \quad (2.5)$$

Assuming phase equilibrium at the interface, the overall mass transfer coefficient can be obtained by the sum of mass transfer resistances represented by the following relationship,

$$\frac{1}{K_{OG}} = \frac{1}{k_G} + \frac{m}{k_L} \quad (2.6)$$

Considering a mass balance across a differential element in the froth of a sieve tray, the expressions for the vapor and liquid-phase mass transfer units obtained are

$$N_G = k_G a_i t_G \quad (2.7)$$

and

$$N_L = k_L a_i t_L \quad (2.8)$$

Where the residence times t_G and t_L are given by

$$t_G = \frac{h_f}{Q_V / A_A} = \frac{h_f}{U_{SM}} \quad (2.9)$$

where h_f is the height of the two-phase mixture above the tray floor.

$$t_L = \frac{h_f}{Q_L / A_A} = \frac{h_f}{Q_{LA}} \quad (2.10)$$

The overall gas-phase mass transfer unit is obtained from the individual phase transfer units:

$$\frac{1}{N_{OG}} = \frac{1}{N_G} + \frac{\lambda}{N_L} \quad (2.11)$$

The point efficiency is then expressed in terms of overall vapor-phase mass transfer units by the following Equation, which assumes that vapor moves across the element in plug flow and the liquid is perfectly mixed in the vertical direction.

$$E_{OG} = 1 - \exp(-N_{OG}) \quad (2.12)$$

2.3 MODELS FOR THE PREDICTION OF TRAY EFFICIENCY

Over the years many procedures have been proposed for estimating tray efficiencies, using empirical methods. However, two main approaches have been used for the development of methods to calculate the efficiency with some degree of rigor. Theoretical prediction methods are based on the two-film theory. For convenience, these two approaches will be termed empirical and fundamental. All models used the important hydraulic parameter, F-factor, for loading. This factor is defined as

$$F_{SM} = U_{SM} \sqrt{\rho_V} \quad (2.12a)$$

U_{SM} = Superficial gas velocity based on active area, m/s.

ρ_V = vapor density, kg/m³

2.3.1 EMPIRICAL METHODS

One of the first attempts to correlate empirically plant or semi-works overall column efficiencies were made by Drickamer and Bradford (1943). They measured the column efficiency of 54 refinery columns and found the values to be related to the molar average viscosity of the liquid feed to the column (If the feed contained vapor, equilibrium liquid composition was used). O'Connell (1946) modified the Drickamer/Bradford correlation to include nonhydrocarbon and high-relative-volatility systems. Later, MacFarland et al. (1972) correlated these efficiency data in terms of dimensionless groups of vapor and liquid properties.

2.3.1.1 O'CONNELL CORRELATION (1946)

The O'Connell correlation has been the standard of industry for several decades. In addition, to the Drickamer/Bradford data, O'Connell added data from 32 commercial and five laboratory columns to give a data base that included hydrocarbon, chlorinated hydrocarbon and alcohol mixtures. O'Connell modified the correlating parameter of Drickamer and Bradford to the product of the molar average viscosity and the relative volatility of the key components, with both parameters evaluated at the arithmetic mean

of the top and bottom temperatures. The agreement between test results and the fitted curve fell within 16% of an “average” curve through the plotted data. The deviation from the curve was attributed to errors in analyses, inaccuracies in physical data, limitations in the method of calculation, and differences in column design. Lockett (1986) expressed the O’Connell plot for bubble cap trays in equation form:

$$E_{OC} = 9.06(\mu_L \alpha)^{-0.245} \quad (2.13)$$

Where E_{OC} is the overall column efficiency in percent, μ_L is the liquid viscosity in (Pa.s), and α is the relative volatility.

This method has been considered a reasonable one for estimating distillation tray efficiency, particularly for conceptual process designs. Kister (1992) recommended it for this purpose because of its reasonable accuracy, good reliability and simplicity.

2.3.1.2 MACFARLAND, SIGMUND, AND VAN WINKLE CORRELATION (1972)

The MacFarland et al. (1972) correlation for predicting Murphree tray efficiency is based on binary data systems for bubble-cap and sieve trays. The correlation expresses efficiency in terms of dimensionless groups which include liquid and vapor properties. MacFarland et al (1972) ignored the vapour Schmidt number and selected the following three dimensionless groups based on 42 existing models.

$$E_{MV} = 7.0 \left(\frac{\sigma}{\mu_L U_{SA}} \right)^{0.14} \left(\frac{\mu_L}{\rho_L D_L} \right)^{0.25} \left(\frac{h_w U_H \rho_G}{\mu_L} \right)^{0.08} \quad (2.14a)$$

or

$$E_{MV} = 6.8 \left(\frac{\sigma}{\mu_L U_{SA}} \right)^{0.115} \left(\frac{\mu_L}{\rho_L D_L} \right)^{0.215} \left(\frac{h_w U_H \rho_G}{\mu_L} \right)^{0.1} \quad (2.14b)$$

2.3.2 THEORETICAL OR SEMI-EMPIRICAL MODELS

Theoretical prediction methods for point tray efficiency are based on the two-resistance theory and use a sequence of steps to convert phase resistance into a tray efficiency.

Almost all theoretical models have evolved from the AIChE modeling of bubble-cap trays developed in the late 1950s. Through the years, the AIChE approach has been corrected and modified. Later versions improved several aspects and updated its hydraulic and mass transfer fundamentals (Chan and Fair, 1984; Chen and Chuang, 1993).

2.3.2.1 AIChE MODEL

In 1952, the Research Committee of the American Institute of Chemical Engineers initiated a fundamental research project to study bubble-cap tray efficiencies in distillation and absorption. Experimental work was carried out over a five-year period. An additional year was needed to correlate the results, develop and test a general method for predicting tray efficiency.

The objective of the program was to study the main factors that affect the efficiency under conditions where entrainment is negligible. The factors are: rate of mass transfer in the vapor phase, rate of mass transfer in the liquid phase, and degree of liquid and vapor mixing on the tray. The variables affecting these factors were found to fall into three main categories: operating, tray design, and system properties. Unfortunately, each of the main factors governing efficiency responded differently to a given change in the operating, design and system variables, and it was not possible to relate tray efficiency directly to these variables in a single correlation. The AIChE recommended procedure for predicting efficiency follows:

- 1) Predict a value for the vapor-phase mass transfer units, N_G , by the following relationship:

$$N_G = \frac{0.776 + 4.57h_w - 0.238F_{SA} + 104.8Q_L}{(Sc_G)^{1/2}} \quad (2.15)$$

- 2) Calculate the liquid holdup on the tray h_L (expressed as inches of clear liquid):

$$h_L = 0.0419 + 0.0135F_{SA} + 2.45Q_L \quad (2.16)$$

- 3) Calculate the average liquid contact time t_L , on the tray (in seconds):

$$t_L = \frac{h_L L_T}{Q_L} \quad (2.17)$$

4) Predict the value for liquid-phase mass transfer units, N_L :

$$N_L = 1.97 \times 10^4 D_L^{0.5} t_L (0.403 F_{SA} + 0.17) \quad (2.18)$$

Calculate the overall vapor-phase transfer units, N_{OG} , to predict point efficiency E_{OG} , using the equations 2.11, 2.12.

2.3.2.2 CHAN AND FAIR (1984)

This model is based on the two-resistance concept (as is the AIChE model). The authors used a distillation data bank obtained on commercial scale columns and for sieve trays only. The model fitted the experimental data within an average absolute deviation of 6.27%, a good improvement over the AIChE model which, for the same database gave an equivalent fit of 22.9%. Note that the AIChE model was really limited to trays with small bubble-caps.

Based on penetration theory (Higbie, 1935) equation 2.19 and distillation efficiency data base, Chan and Fair derived a correlation, equation 2.20 for the vapor volumetric mass transfer coefficient $k_G a_i$.

$$k_G = 2 \left(\frac{D_G}{t_G} \right)^{0.5} \quad (\text{Higbie, 1935}) \quad (2.19)$$

$$k_G a_i = \frac{D_G^{1/2} (1030 f - 867 f^2)}{(h_L)^{1/2}} \quad (2.20)$$

To use the method, the fractional approach to flood, $f (=U_{SA}/U_{AF})$ is defined as the ratio of the vapor velocity through the active, or bubbling, area U_{SA} , to equivalent velocity through the active, or bubbling, area U_{SA} , to equivalent velocity at flood, U_{AF} . The clear liquid height (liquid holdup) h_L is calculated by the method of Bennett et al. (1983),

$$h_L = h_w + c \left(\frac{Q_L}{L_w \alpha_e} \right)^{0.67} \quad (2.21a)$$

α_e is effective relative froth density.

$$\text{Where, } \alpha_e = \exp \left[-12.55 \left(U_A \left(\frac{\rho_G}{\rho_L - \rho_G} \right)^{0.5} \right)^{0.91} \right] \quad (2.21b)$$

$$\text{and, } c = 0.5 + 0.438 \exp(-13.7h_w) \quad (2.21c)$$

The average gas-phase residence time is obtained from

$$t_G = \frac{(1 - \alpha_e)h_L}{\alpha_e U_{SA}} \quad (2.22)$$

The effective relative froth density α_e is calculated by the method of Bennett et al., 1983. Hence, the gas-phase number of transfer units N_G was calculated by equation 2.7.

The volumetric mass transfer coefficient for the liquid k_{L,a_i} , is taken from the relationship of Foss and Gerster (1956):

$$k_{L,a_i} = 1.97 \times 10^4 D_L^{0.5} t_L (0.403 F_{SA} + 0.17) \quad (2.23)$$

The average liquid residence time, t_L and N_L , the liquid-phase number of transfer units are calculated by equation 2.17, 2.8.

Finally, the overall gas-phase mass transfer and point efficiency are calculated in a fashion similar to that of the AIChE model. According to Chen and Chuang (1993) the Chan/Fair model over predicts the efficiency for liquid-phase controlled systems.

2.3.2.3 CHEN AND CHUANG (1993)

These authors developed a new semi empirical model for determining the number of mass-transfer units, hence tray efficiency, for distillation. They estimated the interfacial area of the sieve tray dispersion using Levich theory. Vapor and liquid mass-transfer coefficients were determined by penetration theory. Two required constants were calculated by fitting the model to the tray efficiency data of cyclohexane/n-heptane mixtures, gathered in the facilities of the Fractionation Research, Inc. (FRI).

The authors considered the Hofhuis correlation (Hofhuis, 1980) to calculate the liquid holdup on a sieve tray

The authors considered the Hofhuis correlation (Hofhuis, 1980) to calculate the liquid holdup on a sieve tray

$$h_{l_i} = 0.6 h_w^{0.5} \rho^{0.25} \left[\left(\frac{\rho_G}{\rho_L} \right)^{0.5} \left(\frac{A_A}{L_w} \right) \right]^{0.25}, \text{ for } 25 < h_w \text{ (mm)} < 100 \quad (2.24)$$

The following Equations show the vapor and liquid mass transfer coefficients multiplied by their vapor and liquid contacting time, respectively.

$$k_G t_G \propto (D_G t_G)^{0.5} \quad (2.25)$$

$$k_L t_L \propto \left(\frac{M_G G}{M_L L} \right) (D_L t_L)^{0.5} \quad (2.26)$$

The prediction of the interfacial area was obtained from the following equation. The maximum bubble size was calculated with an equation proposed by Bhavaraju et al. (1978) for stirred vessels that takes into account the effect of liquid viscosity. The equation of Stichlain (1978) was used to calculate the mean void fraction ϵ in the dispersion.

$$a = \frac{6\epsilon}{d_{32}} \propto \frac{6\epsilon}{d_{\max}} \quad (2.27)$$

$$a \approx \frac{1}{\mu^{0.1} \left(\frac{A_H}{A_A} \right)^{0.14}} \left[\frac{\rho_L F_{SM}^2}{\sigma^2} \right]^{1/3} \quad (2.28)$$

Combining the new equations for gas- and liquid-phase mass transfer, the overall gas-phase mass transfer becomes

$$N_{OG} = \frac{C_1 \frac{1}{\mu^{0.1} \left(\frac{A_H}{A_A} \right)^{0.14}} \left[\frac{\rho_L F_{SM}^2}{\sigma^2} \right]^{1/3} (D_G t_G)^{0.5}}{1 + \lambda \frac{C_1 \left(\frac{D_G \rho_G}{D_L \rho_L} \right) \left(\frac{M_L L}{M_G G} \right)}{C_2}} \quad (2.29)$$

Constants C1 and C2 were determined by fitting the number of overall vapor-phase mass-transfer units, N_{OG} , to the experimental data (free of weeping and entrainment conditions) as a function of the slope of the equilibrium line, m . The values obtained for C1 and C2 were 11 and 14, respectively. Finally, the point efficiency is calculated by equation 2.11, 2.12.

2.3.2.4 THE MECHANISTIC MODEL OF PRADO AND FAIR (1990)

These authors proposed a model for the prediction of tray efficiency based on fundamental considerations of sieve tray hydraulics (flow regime) combined with diffusional mechanisms. The correlation includes a term that accounts for weeping, but not a term for entrainment. Experiments conducted in a rectangular sieve tray with several tray geometries supported model development. For studies in which the liquid phase offered the controlling resistance to mass transfer, oxygen was stripped from water. For gas-phase resistance mass transfer, water was evaporated into a dry air stream.

Hole activity (jet and bubble formation), bubble sizes and rise velocities, and average void fraction were the hydraulic factors considered in the model. The range of variables covered was representative for commercial tray design.

The dispersion above the tray is divided vertically into three zones. The zone at the bottom and closest to the tray (hole activity zone) corresponds to the activity at the holes (jetting or bubbling), the middle section (bulk froth zone) is composed of gas bubbles dispersed in the liquid, while the top zone (spray zone) is gas continuous, with liquid drops and ligaments dispersed throughout. Tray hole activity is classified as: jetting, large bubbling, and small bubbling.

2.3.2.5 THE MECHANISTIC MODEL OF GARCIA AND FAIR (2000)

Garcia and Fair extended Prado and Fair (1990) to other systems. However, too many adjustable parameters introduced at different stages of the model have made the model complicated and emphasized on its mechanistic nature.

2.3.2.6 SYEDA ET AL MODEL (2007)

A phenomenological model for froth structure is proposed based on the analysis of froth images of an active sieve tray taken from a 0.153 m distillation column. Froth is defined as a combination of bubbles and continuous jets that break the surface of froth projecting liquid splashes and drops above the surface. To estimate the fraction of small bubbles in froth, a fundamentally sound theoretical expression is derived from turbulent

break-up theory. A new model for predicting point efficiency of cross-flow sieve trays has been developed based on the hydrodynamics of an operating sieve tray represented by the proposed froth structure model. This efficiency model is applicable for both froth and spray regime. Fraction of by-passed or uninterrupted gas jet is considered as the determining factor for froth to spray transition. The net efficiency is estimated by adding up the contributions of both bubbles and jets present in the dispersion.

$$E_{OG} = (1 - F_J)E_B + F_J E_J \quad (2.30)$$

$$E_B = (1 - F_{SB})E_{LB} + F_{SB} E_{SB} \quad (2.31)$$

Where E_{OG} , F_J , F_{SB} , E_J , E_B , E_{LB} , E_{SB} are the overall tray efficiency, volume fraction of gas that penetrates the froth as continuous jet, fraction of small bubbles, efficiency of the jetting zone, efficiency of the large bubble, and tray efficiency of the small bubble, respectively. The model is tested against the efficiency data of cyclo-hexane/n-heptane and i-butane/n-butane mixtures.

Bubbling zone is considered to have bimodal size distribution of bubbles. The small bubbles are the secondary bubbles formed by the turbulent break-up of the primary bubbles originated from the orifice. The large bubbles are the unbroken primary bubbles that remain in the froth due to incomplete break-up.

The specific interfacial area, a_{iG} , and residence time, t_{GLB} , for the large bubbles in froth can be estimated from the following equations, respectively:

$$a_{iG} = \frac{6}{d_{32L}} \quad (2.32)$$

$$t_{GLB} = \frac{h_f}{U_{LB}} \quad (2.33)$$

The following equations are used to estimate the Sauter mean diameter, d_{32L} and rise velocity, U_{LB} of the large bubbles formed at the orifice.

$$d_{32L} = 0.887 D_H^{0.846} u_H^{0.21} \quad (2.34)$$

Here D_H and u_H are hole diameter and hole velocity, respectively.

$$U_{LB} = U_i \times 10^{-1} + \frac{G}{A} \quad (2.35)$$

$$U_i = 25V^{1/6} \quad (2.36)$$

In this empirical equation the volume of the bubble, V , is expressed in cm^3/s and the bubble velocity, U_i , in cm/s .

The mass transfer coefficient for the liquid phase, $k_{L,B}$ is modelled with Higbie penetration theory²¹,

$$k_{L,B} = 1.13 \left(\frac{D_L}{t_{GLB}} \right)^{0.5} \quad (2.37)$$

The mass transfer coefficient for gas phase, $k_{G,B}$, of the large bubbles is estimated from the numerical solution presented by Zaritzky and Calvelo.

$$Sh_\alpha = -11.878 + 25.879(\log Pe_G) - 5.64(\log Pe_G)^2 \quad (2.38)$$

For the range $Pe_G > 200$,

$$Sh_\alpha = 17.9 \quad (2.39)$$

$$\text{Here, } Sh_\alpha = \frac{k_{GLB} d_{32L}}{D_G} \quad \text{and} \quad Pe_G = \frac{d_{32L} U_{LB}}{D_G}$$

Froth height, h_f , is estimated from Hofhius²³ equation of liquid height, h_L (equation 2.24) and Zuideweg's¹ model of froth density, α_e , for mixed and emulsion flow regime.

The effective froth density α_e is estimated as follows:

$$\frac{I}{\alpha_e} = 40 \left[\frac{u_s (FP)^{0.5}}{(gh_L)^{0.5}} \right]^{0.8} + I \quad (2.40)$$

Using the above information, N_{GLB} and N_{LLB} can be calculated from equations (2.7) and (2.8). Equation (2.11) is then used to get the overall mass transfer unit, N_{OGLB} , from which the contribution of the large bubbles, E_{LB} , to the net efficiency is obtained by using the equation (2.17).

In order to estimate the contribution of small bubbles to the total efficiency, it is needed to determine the fraction of small bubbles, F_{SB} , in froth. Due to lack of experimental data and reliable method to estimate this parameter, Syeda et al. derived the expression

of F_{SB} in term of flow field and fluid physical properties from turbulent break-up theory of bubbles. The expression is given by the following equation

$$F_{SB} = \frac{2(1 - e^{-k\bar{\Delta t}})}{2(1 - e^{-k\bar{\Delta t}}) + \left(\frac{d_{32L}}{d_{32S}}\right)^3 e^{-k\bar{\Delta t}}} \quad (2.41)$$

The ratio of large bubble diameter to small bubble diameter, d_{32L}/d_{32S} was considered to be 5 based on the existing literature.

The breakage rate constant k is a function of the turbulent flow field and the fluid physical; properties. Hesketh et al. (1991) showed that the measured deformation times and breakage time of bubbles can be characterized by the natural mode of oscillation of a sphere given by Lamb (1932) and proposed the following functionality of the rate constant k ,

$$k = \left(\frac{3.8}{We_{cr}^{0.9}}\right) \frac{\rho_L^{0.1} \rho_G^{0.3} \omega^{0.6}}{\sigma^{0.4}} \quad (2.42)$$

In distillation, $\omega = u_{sg}$ (Kawase and Moo-Young, 1990); thus the rate constant becomes,

$$k = \left(\frac{3.8}{We_{cr}^{0.9}}\right) \frac{\rho_L^{0.1} \rho_G^{0.3}}{\sigma^{0.4}} (u_{sg})^{0.6} \quad (2.43)$$

The breakage time $\bar{\Delta t}$ can be expressed as

$$\bar{\Delta t} = n t_{GLB} \quad (0 < n < 1) \quad (2.44)$$

The final expression for $k\Delta t$ was obtained as

$$k\bar{\Delta t} = 0.16 \left(\frac{3.8 \rho_L^{0.1} \rho_G^{0.3}}{\sigma^{0.4}}\right) (u_{sg})^{0.6} t_{GLB} \quad (2.45)$$

The small bubbles are considered to be completely saturated, i.e. $E_{SB} = 1$

Fraction of jetting is estimated from the experimental data of Raper et al.(1982) and Zuiderweg's (1983) spray regime model is used to estimate the contribution of jetting zone to the total mass transfer efficiency. The following equations are found from Zuiderweg's (1983) spray regime model.

Fraction of jetting is estimated from the experimental data of Raper et al.(1982) and Zuiderweg's (1983) spray regime model is used to estimate the contribution of jetting zone to the total mass transfer efficiency. The following equations are found from Zuiderweg's (1983) spray regime model.

$$k_{Gj} = \frac{0.13}{\rho_G} - \frac{0.065}{\rho_G^2} \quad (1 < \rho_G < 80 \text{kg/m}^3) \quad (2.46)$$

$$k_{Lj} = \frac{2.6 \times 10^{-5}}{\mu_L^{0.25}} \quad (2.47)$$

$$\frac{1}{K_{OG}} = \frac{1}{k_G} + \frac{m}{k_L} \quad (2.48)$$

$$E_j = 1 - \exp\left(-\frac{ah_f K_{OGj}}{u_s}\right) \quad (2.49)$$

$$ah_f = \frac{40}{F^{0.3}} \left(\frac{F_{bba}^2 h_L FP}{\sigma} \right)^{0.37} \quad (2.50a)$$

$$\text{Here, } h_L = 0.6h_w \left(\frac{\rho}{b} FP \right)^{0.25} \quad (2.50b)$$

$$\text{and at total reflux } FP = \left(\frac{\rho_G}{\rho_L} \right)^{0.5} \quad (2.50c)$$

AICHE, 1958; Chan and Fair, 1984; Chen and Chuang, 1993 did not consider two-phase mixture that is generated on the tray in different regimes. At first Prado and Fair (1990) considered the dispersion structure in the froth regime for air water system. Later, Garcia and Fair (2000) extended this model to other systems. Finally Syeda et al. (2000) developed a single model for both froth and spray regimes that consider a simplified form of two phase mixture generated on the tray. All efficiency models based on tray hydrodynamics used complicated calculations which discourage researchers as well as industry people to adopt such models. So a new user friendly model for prediction of tray efficiency on cross flow sieve trays in distillation, based on the analysis of tray hydrodynamics has been developed in this study.

CHAPTER 3

DATA BASE SELECTION

3.1 INTRODUCTION

Before developing an efficiency model it is necessary to search for available large-scale data in the open literature. Carefully-measured, reliable efficiency data taken at the pilot-plant or semi-industrial level are very scarce. Such data must include hydraulic parameters, mass transfer rates under distillation conditions, and a most important consideration, authenticity. Sources of such data are described briefly in chronological order, and are summarized by fluid flow field and physical properties in tables 3.1 and 3.2. Most of the efficiencies reported are either overall column efficiency or Murphree tray efficiency, it being very difficult to sample locations within a tray to obtain point efficiencies. By far the simplest and most straightforward experimental approach is to use samples taken from clear liquid at the bottoms of downcomers.

The procedure normally followed is: a) obtain tray samples; b) calculate the Murphree efficiency for the entire tray; and c) use a model to convert Murphree efficiencies to local, or point, efficiencies. As discussed earlier, the point efficiency is the fundamental parameter for correlating mass transfer rates. In this chapter, the development of an efficiency data base, using literature values, is described. The complete data base may be found in Appendix B. Finally, a new model for predicting or analyzing sieve tray efficiency will be described in Chapter 4, and will be validated with the data base from Chapters 3.

3.2 TRAY EFFICIENCY SOURCES

All the efficiency data are for binary mixtures operated at total reflux. The sieve trays represented in the data base are all designed for single cross flow of liquid.

Table 3.1 Summary of tray efficiency data bank.

No	Sources	Data Points	System	Pressure (kPa)	Clm dia D _c (m)	Tray Spacing (mm)	Hole area (%)	Hole diameter (mm)	Weir height (mm)
1	Jones and Pyle, 1955	11	Acetic Acid/Water	101.4	0.457	305	8.35	3.18	38.1
2	FRI, 1966a	05	Isopropanol/Water	13.3	1.213	610	12.7	4.76	25.4
3	FRI, 1966a	06	ortho/para xylenes	2.13	1.213	610	12.7	4.76	25.4
4	FRI, 1966b	06	ortho/para xylenes	2.13	1.213	610	13	12.7	25.4
5	FRI, 1966b	06	n-octanol/n-decanol	1.3	1.22	610	13	12.7	25.4
6	FRI, 1966b	06	n-octanol/n-decanol	8.0	1.22	610	13	12.7	25.4
7	Kastanek & Standart, 1967	13	methanol/water	101.4	0.976	400	4.8	4.00	40.0
8	Billet et al., 1969	12	ethyibenzene/styrene	13.3	0.788	500	13.6	12.5	19.0
		10	ethyibenzene/styrene	13.3	0.788	500	13.6	12.5	38.0
9	Sakata and Yanagi, 1979	08	cyclohexane/n-heptane	27.6	1.22	610	8.3	12.7	50.8
10	Sakata and Yanagi, 1979	08	cyclohexane/n-heptan	165	1.22	610	8.3	12.7	50.8
11	Sakata and Yanagi, 1979	08	iso-butane/n-butanc	1138	1.22	610	8.3	12.7	50.8
12	Sakata and Yanagi, 1979	13	iso-butane/n-butane	2068	1.22	610	8.3	12.7	50.8
13	Sakata and Yanagi, 1979	12	iso-butane/n-butane	2758	1.22	610	8.3	12.7	50.8
14	Yanagi and sakata, 1982	05	cyclohexane/n-heptane	34	1.22	610	14	12.7	50.8
15	Yanagi and Sakata, 1982	08	cyclohexane/n-heptane	165	1.22	610	14	12.7	50.8
16	Yanagi and Sakata, 1982	07	iso-butane/n-butane	1138	1.22	610	14	12.7	50.8
17	Korchinsky et al., 1994	06	methanol/water	101.4	0.6	340	12.7	4.8	50.0
18	Korchinsky et al., 1994	06	1-propanol/water	101.4	0.6	340	12.7	4.8	50.0
19	Korchinsky et al., 1994	06	methylcyclohexane/toluene	101.4	0.6	340	12.7	4.8	50.0
20	Nutter and Perry, 1995.	07	cyclohexane/n-heptanc	101.4	0.5	610	14	12.7	50.8

Table 3.2 Summary of physical properties and operating conditions of tray efficiency data bank.

Source	System	Liquid density (kg/m ³)	Gas density (kg/m ³)	Liquid viscosity (mPa.s)	Gas viscosity (mPa.s)	Surface tension (mN/m)	Range of Liquid flow rate (L _r) Kg/m ³	Range of Vapor flow rate (G _r) Kg/m ³
Jones and Pyle, 1955	Acetic Acid/Water	949	0.63	0.289	0.013	55	231-1050	231-1050
FRI, 1966a	Isopropanol/Water	802	0.27	1.562	0.009	21	1674-4175	1669-4178
FRI, 1966b	ortho/para xylenes	845	0.12	0.515	0.007	26	830-3966	747-4486
FRI, 1966b	ortho/para xylenes	847	0.11	0.532	0.007	27	714-2800	691-29613
FRI, 1966b	n-octanol/n-decanol	775	0.07	1.170	0.007	19	529-2518	526-2518
FRI, 1966b.	n-octanol/n-decanol	750	0.34	0.655	0.008	17	1097-5171	1094-5173
Kastanek & Standart, 1967	methanol/water	940	0.83	0.380	0.011	39	791-2096	100-266
Billet et al., 1969	ethyibenzene/styrene	850	0.48	0.377	0.008	25	715-3638	708-3258
	ethyibenzene/styrene	847	0.48	0.377	0.008	25	736-3567	728-3238
Sakata and Yanagi, 1979	cyclohexane/n-heptane	715	0.94	0.370	0.007	20	1987-9953	1900-7675
Sakata and Yanagi, 1979	cyclohexane/n-heptan	658	5.05	0.271	0.009	14	4767-22343	4905-22867
Sakata and Yanagi, 1979	iso-butane/n-butane	493	28.0	0.090	0.010	05	6424-35028	6440-35256
Sakata and Yanagi, 1979	iso-butane/n-butane	428	56.0	0.065	0.010	03	7446-25122	7388-25224
Sakata and Yanagi, 1979	iso-butane/n-butane	380	85.0	0.050	0.011	01	5163 -19104	5039-19230
Yanagi and sakata, 1982	cyclohexane/n-heptane	714	1.14	0.340	0.007	19	4022-10171	4852-10433
Yanagi and Sakata, 1982	cyclohexane/n-heptane	649	5.09	0.264	0.008	14	2433-23763	2490-26250
Yanagi and Sakata, 1982	iso-butane/n-butane	490	28.93	0.090	0.009	05	6290-35311	6468-35284
Korchinsky et al., 1994	methanol/water	895	0.96	0.455	0.011	30	879-1131	1077-1198
Korchinsky et al., 1994	1-propanol/water	875	1.06	0.300	0.012	27	543-730	870-941
Korchinsky et al., 1994	methylcyclohexane/toluene	760	3.01	0.257	0.009	18	1628-1826	1632-1835
Nutter and Perry, 1995	cyclohexane/n-heptane	666	3.05	0.302	0.009	15	571-2599	570-2601

Graphical presentations of the data points will be made in connection with the new model development and validation (Chapter 5).

3.2.1 JONES AND PYLE (1955)

These researchers published performance data for sieve and bubble-cap trays used to separate water and acetic acid at atmospheric pressure. The work was conducted at the Experimental Station of the DuPont Company. The column diameter was 0.457 m (18 inches).

3.2.2 KASTANCK AND STANDART (1967)

This work was carried out in Czechoslovakia at the Institute for Chemical Process Fundamentals, Prague. As part of a general research program, Kastanck and Standart measured the efficiencies of several common tray devices, including sieve trays. An industrial-scale test column of 0.976 m inside diameter (3.20 ft) was operated with the methanol/water test mixture at atmospheric pressure.

3.2.3 BILLET, CONRAD AND GRUBB (1969)

Results for vacuum distillation were published by Billet et al. for the ethylbenzene/styrene system in a column with a 0.788 m. (31 inch) inside diameter. Sieve tray efficiencies were reported for two weir heights, 19 and 38 mm, and total reflux, and an operating pressure of 13.3 kPa.

3.2.4 SAKATA AND YANAGI (1979); YANAGI AND SAKATA (1982)

One of the most valuable sources of sieve tray data are the laboratories of Fractionation Research Inc. (FRI). Two journal publications containing performance data have been presented by Sakata and Yanagi and by Yanagi and Sakata. The tests were conducted in an industrial-scale column with 1.22 m inside diameter (48 inches) using two test mixtures; cyclohexane/n-heptane and i-butane/n-butane. The tray geometries were different for each publication. The first paper reported overall efficiency data for both test mixtures, using five different pressures, and thus five different sets of property and hydraulic conditions. In general, total reflux conditions were maintained, but with different original charge concentrations. The second paper covered only three sets of

operating conditions for the two test mixtures. Many hydraulic and efficiency models have been developed on the basis of the data published by these authors.

3.2.5 KORCHINSKY, EASHANI AND PLAKA (1994)

Tray point efficiency data were published by Korchinsky et al. based on tests at the University of Manchester Institute of Science and Technology (UMIST), Manchester, UK. Experiments were conducted in a 0.61 m. I.D. (24 inches) column at atmospheric pressure using three different systems; methanol/water, isopropanol/water and toluene/methylcyclohexane. Korchinsky et al. reported point efficiencies based on average conditions on the trays. They use their experimental results to make comparisons between several published models for predicting efficiency.

3.2.6 NUTTER AND PERRY (1995)

Overall efficiency data were presented for a sieve tray as well as for a fixed valve tray using the cyclohexane/n-heptane mixture at atmospheric pressure and total reflux. The test unit had an inside diameter of 0.50 m (19.7 inches). Weeping and entrainment data were gathered along with the efficiency data.

3.2.7 EARLY FRI DATA

Fractionation Research, Inc. (FRI) elected to release older experimental data, and these included sieve tray efficiency data for three systems, n-octanol/n-decanol at 10 and 60 mm Hg. (1.33 and 8.0 kPa), otho/para xylenes at 16 mm Hg abs (2.13 kPa abs), and isopropanol/water at 100 mm Hg abs (13.3 kPa abs). All data were taken in the 1.22 m (48-inch) column described by Sakata/Yanagi and Yasnagi/Sakata, at total reflux. The sources are cited here under Fractionation Research, Inch.

3.3 CONVERSION OF OVERALL AND MURPHREE EFFICIENCIES TO POINT EFFICIENCIES

For all the data reported as overall column efficiency (E_{OC}), conversion to Murphree tray efficiency of tray n , requires the use of the Lewis relationship (Lewis, 1936):

$$E_{MV} = \frac{\lambda^{E_{OG}} - 1}{\lambda - 1} \quad (3.1)$$

$$\lambda = m \frac{G_M}{L_M} \quad (3.2)$$

Where m is the slope of the equilibrium curve. For many cases, the average slope of the curve is about unity, and since for total refluxes $L_M = G_M$, the value of E_{OG} was not greatly different from E_{MV} .

When converting from Murphree efficiency to point efficiency a model for the mixing of vapor and liquid is needed. The AIChE (1958) and Chan-Fair (1984) models use a variation of the "Case I" of Lewis (1936). This case is for the special situation of complete vapor mixing between trays and no horizontal liquid mixing on the tray (i.e., plug flow). For the present work, plug flow was not assumed, and a conversion model was employed together with the eddy diffusion model of Bennett and Grimm (1991). On the basis of the AIChE model, the Murphree and point efficiencies are related as follows:

$$\frac{E_{MV}}{E_{OG}} = \frac{1 - e^{-(\eta Pe)}}{(\eta + Pe) \left\{ 1 + \left[\frac{\eta + Pe}{\eta} \right] \right\}} + \frac{[e^\eta - 1]}{\eta \left\{ 1 + \left[\frac{\eta}{(\eta + Pe)} \right] \right\}} \quad (3.3)$$

$$\eta = \frac{Pe}{2} \left[\left(1 + \frac{4\lambda E_{OG}}{Pe} \right)^{1/2} - 1 \right] \quad (3.4)$$

The dimensionless Peclet number is defined as:

$$Pe = \frac{L_T^2}{Det_L} \quad (3.5)$$

and the liquid path length of the tray, L_T , is the distance between the inlet and outlet weirs. Very low values of Pe represent small trays or high diffusive backmixing; thus, as $Pe \rightarrow 0$, Equation 3.3 reduces to the completely mixed form

$$\frac{E_{MV}}{E_{OG}} = 1 \quad (3.6)$$

High values of $Pe (Pe \rightarrow \infty)$ indicate very little backmixing (essentially plug flow) and Equation 3.3 becomes:

$$E_{OG} = \frac{\ln[\lambda E_{MV} + 1]}{\ln \lambda} \quad (3.7)$$

The correlation of Bennett and Grimm (1991) was chosen as appropriate for determining De because it offers two main improvements over earlier correlations: a) it is a phenomenological-based model, not limited to air/water, and b) the correlation gives significantly lower average actual and relative errors, and a lower standard deviation of the actual error, than other available correlation do. The eddy diffusion coefficient is a function of the height of the two-phase layer:

$$De = 0.02366 [h_{2\phi}]^{3/2} \quad (3.8)$$

The value of $h_{2\phi}$ is determined from individual heights of vapor continuous and liquid continuous region:

$$h_{2\phi} = h_{lc} + \left[\frac{0.794 K_S^2}{(A_H / A_A) \phi_e} \right] \quad (3.9)$$

with h_{lc} from Bennett et al. (1983):

$$h_{lc} = h_w + C \left[\frac{Q_{LW}}{\phi_e} \right]^{2/3} \quad (3.10)$$

where

$$C = 0.501 + 0.439 \exp[-137.8 h_w] \quad (3.11)$$

The average residence time of the liquid on the tray t_L in Equation 3.5 is based on liquid holdup in the tray froth (clear liquid height) and given in equation 2.17

For calculating liquid holdup on a tray, the model of Bennett et al. (1983) is judged to be the most reliable available, and is supported by a very large data base. It was selected for use in the present work. The model is as follows:

$$h_L = \phi_e \left[h_W + C \left[\frac{Q_{LW}}{\phi_e} \right]^{2/3} \right] \quad (3.12)$$

where

$$\phi_e = \exp[-12.55 K_s^{0.91}] \quad (3.13)$$

$$K_s = U_{SA} \left(\frac{\rho_v}{\rho_L - \rho_v} \right) \quad (3.14)$$

Constant C is obtained from equation, 3.11.

The complete data base is given in Appendix B. Finally, a new model for predicting or analyzing sieve tray efficiency will be described in Chapter 4, and will be validated with the data base from Chapters 3.

CHAPTER 4

MODEL DEVELOPMENT

4.1 MODEL STRUCTURE

In order to develop user-friendly tray efficiency model a simple dispersion structure needs to be selected. For this purpose a close examination of the existing hydrodynamic model for gas/liquid dispersion on sieve trays is done. Prado and Fair (1990) proposed their mechanistic hydrodynamic model for air/water system based on gas hold-up data.

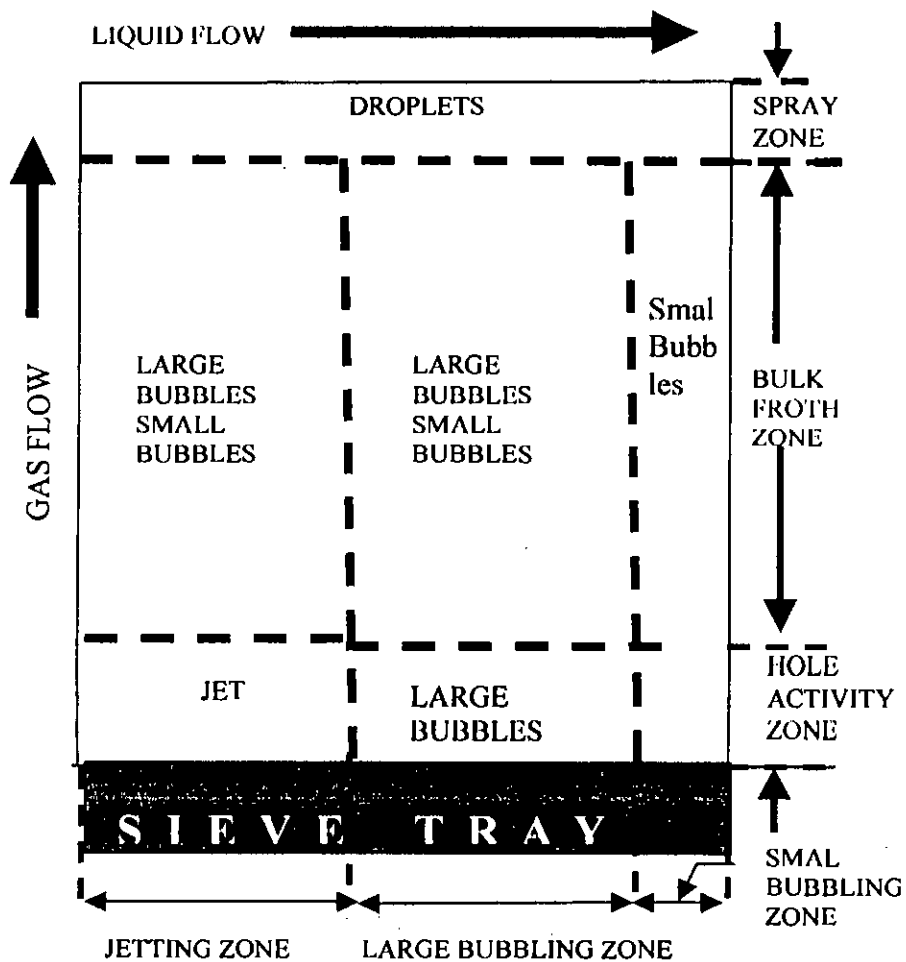


Figure 4.1 Schematic of the hydrodynamic model used by Prado and Fair (1990).

Their hydrodynamic model was later adopted by Garcia and Fair (2000) and extended for other binary systems. As shown in Figure 4.1 dispersion above the tray is divided into six zones. The zone at the bottom and closest to the tray (hole activity zone) corresponds to the activity at the holes (jetting or bubbling), the middle section (bulk froth zone) is composed of gas bubbles dispersed in the liquid, while the top zone (spray zone) is gas continuous, with liquid drops and ligaments dispersed throughout.

Bennett et al. (1997) proposed a two zone froth structure model consists of a liquid continuous region at the tray deck and a vapor continuous region on top of the liquid continuous region. Figure 4.2 shows the schematic of Bennett et al. (1997) model.

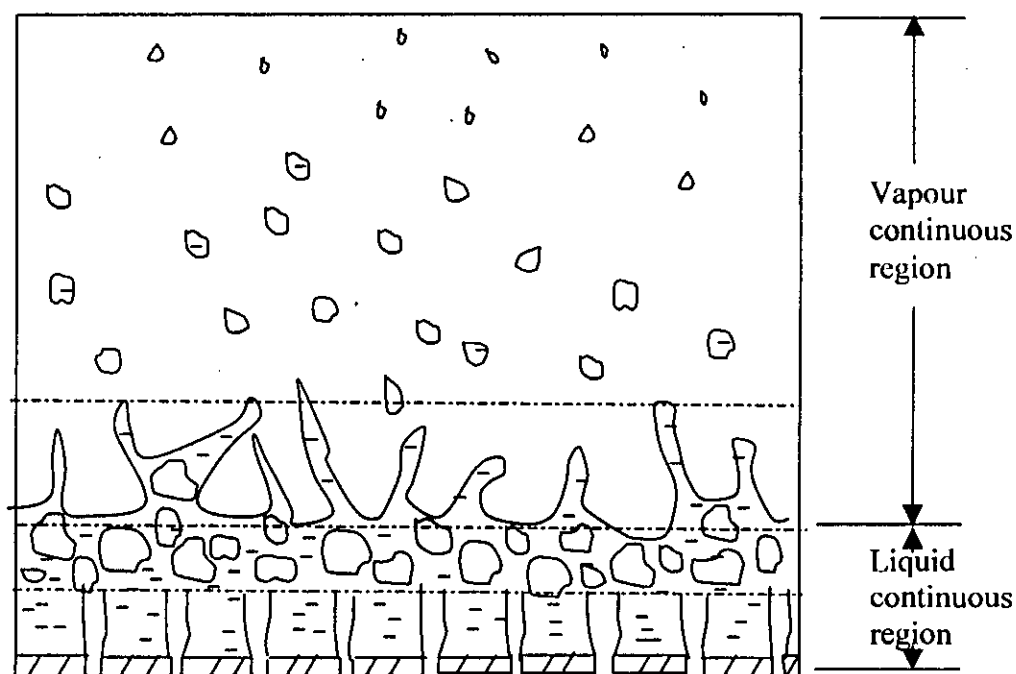


Figure 4.2 Schematic of the two-zone model adopted by Bennett et al. (1997)

In a very recent study Syeda et al. (2007) proposed another two-zone froth structure model based on froth images on a distillation tray. According to this model gas/liquid dispersion on a sieve tray is treated as a mixture of jets and bubbles. They divided the froth into jetting and bubbling zones. The jetting zone formed at the sieve tray holes, crosses the froth uninterrupted and throw liquid splashes above by tearing down the liquid surface. Bubbling zone is considered to have bimodal size distribution of bubbles due to turbulent break-up. The large bubbles are the unbroken formation bubbles originated from tray holes that remain in the froth due to incomplete break-up. The

small bubbles are the secondary bubbles formed by the turbulent break-up of formation bubbles. Both zones remain intimately mixed with each other in real froth. Figure 4.3 gives the details of Syeda et al. (2007) model.

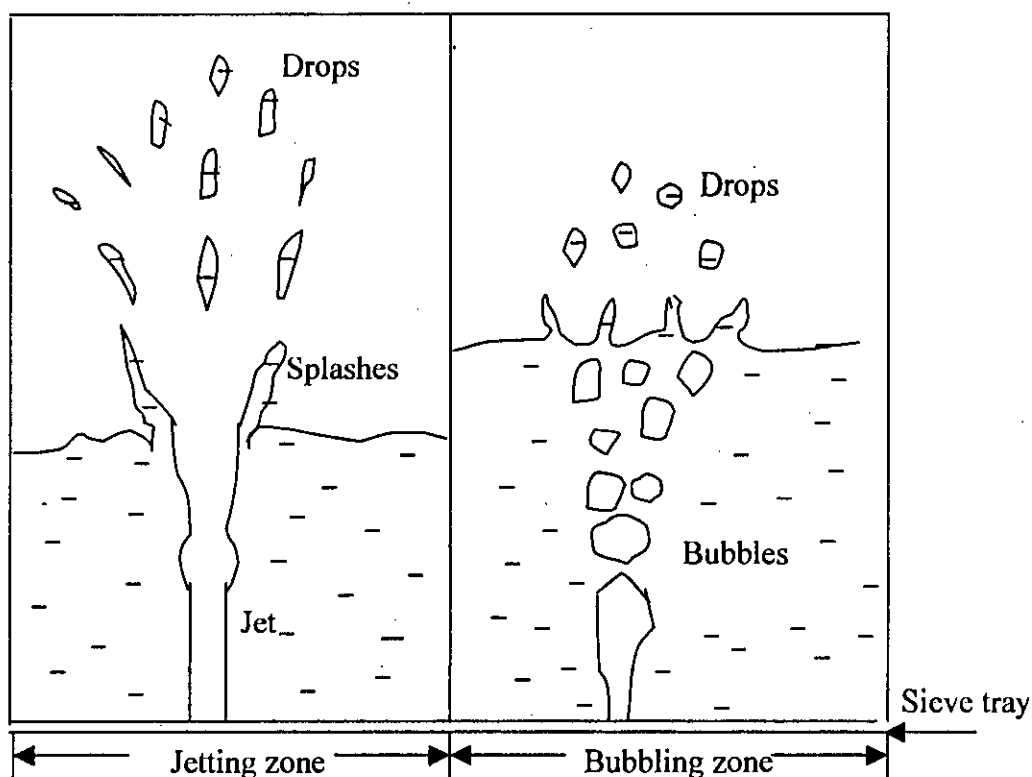


Figure 4.3 Schematic of the froth structure model proposed by Syeda et al. (2007)

It is evident from the schematics that Prado and Fair (1990) model is far more complicated than both Bennett et al (1997) and Syeda et al (2007) model. Both Bennett et al (1997) and Syeda et al (2007) used their froth structure model towards developing tray efficiency models. Bennett et al (1997) validated their efficiency model in froth regime and ignored spray regime. Thus their model has limited application. On the other hand, both froth structure model and tray efficiency model proposed by Syeda et al are validated for froth and spray regime which made their model somewhat more attractive than Bennet et al's one. For present study we base our tray efficiency model on the froth structure proposed by Syeda et al (2007). We, however, take different approach from Syeda et al. while developing the tray efficiency model in order to minimize and simplify the calculation steps as well as to broaden the applicability of the model for systems with range of physical properties.

For the froth structure proposed by Syeda et al (2007) and shown in figure 4.3 the tray efficiency is estimated by combining the contribution of both bubbling and jetting zones that exist on the tray. Equation 2.31 and 2.32 are given below

$$E_{OG} = (1 - F_J)E_B + F_J E_J \quad (2.31)$$

$$E_B = (1 - F_{SB})E_{LB} + F_{SB} E_{SB} \quad (2.32)$$

Where E_{OG} , F_J , F_{SB} , E_J , E_B , E_{LB} , E_{SB} are the overall tray efficiency, volume fraction of gas that penetrates the froth as continuous jet, fraction of small bubbles, efficiency of the jetting zone, efficiency of the large bubble, and tray efficiency of the small bubble, respectively.

Among the five parameters F_J , F_{SB} , E_J , E_{LB} , E_{SB} used in equations 2.31 and 2.32 there are more than one correlations for F_{SB} (fraction of small bubbles) and F_J (fraction of jetting) in literature. Furthermore, since the small bubbles in froth can be assumed to reach equilibrium when mass transfer rate is high the efficiency of small bubbles can be considered as unity, i.e.

$$E_{SB} = 1$$

Therefore the main challenge of developing a new model expressed by the equations 2.31 and 2.32 is to find suitable ways to estimate the terms E_J and E_{LB} . Previous studies simulate mass transfer processes in single bubble and single jet and employ five to ten step calculations to get the value of E_J and E_{LB} . The accuracy in predicting tray efficiency achieved by employing such rigorous calculation is not more than $\pm 25\%$. In present study our target is to achieve same or higher level of accuracy without adopting the complicated calculation steps for E_J and E_{LB} . With this purpose in mind we first select the correlations for F_J and F_{SB} from existing literature.

4.2 DETERMINATION OF FRACTION OF JETTING, F_J

Raper et al. (1982) studied the fraction of jetting with respect F-factor on sieve trays. Equation 4.3 gives an excellent fit of the experimentally measured data of Raper et al. (1982) for the average value of fraction of jetting, F_J , as a function of F-factor, F_{SA}

$$F_J = -0.1786 + 0.9857(1 - e^{-1.43F_{SA}}) \quad (4.1)$$

4.3 DETERMINATION OF FRACTION OF SMALL BUBBLES, F_{SB}

Garcia and Fair (2000) and Syeda et al (2007) proposed two different correlations for estimating F_{SB} . As mentioned earlier, Garcia and Fair (2000) correlation for F_{SB} is arbitrary and lacks in theoretical base. Therefore, we adopt the F_{SB} correlation of Syeda et al. (2007), which is based on the theory of bubble break-up in turbulent flow field.

$$F_{SB} = \frac{2(1 - e^{-k\bar{\Delta}})}{2(1 - e^{-k\bar{\Delta}}) + \left(\frac{d_{32L}}{d_{32S}}\right)^3 e^{-k\bar{\Delta}}} \quad (2.41)$$

Where,

$$k\bar{\Delta} = 0.16 \left(\frac{3.8\rho_L^{0.1}\rho_G^{0.3}}{\sigma^{0.4}} \right) (u_S g)^{0.6} t_{GLB} \quad (2.45)$$

$$t_{GLB} = \frac{h_f}{(Q_V/A_A)} = \frac{h_f}{U_{SA}}$$

h_f is calculated by the method of Bennett et al. (1983), Given in equations (2.21a), (2.21b) and (2.21c).

4.4 DETERMINATION OF EFFICIENCIES, E_{LB} AND E_L

Semi-empirical model:

All semi-empirical models employ basic mass transfer theory in estimating efficiencies. Based on the Higbie penetration (Higbie, 1935) the following equations for mass transfer co-efficient are postulated

$$k_G = C_1 \left(\frac{D_G}{t_G} \right)^{0.5} \quad (4.2)$$

$$k_L = C_2 \left(\frac{D_L}{t_L} \right)^{0.5} \quad (4.3)$$

Substituting equations (4.2) and (4.3) into equations (2.7) and (2.8) respectively, we get

$$N_G = C_1 a (D_G t_G)^{0.5} \quad (4.4)$$

$$N_L = C_2 a (D_L t'_L)^{0.5} \left(\frac{M_G G}{M_L L} \right) \quad (4.5)$$

Here, the vapor residence time in the two-phase dispersion is expressed as

$$t_G = \frac{h_f \varepsilon}{u_s} \quad (4.6)$$

Similarly, the liquid residence time is

$$t_L = t'_L \left(\frac{M_G G}{M_L L} \right) \quad (4.7)$$

Where

$$t'_L = t_G \frac{\rho_L}{\rho_G} \quad (4.8)$$

Finally, by combining equations (2.11), (4.4) and (4.5), we get the expression for the overall mass transfer unit.

$$\begin{aligned} N_{OG} &= \frac{N_G}{1 + \lambda(N_G/N_L)} \\ &= \frac{C_1 a (D_G t_G)^{0.5}}{1 + \lambda(C_1/C_2) (M_L L/M_G G) (D_G \rho_G/D_L \rho_L)^{0.5}} \end{aligned} \quad (4.9)$$

Equation 4.9 can be applied to determine both E_{LB} and E_J . The unknowns in this equation are interfacial area a and two constants C_1 and C_2 . Previous studies adopted different approaches in determining interfacial area a for bubble dominated regimes. For jets such effort is scarce. In our model to keep the expression simple we assume that interfacial area per unit volume for large bubbles is constant and is denoted by a_{LB} . Similarly, for jets interfacial area per unit volume is considered constant and is denoted by a_j . Earlier semi-empirical studies showed that the constants C_1 and C_2 employed in equations are of same order and close to each other. In this model we assume that $C_1 \cong C_2$ so that the ration C_1/C_2 becomes 1. Thus the final form of E_{LB} and E_J become as follow

$$E_J = 1 - \exp\left(-\frac{B(D_G t_G)^{0.5}}{1 + \lambda(M_L L / M_G G)(D_G \rho_G / D_L \rho_L)^{0.5}}\right) \quad (4.9a)$$

$$E_{LB} = 1 - \exp\left(-\frac{A(D_G t_G)^{0.5}}{1 + \lambda(M_L L / M_G G)(D_G \rho_G / D_L \rho_L)^{0.5}}\right) \quad (4.9b)$$

Where the constant $A=C_1 a_{LB}$ and the constant $B=C_2 a_J$.

The overall point efficiency is obtained by replacing equation, 2.31 and 2.32 by equations (4.9a) and (4.9b).

The constants A and B are determined by comparing the model with the data base. The best fit with minimum error is found for $A=11$ and $B=14$ with error $\pm 35\%$.

Empirical model:

The semi-empirical model gives prediction within $\pm 35\%$ error band. In order to get better prediction empirical method is adopted to determine E_{LB} and E_J . One way to develop empirical correlation is to do dimensional analysis and express the unknown parameters in terms of dimensionless groups.

Tray efficiency is a function of flow properties i.e. liquid and vapor load, physical properties of the system and tray geometry. Consideration of all parameters eventually leads to the following four dimensionless groups

$$\left(\frac{\sigma}{\mu_L U_{SM}}\right), \left(\frac{\mu_L}{\rho_L D_L}\right), \left(\frac{\mu_G}{\rho_G D_G}\right) \text{ and } \left(\frac{h_w U_H \rho_G}{\mu_L}\right)$$

Since the efficiency of large trays is considered only, the effect of diameter is not considered in these dimensionless groups. The first group is denoted as surface tension number and gives an estimation of the stability of gas dispersion in liquid. The second and third dimensionless groups are liquid and vapour Schmidt numbers and approximate the mass transfer process in liquid and vapour phases. The last term is the modified Reynolds number and approximates the nature of the gas liquid dispersion. The effect of vapour Schmidt number on tray efficiency is open to doubt and almost all existing models and correlations do not consider vapour Schmidt number in their models. MacFarland et al (1972) ignored the vapour Schmidt number and selected the

three dimensionless groups among the abovementioned four groups based on 42 existing models. For present study the dimension less groups used by MacFarland et al (1972) are adopted to express the extent of large bubbles saturation, E_{LB} and the extent of jet saturation, E_J .

$$E_{LB} = C_3 \left(\frac{\sigma}{\mu_L U_{SA}} \right)^{0.115} \left(\frac{\mu_L}{\rho_L D_L} \right)^{0.215} \left(\frac{h_w U_H \rho_G}{\mu_L} \right)^{0.1} \quad (4.10a)$$

$$E_J = C_4 \left(\frac{\sigma}{\mu_L U_{SA}} \right)^{0.115} \left(\frac{\mu_L}{\rho_L D_L} \right)^{0.215} \left(\frac{h_w U_H \rho_G}{\mu_L} \right)^{0.1} \quad \text{(Proposed model-1)} \quad (4.10b)$$

Where, $\frac{\mu_L}{\rho_L D_L}$ = Schmidt Number, and $\frac{h_w U_H \rho_G}{\mu_L}$ = Reynolds Number

Constant C_3 and C_4 are two proportionality constants that include effects of other parameters that have been ignored while deriving the dimensionless groups. In present model stability of large bubbles is considered in the term fraction of small bubbles, F_{SB} (equation 2.41) where the effect of surface tension has been included. Furthermore, the effect of vapor load that determines the nature of dispersion is incorporated in the model by the term fraction of jetting F_J (equation 4.1). These two considerations make the surface tension number and Reynolds number less significant in the model. Thus the saturation of large bubbles and jets becomes the function of liquid Schmidt number only. The equations 4.10a and 4.10b can be further simplified and expressed in terms of liquid Schmidt number as follows

$$E_{LB} = C_5 \left(\frac{\mu_L}{\rho_L D_L} \right)^{0.215} \quad (4.11a)$$

and

$$E_J = C_6 \left(\frac{\mu_L}{\rho_L D_L} \right)^{0.215} \quad (4.11b)$$

Analysis of Schmidt number in equations 4.11a and 4.11b shows that the value of l/D_L dominates over $\left(\frac{\mu_L}{\rho_L} \right)$ and the saturation of large bubbles and jets can be expressed in terms of liquid diffusivities only.

$$E_{LB} = C_7 D_L^{-0.215} \quad (4.12a)$$

$$E_J = C_8 D_L^{-0.215} \quad \text{(Proposed Model-2)} \quad (4.12b)$$

The values of the constants C_3 , C_4 , C_7 and C_8 are obtained by comparing equations 2.31 and 2.32 with the database using the respective expressions of E_{LB} and E_J . The values of the constant that give the minimum average absolute error for respective expressions are adopted. The average absolute error was calculated by the following equation,

$$Error\% = \frac{\sum \frac{Estimated - Experimental}{Experimental}}{N}$$

Table 4.1 gives the values and respective error percentage for the four constants.

Table 4.1 Determination of constants C_3 , C_4 , C_7 and C_8

Constants	Values	%Error
C3	4.8	12.88
C4	7.2	
C7	0.7	13.07
C8	1.0	

In order to further simplify the model an attempt to express E_{LB} and E_J by two fractional numbers was made. These two fractional numbers give the average saturation of large bubbles and jets for the range of data used in present study.

$$E_{LB} = 0.4 \quad (4.13a)$$

$$E_J = 0.7 \quad \text{(Proposed model-3)} \quad (4.13b)$$

The average absolute error of predicted point efficiency with equations 4.13a and 4.13b is 8.43 %, which is less than any value mentioned in Table 4.1.

Thus the final expression for the proposed model becomes

$$E_B = (0.4(1 - F_{SB}) + 1.0F_{SB})(1 - F_J) + 0.7F_J$$

The gradual steps and equations used in final proposed model (proposed model-3) are given in table 4.2.

Table 4.2 Steps and Equations Used in Proposed Model-3

Froth structure	Given in Fig 4.1
Efficiency equations	$E_{OG} = (1 - F_J)E_B + F_J E_J$ $E_B = (1 - F_{SB})E_{LB} + F_{SB}E_{SB}$
E_{LB}	0.4
E_J	0.7
E_{SB}	1
F_J	$F_J = -0.1786 + 0.9857(1 - e^{-1.43F_{SL}})$
F_{SB}	$F_{SB} = \frac{2(1 - e^{-k\bar{\Delta}})}{2(1 - e^{-k\bar{\Delta}}) + \left(\frac{d_{32L}}{d_{32s}}\right)^3 e^{-k\bar{\Delta}}}$

Finally the following Assumptions and range of applicability are taken into consideration for model development.

- (1) Weeping and flooding are not considered in the froth structure.
- (2) Effect of liquid height is considered in determining contact time of large bubbles.
- (3) For jets, effect of liquid height h_L , is ignored.
- (4) Chen & Chuang (1993), Garcia and Fair (2000) and Syeda et al. (2007) assumed turbulent flow field on sieve trays within froth to spray regime. In present model similar assumption is made.
- (5) In present model it is also assumed that bubbles formed in tray holes go through turbulent break up but could not reach equilibrium due to short contact time. Thus the froth has bimodal bubble size distribution. The large bubbles represent the

unbroken initial bubbles, the small bubble are the secondary bubbles formed by incomplete break-up.

- (6) Based on literature the diameter ratio of large to small bubbles is considered to be 5:1.
- (7) The rate of bubble break-up is assumed to be of first order. The rate constant is determined based on the turbulent breakup theory and by using the physical properties of both gas and liquid phases of the dispersion.
- (8) The model estimates point efficiency E_{OG} and uses Bennett and Grimm's liquid mixing model to convert E_{OG} to tray efficiency E_{MV} . Bennett and Grimm's model considers the effect of liquid gradient and liquid mixing on tray efficiency. The present model needs to be applied together with Bennett and Grimm's model to get E_{MV} from the predicted E_{OG} .
- (9) The model is generally applicable to all binary mixtures except those with foaming tendency. In such cases correction based on foaming factor will be necessary.

CHAPTER 5

RESULT & DISCUSSION

The semi-empirical approach based on basic mass transfer theory was not successful as the model gives higher error. Thus although the semi-empirical model gives more detail of the mass transfer process in large bubbles and jets this model was not adopted. All three forms of the empirical model give better prediction than the semi-empirical model. The error band of the empirical models is also comparable with that of the latest models. Therefore, the empirical models are considered to be the proposed models of present study.

In order to validate the proposed models, implementation and testing of the proposed models are covered in this chapter. Twenty sets of experimental data (153 points), which are given in Appendix B, are used to predict point efficiencies by present models. In literature efficiencies are given in the form of overall column efficiency or Murphree vapor efficiency. The conversion procedure of overall column efficiency or Murphree vapor efficiency to point efficiency has been given in Chapter 3. Figures 5.1-5.16 show the predicted values using the final proposed model (Model-3) against experimental data. Predictions by other two proposed models (Model-1, Model-2) are also shown in Figures. The important hydraulic parameter, F-factor, used to account for loading, is defined as

$$F_{SM} = U_{SM} \sqrt{\rho_V}$$

U_{SM} = Superficial gas velocity based on active area, m/s.

ρ_V = vapor density, kg/m³

Finally parity plots, Figures 5.17-5.19 show the prediction by the limits $\pm 25\%$ for 153 data points. The models fit these diversified data satisfactory. Table 5.1 shows the used range of operating pressure and physical properties for model validation.

Table 5.1 Range of operating pressure and physical properties used in model validation

Range	Pressure (kPa)	Liquid density (kg/m ³)	Gas density (kg/m ³)	Liquid viscosity (mPa.s)	Gas viscosity (mPa.s)	Surface tension (mN/m)
Max	2758	949	85.0	1.56	0.013	55
Min	1.3	380	0.07	0.05	0.007	01

Figures 5.1-5.5 include test results for aqueous mixtures of acetic acid, isopropanol and methanol respectively. All systems, except one set of isopropanol/water, were distilled at atmospheric pressure. Isopropanol/water system was run at 13.3 kPa. Table 5.2 shows pressures, average Schmidt numbers and characteristics of these systems. At atmospheric pressure average Schmidt number for these systems are close to each other. For vacuum system (i.e. iso-propanol/water system), however, the Schmidt number obtained was very high.

Table 5.2 Pressure, average Schmidt number, characteristics of aqueous systems

System	Pressure (kPa)	Average Schmidt number	Characteristics
Acetic Acid/Water	101.4	56	-
Isopropanol/Water	13.3	3342	-
Isopropanol/water	101.4	67	-
methanol/water	101.4	60	Foaming
methanol/water	101.4	63	Foaming

Tables B.1.1, B.2.1, B.18.1, B.7.1, B.17.1, give flow field properties, physical properties and efficiencies (experimental and calculated) of these systems respectively. Calculation steps of fraction of jetting and fraction of small bubbles are given in tables B.1.2, B.2.2, B.18.2, B.7.2, B.17.2, respectively and Tables B.1.3, B.2.3, B.18.3, B.7.3, B.17.3, gives efficiencies of bubbles and jetting of respective systems. Acetic acid/water, and isopropanol/water (Systems) show good agreements (Figures 5.1-5.3), although Schmidt numbers are widely varied. For methanol/water system, Figures 5.4

and 5.5 the measured efficiencies are much higher than other systems although they have comparable Schmidt numbers to that of acetic acid system. The proposed model predicts lower than the measured efficiency. Thus this higher efficiency of methanol/water can not be explained by Schmidt number only. This is in fact due to the foaming tendency of methanol water system. Syeda et al. (2004) and Zuiderweg (1982) reported that methanol/water system has foaming tendency and give higher efficiency than non foaming systems. The proposed froth structure does not consider foaming in the dispersion; thus under predicts efficiency of foaming systems.

Figures 5.6-5.16 give test results for hydrocarbon systems. Table 5.3 shows pressures,, average Schmidt numbers and characteristics of these systems . Tables B.3.1, B.4.1, B.8.1, B.9.1, B.10.1, B.14.1, B.15.1, B.20.1, B.12.1, B.13.1, B.16.1 give flow field properties, physical properties and efficiencies (experimental and calculated) of these systems respectively. Calculation steps for fraction of jetting and fraction of small bubbles are given in tables B.3.2, B.4.2, B.8.2, B.9.2, B.10.2, B.14.2, B.15.2, B.20.2, B.12.2, B.13.2, B.16.2 respectively and tables B.3.3, B.4.3, B.8.3, B.9.3, B.10.3, B.14.3, B.15.3, B.20.3, B.12.3, B.13.3, B.16.3 gives efficiencies of bubbles and jetting of respective system.

Table 5.3 Pressure, average Schmidt number and characteristics of hydrocarbon systems

System	Pressure (kPa)	Average Schmidt number	Characteristics
ortho/para xylenes	2.13	240	-
ortho/para xylenes	2.13	240	-
ethyibenzene/styrene	13.3	138	
cyclohexane/n-heptane	27.6	118	-
cyclohexane/n-heptane	165	54	-
cyclohexane/n-heptane	34	110	-
cyclohexane/n-heptane	165	52	-
cyclohexane/n-heptane	101.4	68	-
iso-butane/n-butane	2068	9	Entrainment
iso-butane/n-butane	2758	7	Entrainment
iso-butane/n-butane	1138	8	Entrainment

Ortho/para xylenes and ethylbenzene/styrene systems (Figures 5.6-5.9) show a close fit (+5%) to the experimental data. For this system average Schmidt numbers are close to each other. From Figures 5.10-5.13 it is found that for cyclohexane/n-heptane systems the proposed model shows very good agreement with experimental data. At high pressure (Figures 14-16) the vapor rate is high, and due to excessive liquid entrainment or excessive backup of liquid in the down comer the true point efficiency is somewhat higher than the measured efficiency, Figures 14-16. In all cases prediction is higher than experimental data which ensures the applicability in high pressure systems.

Table 5.4 Comparison of Proposed Model-3 with Garcia-Fair and Chan-Fair Model

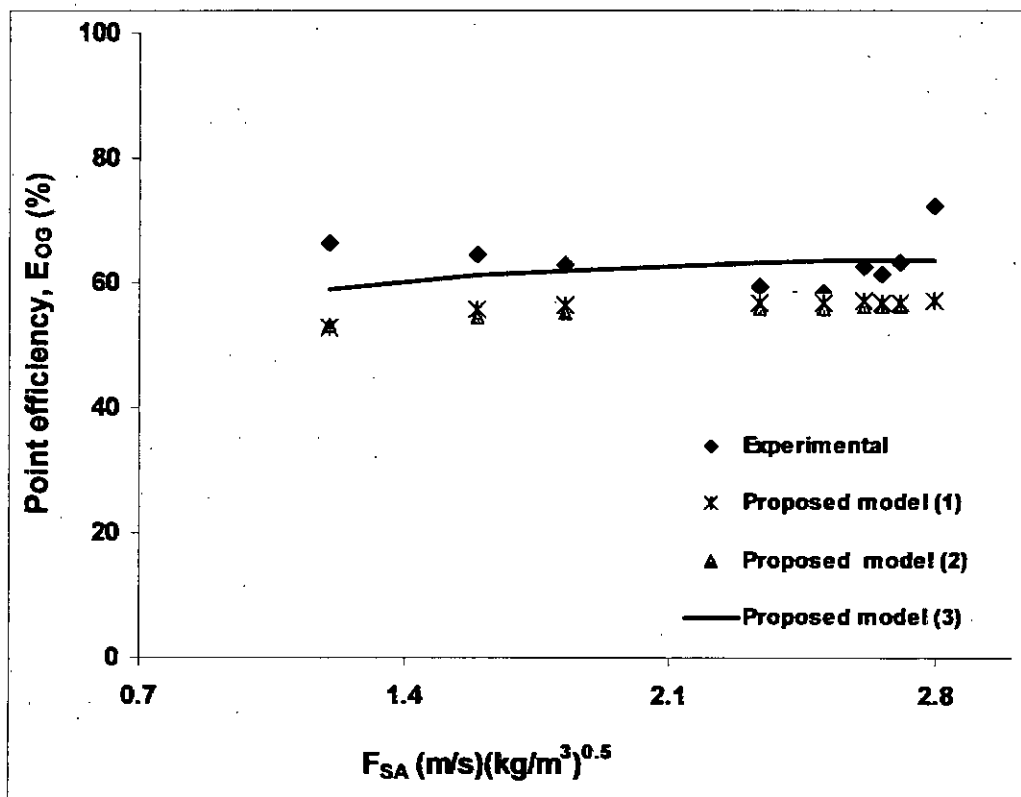
Parameters	Proposed model-3	Garcia-Fair Model	Chan-Fair Model
Average deviation, all points (%)	4.80	-10.8	28.7
Mean Absolute Deviation (%)	10.8	21.4	44.1

$$\% \text{ Deviation} = 100.0 (E_{OG} \text{ Calculated} - E_{OG} \text{ Experimental}) / E_{OG} \text{ Experimental}$$

$$\text{Average Deviation} = (\sum \% \text{ deviation}) / \text{number of data points}$$

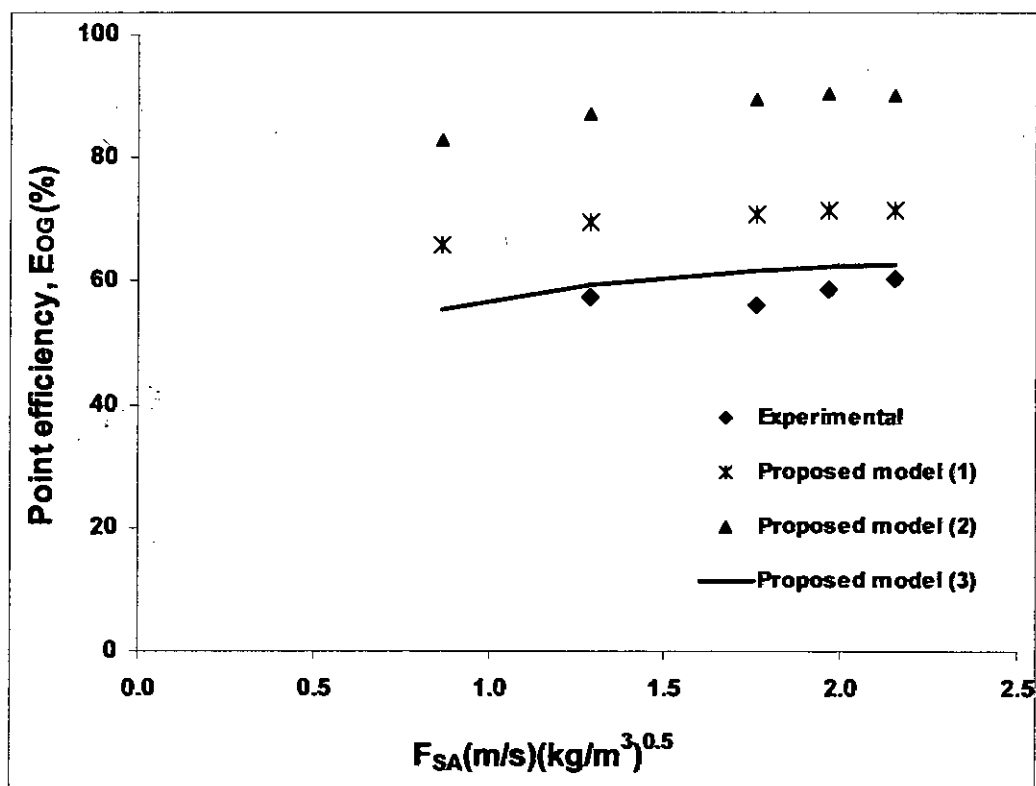
$$\text{Mean Absolute Deviation} = (\sum \text{ABS} (\% \text{ deviation})) / \text{number of data points}$$

Finally, a master parity plots are shown in Figures 5.17-5.19 for all of the data points. Limits of $\pm 25\%$ are shown; these limits are considered to be reasonable for fitting such a diverse set of systems, geometries, experimentalists, analytical procedures, degrees of thermodynamic non-ideality, and so on. An analysis of the fit of proposed Model-3 is shown in Table 5.4, and comparisons with the fit of Garcia and Fair model (2000) and Chan and Fair model (1984) are also included. The standard deviation of final proposed Model is 8. It is evident from Table 5.4 that the predictions of the proposed model are better than the two major existing models.



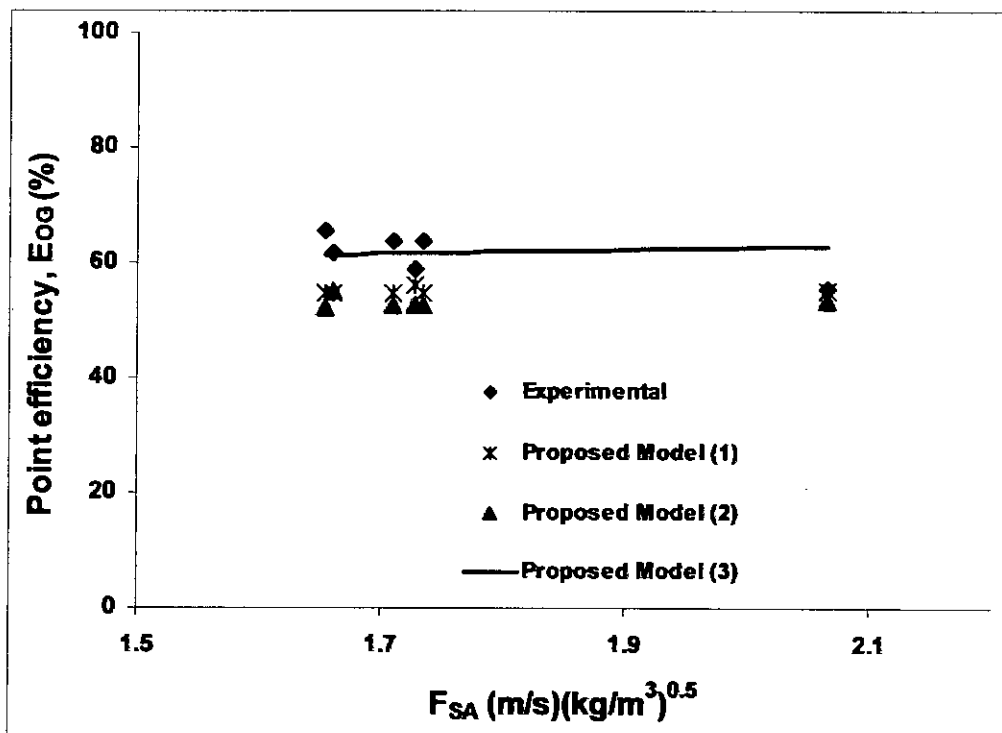
System	acetic acid/water
Operating Pressure	101.4 kPa
Hole diameter (mm)	3.175
Hole area (%)	8.35
Weir height (mm)	38.1
Column diameter (m)	0.457
Source	Jones and Pyle, 1955 (C)

Figure 5.1 Comparison of predicted and experimental point efficiencies acetic acid/water system at 101.4 kPa operating pressure.



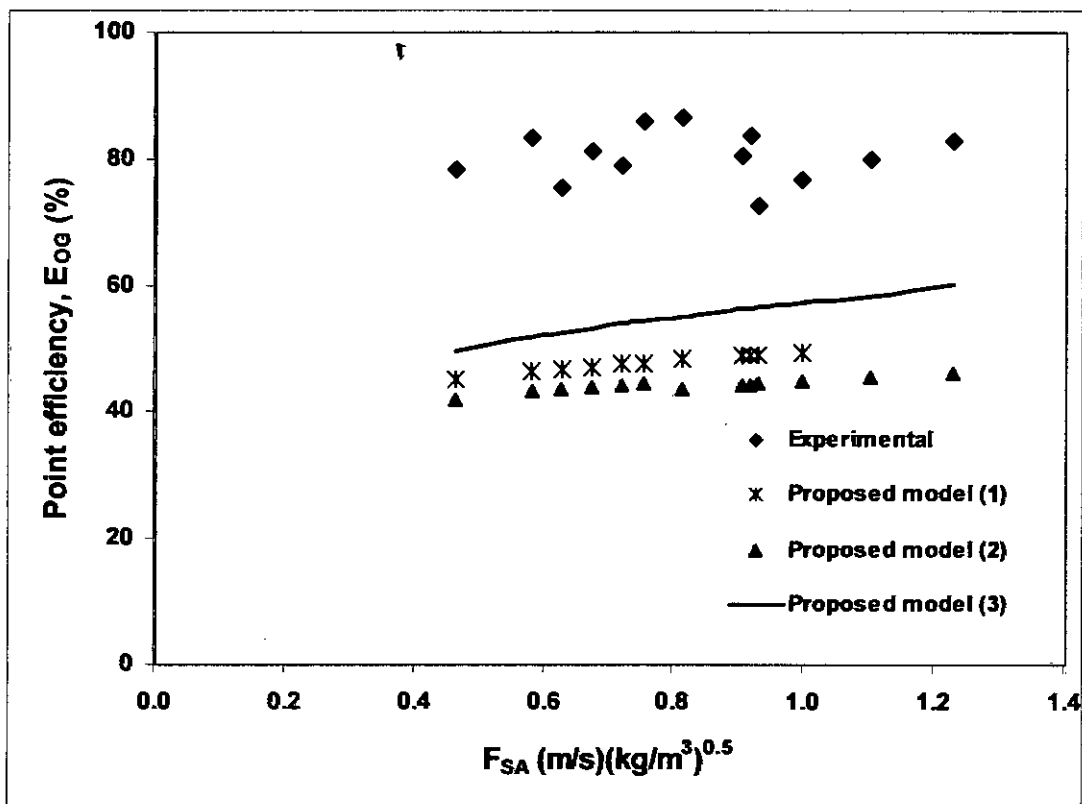
System	isopropanol/water
Operating Pressure	13.3 kPa
Hole diameter (mm)	4.8
Hole area (%)	12.7
Weir height (mm)	25.4
Column diameter (m)	1.22
Source	FRI, 1966a

Figure 5.2 Comparison of predicted and experimental point efficiencies for the isopropanol/water system at 13.3 kPa operating pressure.



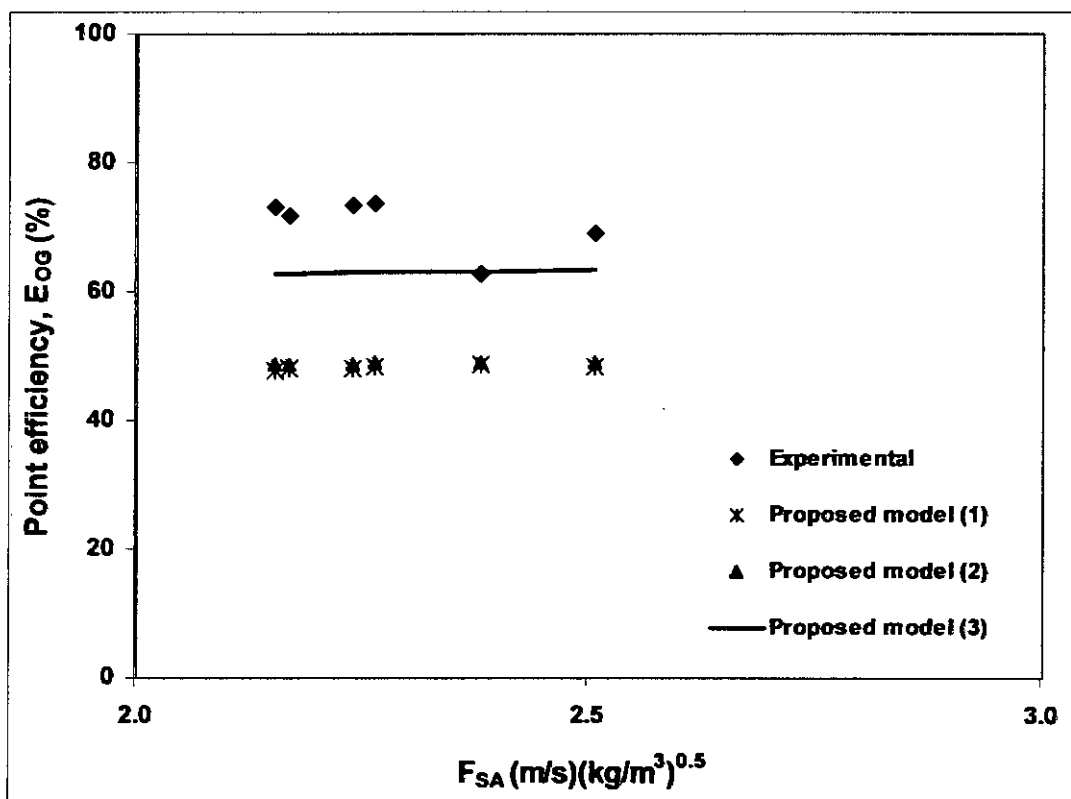
System	iso-propanol/water
Operating Pressure	101.4 kPa
Hole diameter (mm)	4.8
Hole area (%)	12.7
Weir height (mm)	50
Column diameter (m)	0.60
Source	Korchinsky et al., 1994

Figure 5.3 Comparison of predicted and experimental point efficiencies for the isopropanol/water system at 101.4 kPa operating pressure.



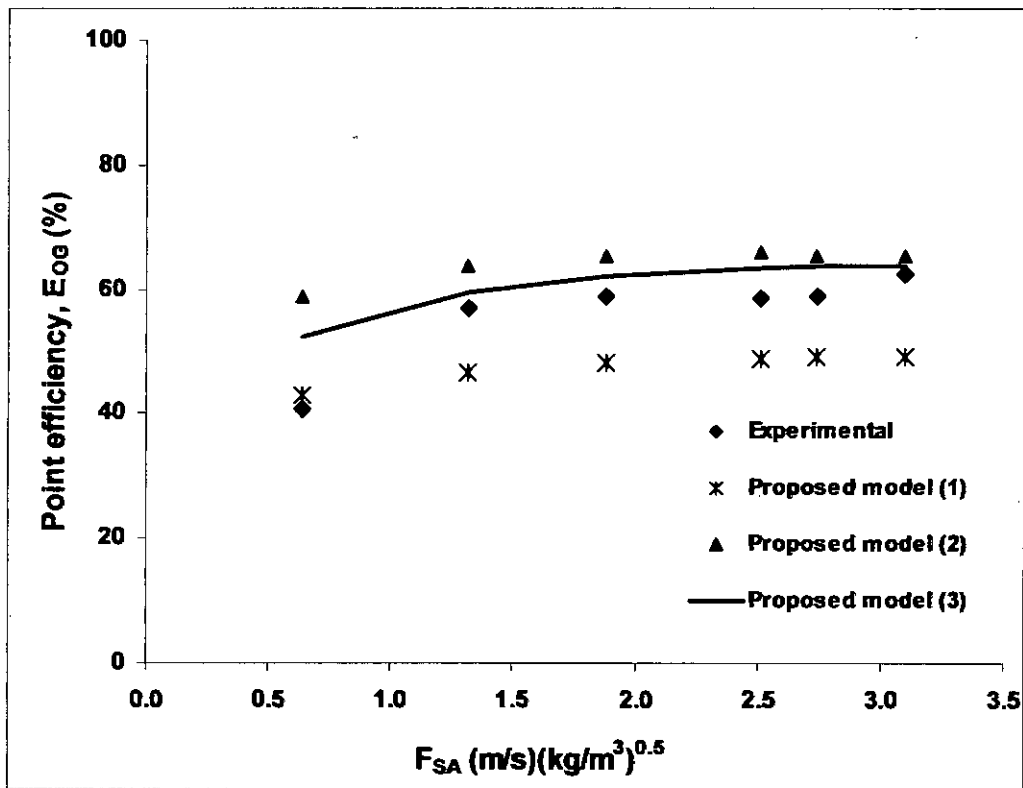
System	methanol/water
Operating Pressure	101.4 kPa
Hole diameter (mm)	4
Hole area (%)	4.8
Weir height (mm)	40
Column diameter (m)	0.976
Source	Kastanek and Stander, 1967

Figure 5.4 Comparison of predicted and experimental point efficiencies for the methanol/water system at 101.4 kPa operating pressure.



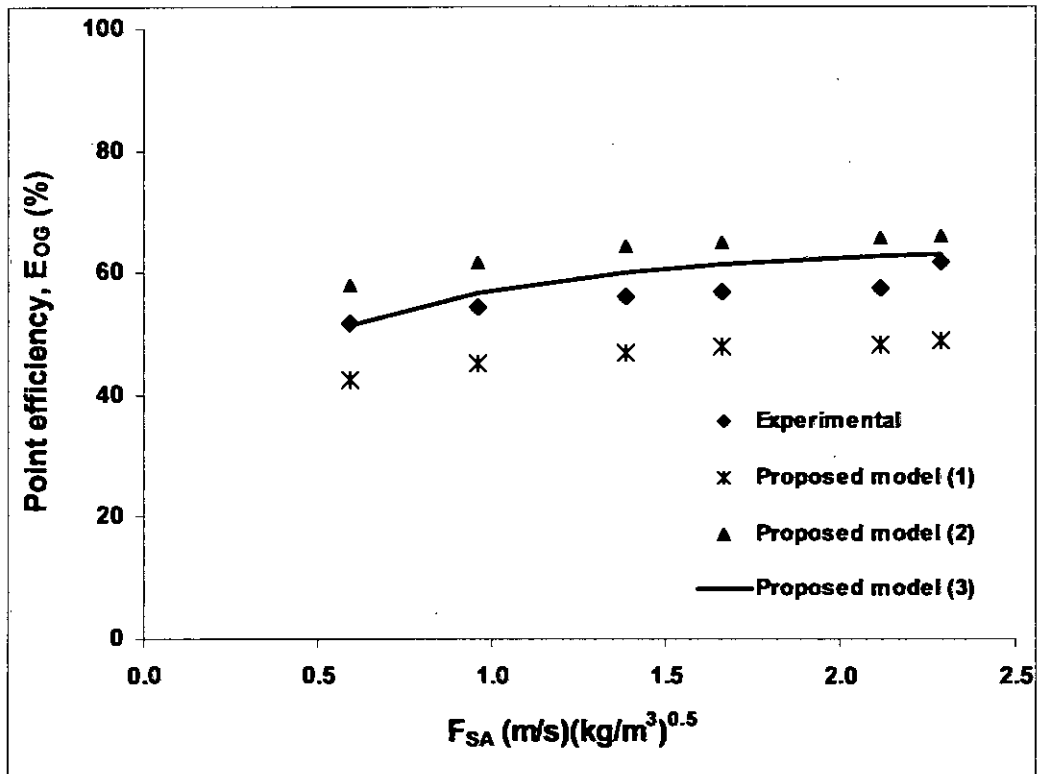
System	methanol/water
Operating Pressure	101.4 kPa
Hole diameter (mm)	4.8
Hole area (%)	12.7
Weir height (mm)	50
Column diameter (m)	0.60
Source	Korchinsky et al., 1994

Figure 5.5 Comparison of predicted and experimental point efficiencies for the methanol/Water system at 101.4 kPa operating pressure



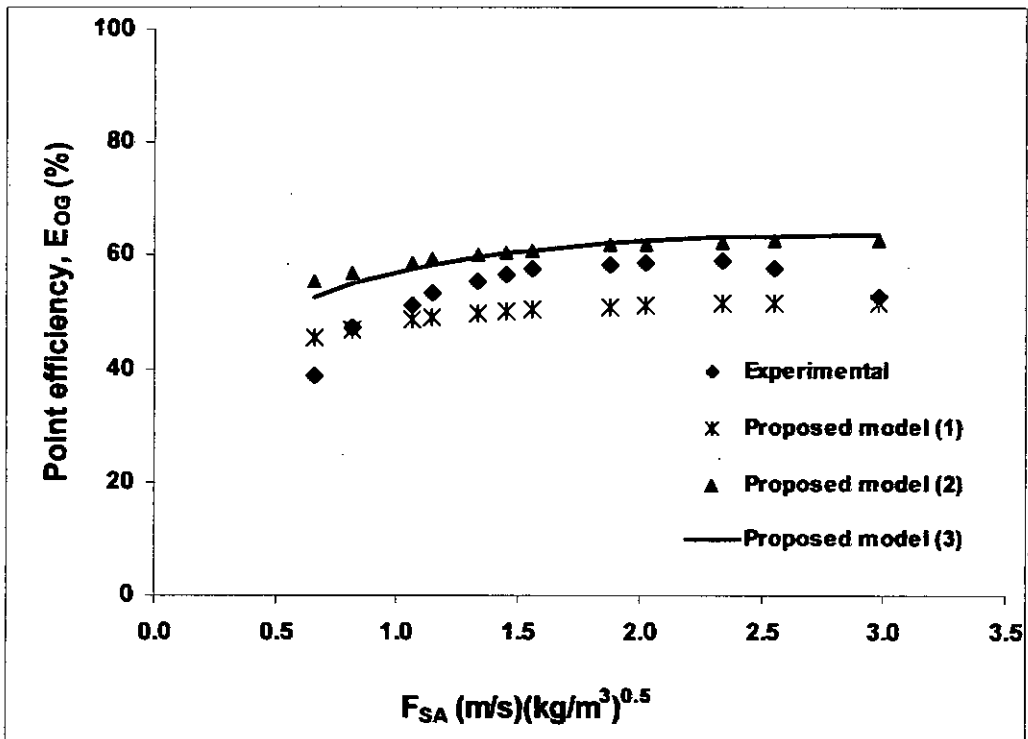
System	ortho/para xylenes
Operating Pressure	2.13 kPa
Hole diameter (mm)	4.8
Hole area (%)	12.7
Weir height (mm)	25.4
Column diameter (m)	1.22
Source	FRI, 1966a

Figure 5.6 Comparison of predicted and experimental point efficiencies for the ortho/para xylenes system at 2.13 kPa operating pressure.



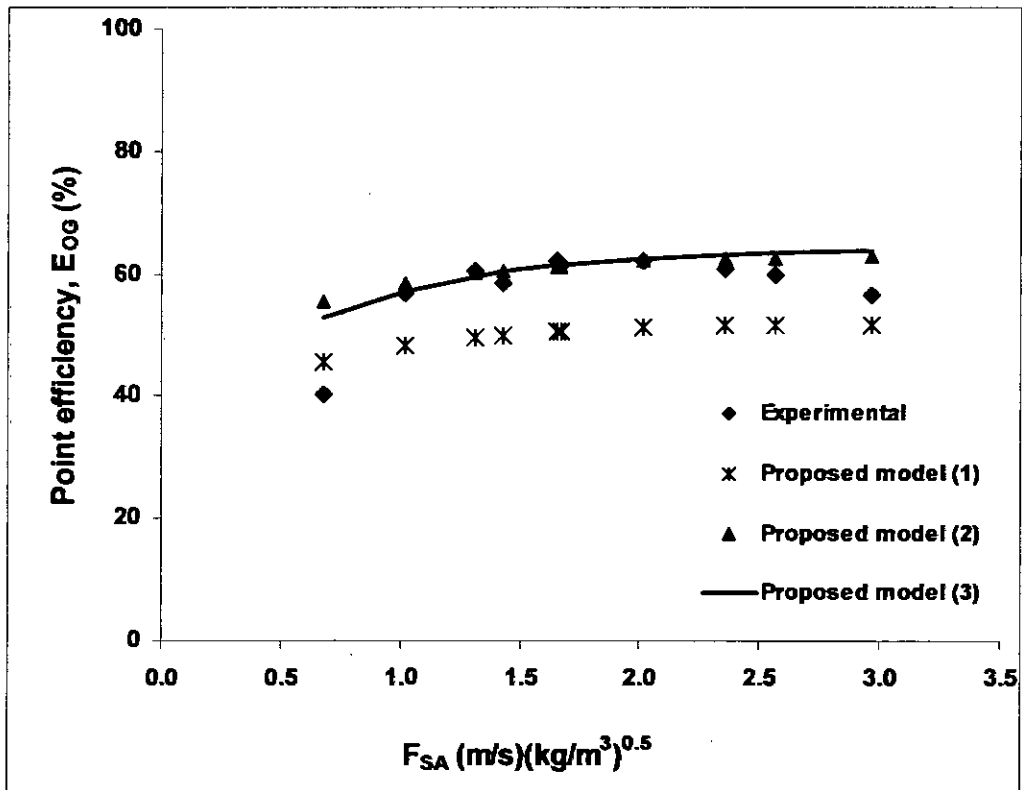
System	ortho/para xylenes
Operating Pressure	2.13 kPa
Hole diameter (mm)	12.7
Hole area (%)	13.0
Weir height (mm)	25.4
Column diameter (m)	1.22
Source	FRI, 1966b

Figure 5.7 Comparison of predicted and experimental point efficiencies for the ortho/para xylenes system at 2.13 kPa operating pressure.



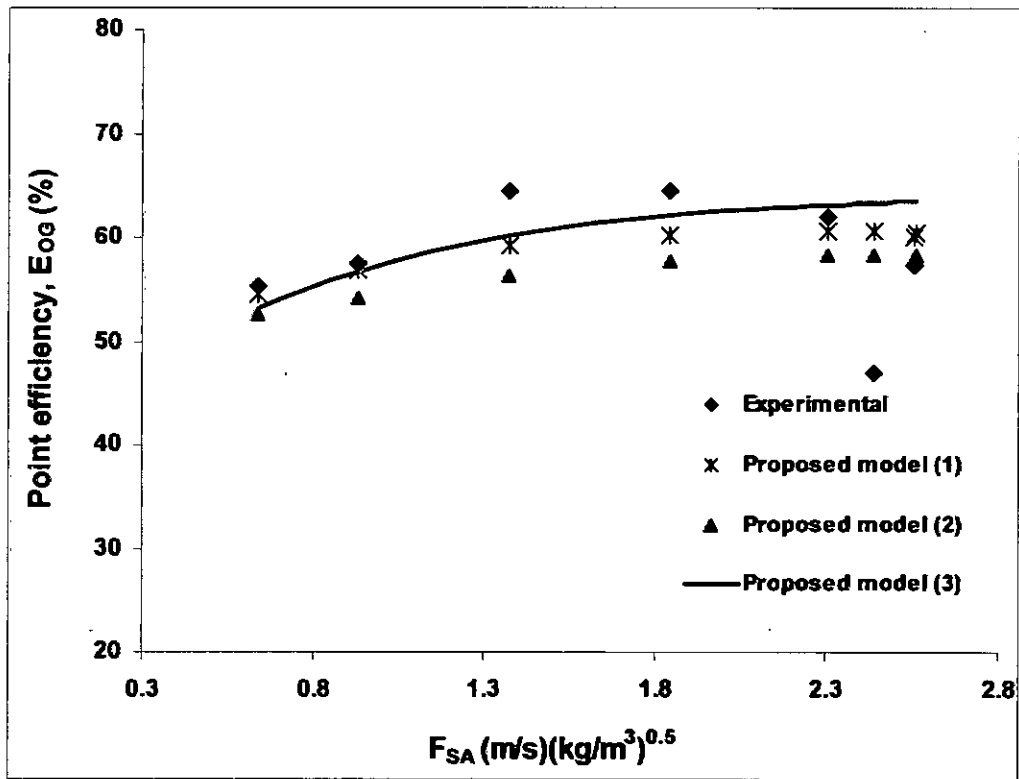
System	ethylbenzene/styrene
Operating Pressure	13.3 kPa
Hole diameter (mm)	12.5
Hole area (%)	13.6
Weir height (mm)	19
Column diameter (m)	0.788
Source	Billet et al., 1969

Figure 5.8.1 Comparison of predicted and experimental point efficiencies for the ethylbenzene/styrene system at 13.3 kPa operating pressure, $h_w = 19\text{mm}$.



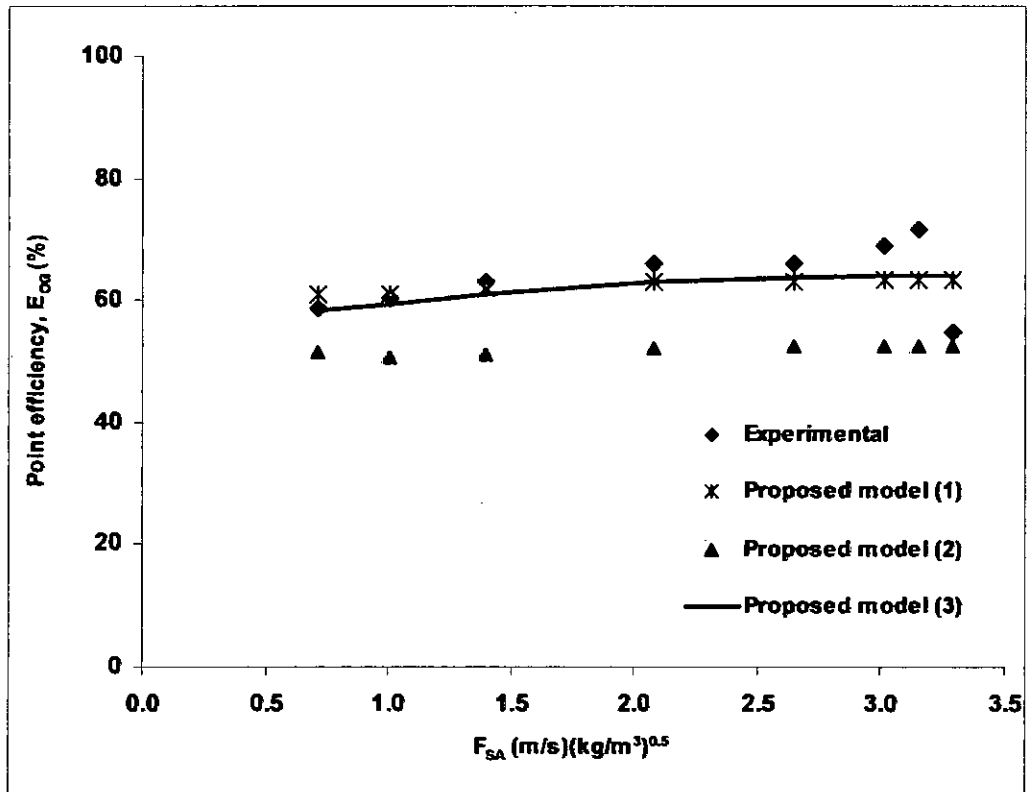
System	ethylbenzene/styrene
Operating Pressure	13.3 kPa
Hole diameter (mm)	12.7
Hole area (%)	13.6
Weir height (mm)	38
Column diameter (m)	0.788
Source	Billet et al., 1967

Figure 5.8.2 Comparison of predicted and experimental point efficiencies for the ethylbenzene/styrene system at 13.3 kPa operating pressure, $h_w=38$ mm.



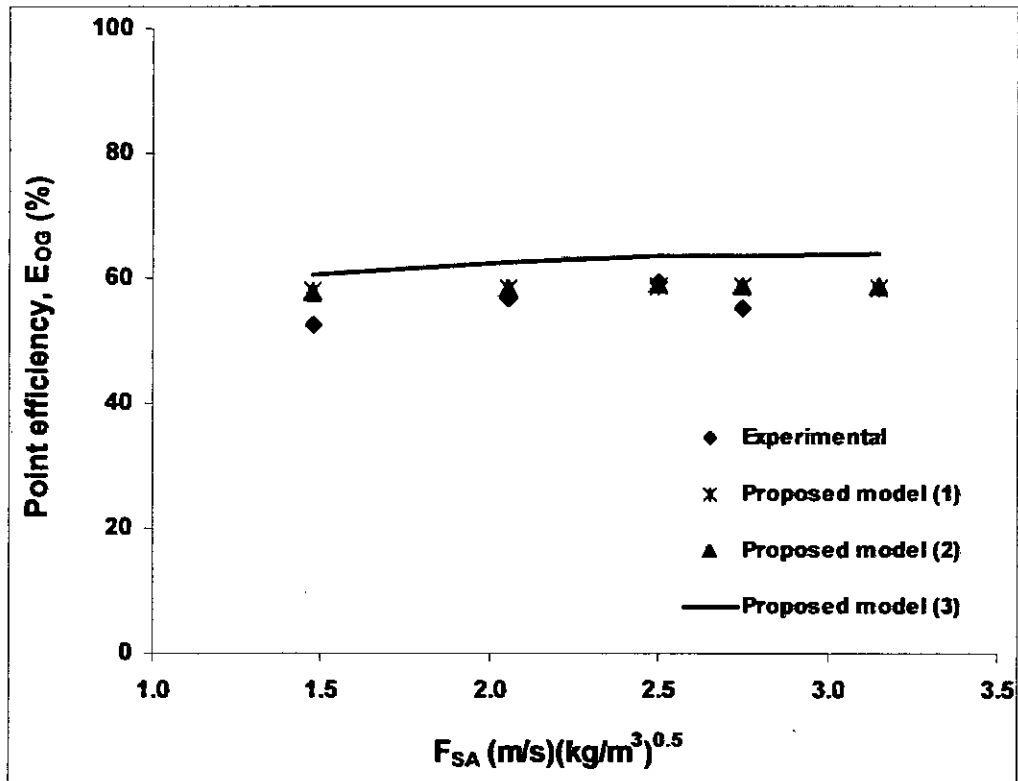
System	cyclohexane/n-heptane
Operating Pressure	27.6 kPa
Hole diameter (mm)	12.7
Hole area (%)	8.3
Weir height (mm)	50.8
Column diameter (m)	1.22
Source	Sakata and Yanagi, 1979

Figure 5.9 Comparison of predicted and experimental point efficiencies for the cyclohexane/n-heptane system at 27.6 kPa operating pressure.



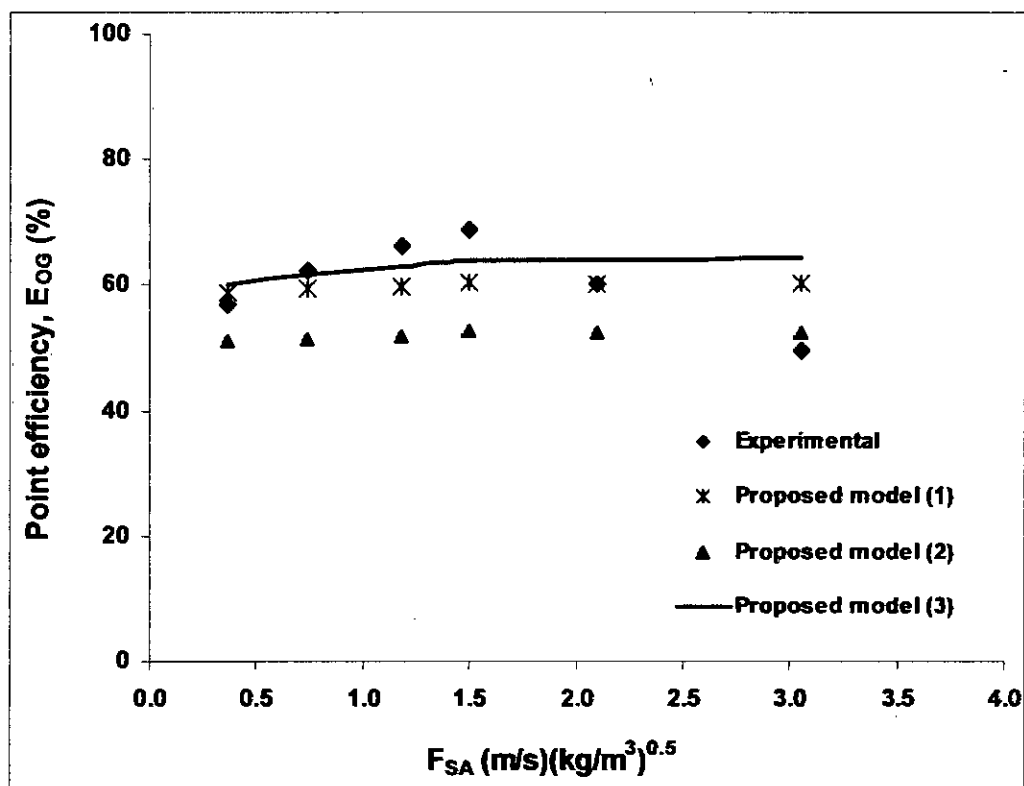
System	cyclohexane/n-heptane
Operating Pressure	165 kPa
Hole diameter (mm)	12.7
Hole area (%)	8.3
Weir height (mm)	50.8
Column diameter (m)	1.22
Source	Sakata and Yanagi, 1979

Figure 5.10 Comparison of predicted and experimental point efficiencies for the cyclohexane/n-heptane system at 165 kPa operating pressure.



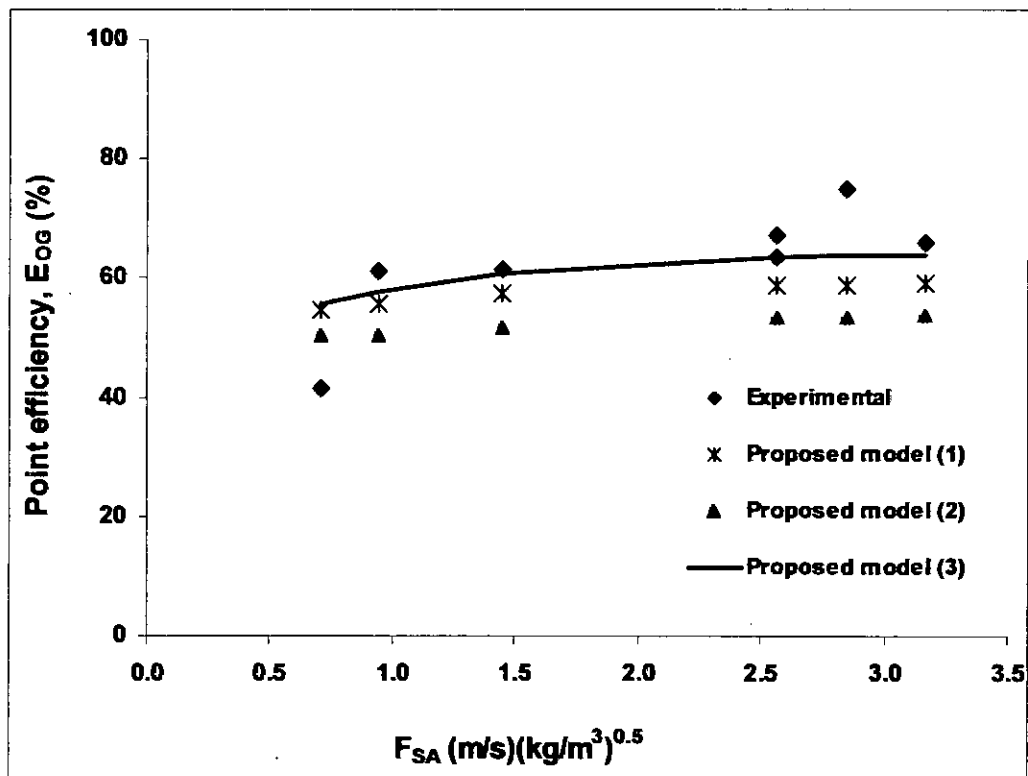
System	cyclohexane/n-heptane
Operating Pressure	34 kPa
Hole diameter (mm)	12.7
Hole area (%)	14
Weir height (mm)	50.8
Column diameter (m)	1.22
Source	Yanagi and Sakata, 1982

Figure 5.11 Comparison of predicted and experimental point efficiencies for the cyclohexane/n-heptane system at 34 kPa operating pressure



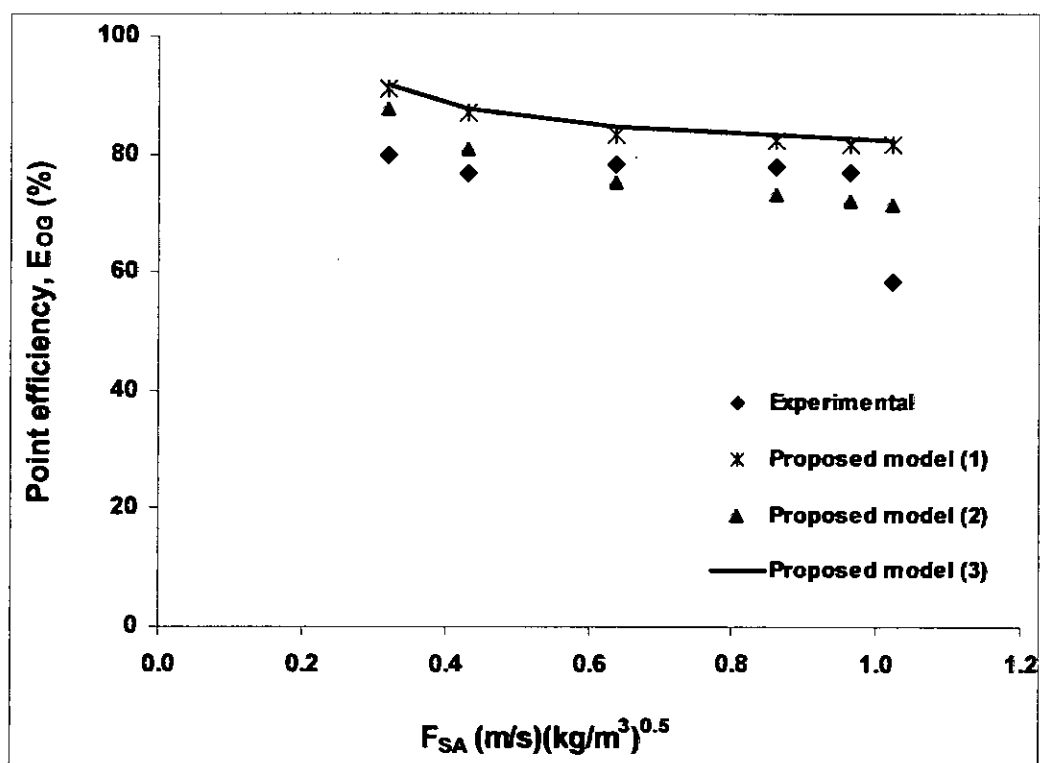
System	cyclohexane/n-heptane
Operating Pressure	165 kPa
Hole diameter (mm)	12.7
Hole area (%)	14
Weir height (mm)	50.8
Column diameter (m)	1.22
Source	Yanagi and Sakata, 1982

Figure 5.12 Comparison of predicted and experimental point efficiencies for the cyclohexane/n-heptane system at 165 kPa operating pressure



System	cyclohexane/n-heptane
Operating Pressure	101.4 kPa
Hole diameter (mm)	12.7
Hole area (%)	14
Weir height (mm)	50.8
Column diameter (m)	0.50
Source	Nutter and Perry, 1995

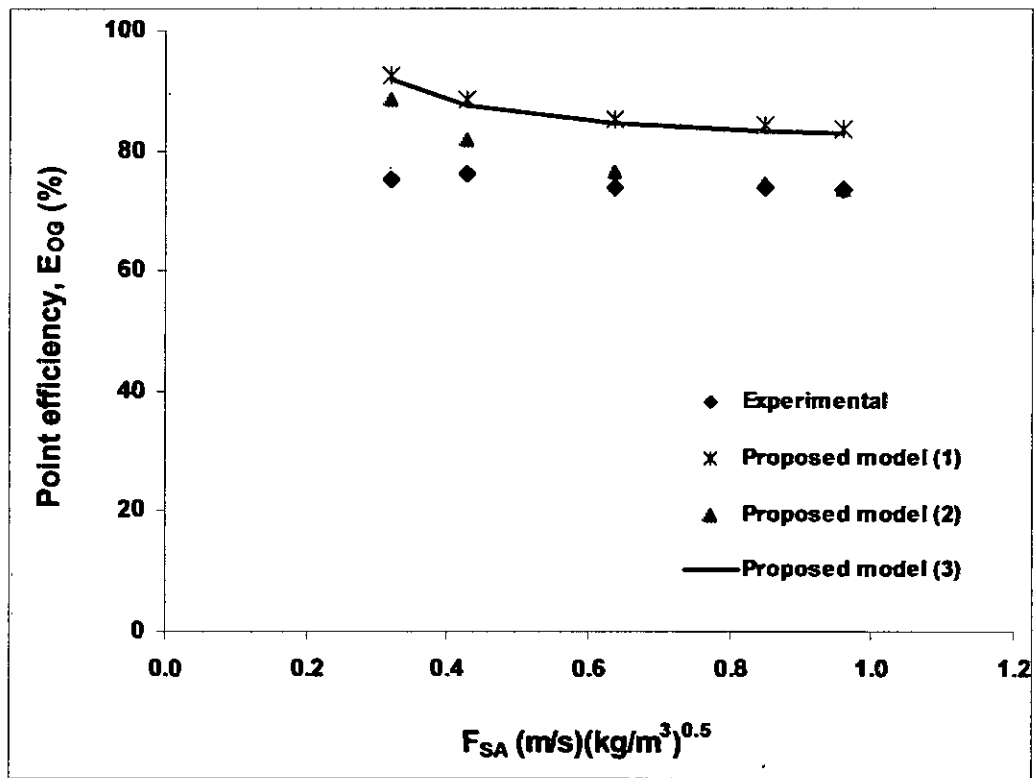
Figure 5.13 Comparison of predicted and experimental point efficiencies for the cyclohexane/n-heptane system at 101.4 kPa operating pressure



104312

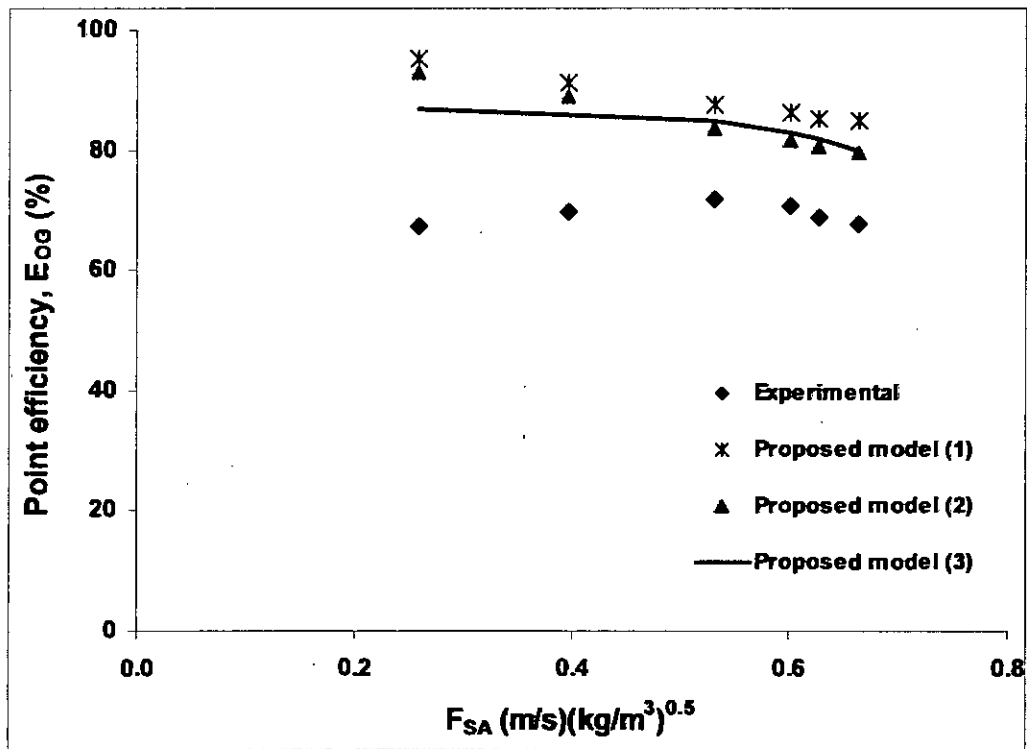
System	iso-butane/n-butane (95% mole iso-butane mixture)
Operating Pressure	2068 kPa
Hole diameter (mm)	12.7
Hole area (%)	8.3
Weir height (mm)	50.8
Column diameter (m)	1.22
Source	Sakata and Yanagi, 1979

Figure 5.14.1 Comparison of predicted and experimental point efficiencies for the iso-butane/n-butane system at 2068 kPa operating pressure and 95% mole of iso-butane mixture.



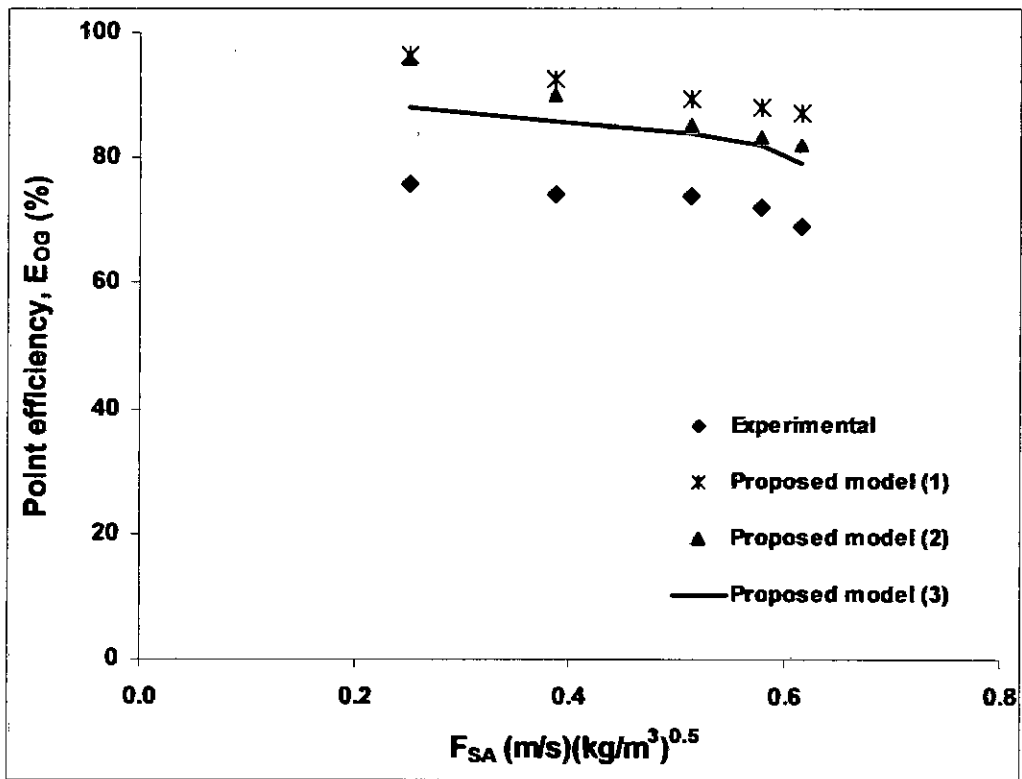
System	iso-butane/n-butane (50 % mole iso-butane mixture)
Operating Pressure	2068 kPa
Hole diameter (mm)	12.7
Hole area (%)	8.3
Weir height (mm)	50.8
Column diameter (m)	1.22
Source	Sakata and Yanagi, 1979

Figure 5.14.2 Comparison of predicted and experimental point efficiencies for the iso-butane/n-butane system at 2068 kPa operating pressure and 50% mole of iso-butane mixture.



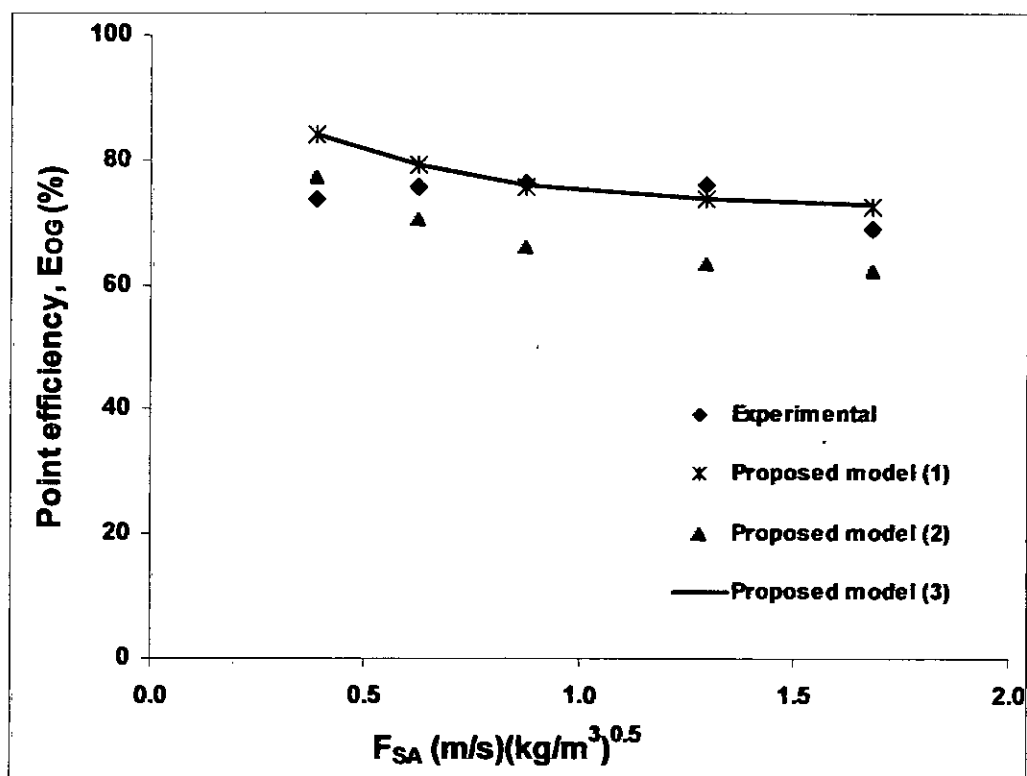
System	iso-butane/n-butane (95% mole iso-butane mixture)
Operating Pressure	2758 kPa
Hole diameter (mm)	12.7
Hole area (%)	8.3
Weir height (mm)	50.8
Column diameter (m)	1.22
Source	Sakata and Yanagi, 1979

Figure 5.15.1 Comparison of predicted and experimental point efficiencies for the iso-butane/n-butane system at 2758 kPa operating pressure and 95% mole of iso-butane mixture.



System	iso-butane/n-butane (50% mole iso-butane mixture)
Operating Pressure	2758 kPa
Hole diameter (mm)	12.7
Hole area (%)	8.3
Weir height (mm)	50.8
Column diameter (m)	1.22
Source	Sakata and Yanagi, 1979

Figure 5.15.2 Comparison of predicted and experimental point efficiencies for the iso-butane/n-butane system at 2758 kPa operating pressure and 50% mole of iso-butane mixture



System	iso-butane/n-butane
Operating Pressure	1138 kPa
Hole diameter (mm)	12.7
Hole area (%)	14
Weir height (mm)	50.8
Column diameter (m)	1.22
Source	Yanagi and Sakata, 1982

Figure 5.16 Comparison of predicted and experimental point efficiencies for the iso-butane/n-butane system at 1138 kPa operating pressure

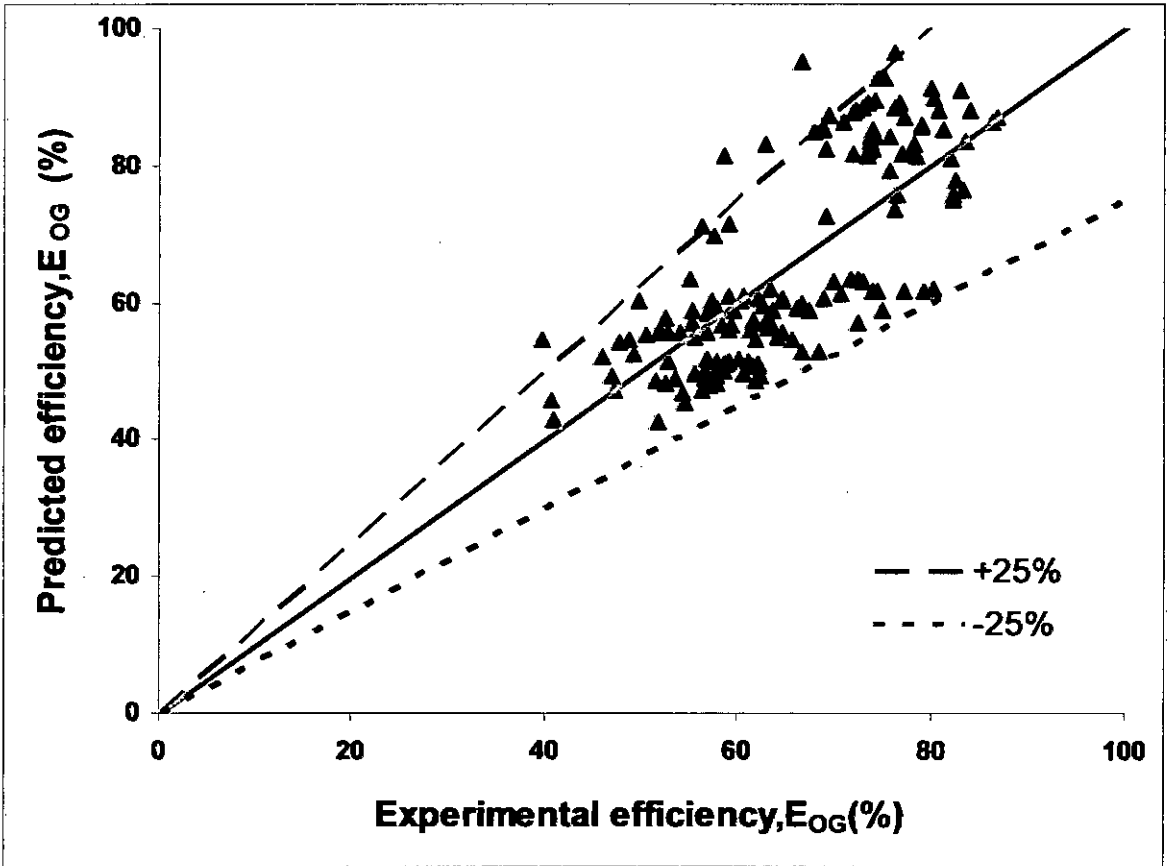


Figure 5.17 Parity plot for the experimental and calculated point efficiency with Proposed Model-1

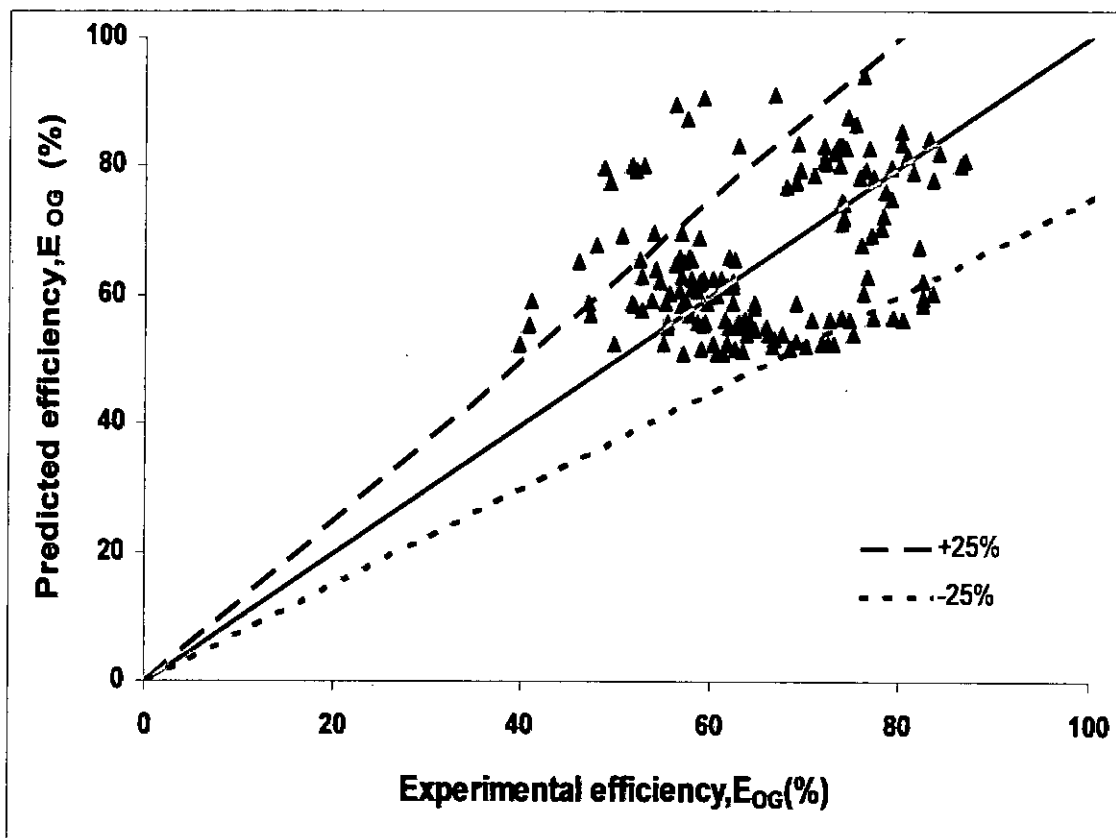


Figure 5.18 Parity plot for the experimental and calculated point efficiency with Proposed Model-2

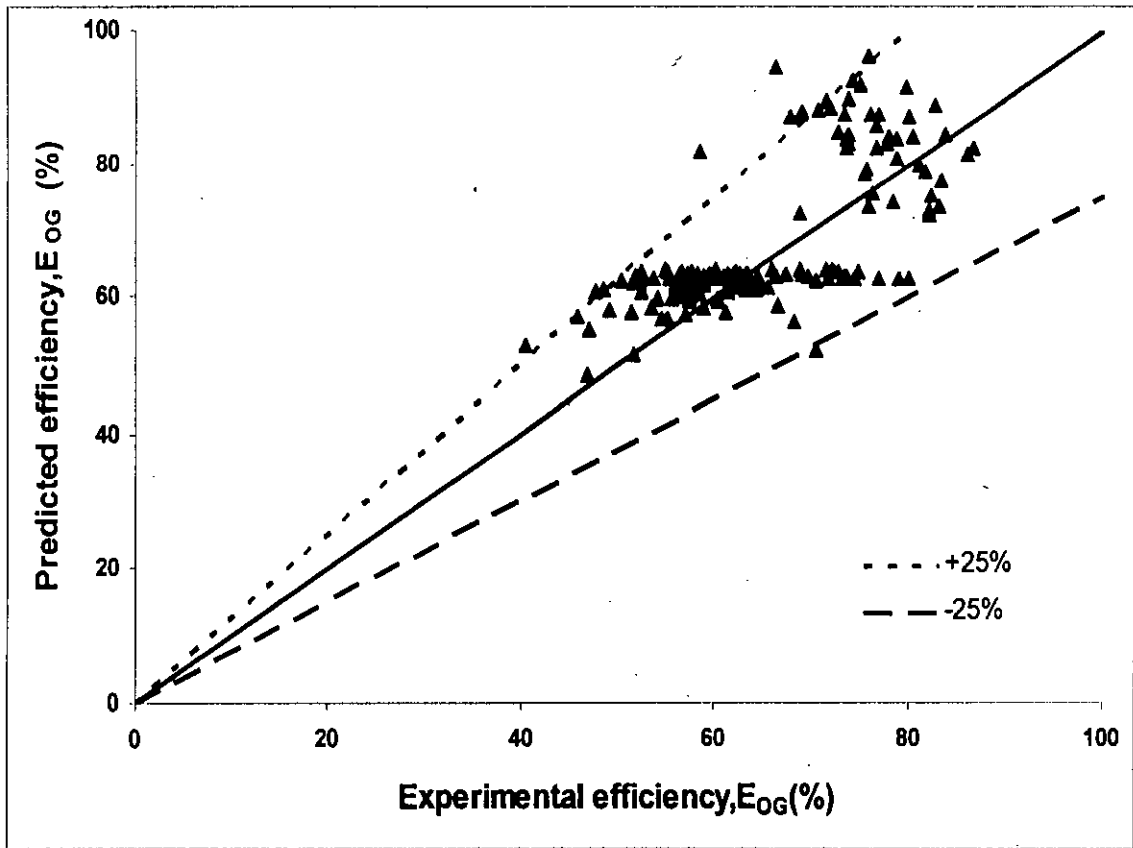


Figure 5.19 Parity plot for the experimental and calculated point efficiency with Proposed Model-3

Literature shows that the latest trend of tray efficiency modeling (Bennett et al., 1997; Garcia and Fair, 2000; Syeda et al., 2007) is to consider the hydrodynamics as the controlling factor in determining efficiencies. Consideration of tray hydrodynamics incorporated with mass transfer theory, however, has made the efficiency calculation ever more complicated. The unique feature of the proposed model is that it correlates tray hydrodynamics with efficiency at the same time it avoids complicated calculation steps.

The simple form of the proposed models is only comparable with the early empirical models (O'Connell, 1946; MacFarland et al., 1972) where only one or two-step calculations were required. The empirical models, however, are generally applicable for estimating E_{mv} and for the data base used the prediction was found to be within $\pm 40-50\%$ error band.

The semi-empirical models without hydrodynamic considerations, on the other hand, give more insight of the mass transfer process; predict both point efficiency E_{OG} and tray efficiency E_{MV} . The parameters used in these models are often arbitrary. Like empirical models the semi-empirical models use adjustable constants to fit the experimental data. These models are reported to predict somewhat better ($\pm 30\%$) than the empirical models.

The semi-empirical models based on hydrodynamics are reported to perform even better ($\pm 25\%$) at the expense of complicated calculations and several adjustable constants. Generally at least five steps are required to estimate the efficiency of large bubbles, E_{LB} by these models. Furthermore, no definitive information is available for determining the efficiency of jets, E_J . Decades ago Raper et al. (1982) failed to find an appropriate expression for E_J . Garcia and Fair (2000) ignored the contribution of spray. Syeda et al (2007) in their recent study treated jetting zone as spray regime and used Zuideweg's (1983) four steps spray regime model to estimate E_J .

In order to overcome the constraints the initial form of the proposed model adopts the three dimensionless groups of MacFarland et al. (1972) empirical model to express E_{LB} and E_J .

The final simple form of the present model contains two adjustable parameters that have important implications. The first constant 0.4 gives the average efficiency or saturation of large bubbles, E_{LB} , the second constant 0.7 gives the average efficiency of jets E_J . For small bubbles the efficiency or saturation is assumed to be 1. The present model does not use diffusivities which are often a nightmare to obtain with reasonable accuracy. The effect of vapor load on efficiency is realized by fraction of jetting F_J and fraction of small bubbles F_{SB} . The physical properties are included in the term k in F_{SB} , which makes the model applicable for systems with a range of physical properties at a range of pressure levels. The effect of column diameter is neglected since the data of only columns with large diameters are used.

The weir height of tray does not affect the efficiency of jets or spray, which justifies a constant value of E_J independent of weir height. However, the saturation of bubbles is affected by tray liquid height, i.e. the weir height, which is incorporated in the term Δt of F_{SB} .

The model is applicable to both froth and spray regime. It does not require prior knowledge of the flow regimes or the incipience of spray regime, which could create a degree of uncertainty since transition of flow regime is not a distinct phenomenon and theories related to transition are still very vague. The proposed model overcomes the problem by introducing the term fraction of jetting, F_J . In froth regime the model considers F_J to be within zero to one i.e. $0 < F_J < 1$. As F_J increases with a higher gas load, transition to spray regime occurs gradually and F_J becomes unity as spray regime is reached. No drastic change in dispersion structure occurs during this transition. This approach is justified by the smooth transition of experimental efficiency data from froth to spray regime. This approach is inherited from Syeda et al (2007) model and is somewhat different from the two previous approaches of earlier models where either same efficiency model is used for both froth and spray regimes without taking into account change of dispersion structure (AIChE, 1958; Chan and Fair, 1984; Chen and Chuang, 1993) or two completely different models are used for froth and spray regime (Zuideweg, 1983). Since the dispersion structure in froth regime is just inverse to that of spray regime, using the same efficiency model for both regimes without considering the change in the dispersion structure is the incorrect way to estimate the tray efficiency. On the other hand, when two separate models are used for the two regimes difficulties

arise in identifying the exact transition point. By including the fraction of jetting, the new model takes into account the difference in dispersion structure that exists between froth and sprays regimes and provides a logical solution to the dilemma of whether to use the same or separate models for both froth and spray regimes.

The final form of the model is kept very simple and user friendly. However, the model is empirical in nature and does not adopt any basic mass transfer theory. Therefore the detail of the mass transfer process, for example values of N_G , N_L , liquid and gas phase resistance etc can not be obtained from the model. Such information is readily available from existing semi-empirical models, although some of them are not user friendly and some of them give higher error.

While the model has been confirmed for binary systems in columns of diameter up to 1.2 meters, the extension to multicomponent systems and larger columns should not be difficult or unsafe, so long as proper fundamental considerations are taken into account. This would involve, among other things the use of diffusion coefficients corrected for composition, and straightforward averages for other physical properties.

CHAPTER 6

CONCLUSION

Based on the hydrodynamics of an operating sieve tray a user-friendly model to predict point efficiency has been developed by considering froth as a mixture of bubbles and continuous gas jets with liquid drops and splashes. The contributions of both bubbles and jets are included to the total point efficiency. The proposed models predict point efficiency for twenty sets of data (153 points) with an approximate accuracy $\pm 25\%$. The model is equally applicable for froth and spray regimes. Finally, the model have been validated for binary systems in columns of diameter up to 1.2 meters.

CHAPTER 7

SUGGESTIONS FOR FUTURE WORK

Although the proposed model successfully predicted a wide range of data within + 25%, the data points in parity plots (Figures 17, 18 and 19) is distributed arbitrarily within the error band. Thus this model only gives an approximate prediction.

Analysis of the model based on narrow range of physical properties is recommended for developing more accurate for future studies.

The model is largely dependent on the considered froth structure as well as on the accuracy of fraction of small bubble, F_{SB} and fraction of jetting F_J . The fraction of jetting F_J is calculated from a data fit equation based on air water system. Fraction of small bubbles, F_{SB} , is calculated from turbulent break-up theory since no measured data is available. In both cases, future studies to achieve more accurate estimation are recommended.

The models applicability for multicomponent systems and larger column needs to be investigated.

REFERENCES

1. AIChE Bubble Tray Design Manual; New York, 1958.
2. Ashley, M. J., and G. G. Haselden, "*Effectiveness of Vapor-Liquid Contacting on a Sieve Plate*", Trans. Inst. Chem. Engg. 50, 119-124, (1972).
3. Bennett, D.L., Agrawal, R. and Cook, P.J., "New Pressure Drop Correlation for Sieve Tray Distillation Columns", AIChE J., 29 (3), 434-442 (1983).
4. Bennett, D.L., Grimm, H.J., "Eddy Diffusivity for Distillation Sieve Trays," AIChE J., 37 (4), 589-596 (1991).
5. Bhavaraju, S.M., Russell, T.W.F., and Blanch, H.W., "The Design of Gas Sparged Devices for Viscous Liquid Systems," AIChE J., 24 (3), 454-466 (1978).
6. Billet, R., Conrad, S. and Grubb, C. M., "*Some Aspects of the Choice of Distillation Equipment*", Inst. Chem. Eng. Symp. Ser., 32, 5:111, (1969).
7. Calderbank, P.H., "Physical Rate Process in Industrial Fermentation, Part I. The International Area in Gas-Liquid Contacting with Mechanical Agitation," Trans IChemE, 36, 443-463 (1958).
8. Calderbank, P.H., and Moo-Young, M.B. "The Mass Transfer Efficiency of Distillation and Gas-Absorption Plate Columns, Part II: Liquid-Phase Mass Transfer Coefficients in Sieve-Plate Columns", Internatioanal Symposium on Distillation. Instn. Chem. Engrs., 51-72 (1960).
9. Chan, H. and J. R. Fair, "*Prediction of Point Efficiencies on Sieve Trays*", Ind. Eng. Chem. Process Des. Dev. 23, 814-819, (1984).
10. Chen, G. X. and K. T. Chuang, "*Prediction of Point Efficiency for Sieve Tray in Distillation*", Ind. Eng. Chem.Res. 32 (4), 701-708, (1993).
11. Colwell, J.C., "Clear Liquid Height and Froth Density on Sieve Trays," Ind. Eng. Chem. Proc. Des. Dev. 20 (2), 298-307 (1981).
12. Darton, R.C., "Distillation and Absorption Technology: Current Market and New Developments," Trans. IChemE, 70, Part A, 435 (1992).
13. Davidson, J.F., and Schuler, B.O.G., "Bubble Formation at an Orifice in a Viscous Liquid," Trans. IChemE, 38, 144-154 (1960a).
14. Davidson, J.F., and Schuler, B.O.G., "Bubble Formation at an Orifice in an Inviscid Liquid," Trans. IChemE, 38, 335-342 (1960b).

15. Drickamer, H.G., and Bradford, J.R., "Overall Plate Efficiency of Commercial Hydrocarbon Fractionating Column as a Function of Viscosity", *Trans AIChE*, **39**, 319 (1943).
16. Fair, J.R., "The Last Frontier in Distillation Technology," Paper presented at Separations Conference, Amsterdam, Netherlands (May 1991).
17. Fair, J.R., Null, H.R., and Bolles, W.L., "Scale-up of Plate Efficiency from Laboratory Oldershaw Data", *Ind. Eng. Proc. Design Devel.*, **22** (1) 53-58 (1983).
18. Fane, A.G., J.K. Lindsey and H. Sawstowski, "Operation of a Sieve Plate in the Spray Regime of Column Operation," *Indian Chem. Engr. (Jan.)* **45**, (1977).
19. Fractionation Research, Inc. Research Progress Reports for June and July 1966. Obtainable from Oklahoma State University Archives, Stillwater, OK.
20. Gracia, J. Antonio and James, R. Fair, "*A Fundamental Model for the Prediction of Distillation Sieve Tray Efficiency. 1. Database Development*", *Ind. Eng. Chem. Res.*, **39**, 1809-1817, (2000).
21. Gracia, J. Antonio and James, R. Fair, "*A Fundamental Model for the Prediction of Distillation Sieve Tray Efficiency. 2. Model Development and Validatio*", *Ind. Eng. Chem. Res.*, **39**, 1818-1825, (2000).
22. Hesketh, R.P., Etchells, A.W. and Russell, T.W.F., "Bubble Breakage in Pipeline Flow," *Chem. Eng. Sci.*, **46** (1) 1-9, (1991).
23. Higbie, R., "The Rate of Absorption of a Pure Gas into a Still Liquid during Short Periods of Exposure", *Trans. AIChE*, **31**, 365 (1953).
24. Hofer, H., "*Influence of Gas-Phase Dispersion on Plate Column Efficiency*", *Ger. Chem. Eng.* **6**, 113-118, (1983).
25. Hofhuis, P.A.M., and Zuiderweg, F.J., "Sieve Plates: Dispersion Density and Flow Regimes", *ICChemE Symp. Ser.*, **56**, 2.2/1-2.2/26 (1979).
26. Idogawa, K., Ikeda, K., Fukuda, T., and Morooka, S., "Effects of Gas and Liquid Properties on the Behavior of Bubbles in a Column Under High Pressure," *Intern Chem Eng.*, **27**, 93 (1987).
27. Jiang, P., Lin, T-J., Luo, X., and L-S Fan., "Flow Visualization of High Pressure (21 MPa) Bubble Column: Bubble Characteristics," *Trans. IChemE*, **73**, Part A, 269 (April 1995).
28. Jones, J. B. and Pyle C., "*Sieve and Bubble-Cap Plates*", *Chem. Eng. Prog.*, **51**, 424, (1955).
29. Kaltenbacher, E., "*On the Effect of The Bubble Size Distribution and the Gas-Phase Diffusion on the Selectivity of Sieve Trays*", *Chem. Eng. Fund.*, **1**(1), 47-68, (1982).

30. Kastanek, F. and Standart, G., "*Studies on Distillation. XX. Efficiency of Selected Types of Large Distillation Trays at Total Reflux*", Sep. Sci., 2, 439, (1967).
31. Kawase, Y. and Moo-Young, M., "Mathematical Models for Design of Bioreactors: Applications of Kolmogoroff's Theory of Isotropic Turbulence." The Chem. Eng., 43, B19-B36, (1990).
32. Kister, H.Z., "Distillation Design," New York, McGraw-Hill Inc. (1992).
33. Kister, H.Z., "Distillation Operation," New York, McGraw-Hill Inc. (1990).
34. Klug, P. and A. Vogelpohl, "*Bubble Formation with Superimposed Liquid Motion at Single-hole Plates and Sieve Plates*", Ger. Chem. Eng. 6, 311-317, (1983).
35. Korchinsky, W. J., Ehsani, M. R. and Plaka, T., "*Sieve Plate Point Efficiencies: 0.6 m Diameter Column*", Inst. Chem. Eng., 72A, 465, (1994).
36. Kumar, R. and Kuloor, N.R., "Studies in Bubble Formation-II. Bubble Formation Under Constant Pressure Conditions," Chem. Eng. Sci., 24, 749-761 (1969).
37. Kupferberg, A. and Jameson, G.J., "Bubble Formation at a Submerged Orifice Above a Gas Chamber of Finite Volume," Trans. IChemE., 47, T241-250 (1969).
38. Lamb, H., "Hydrodynamics," 6th Edn. Cambridge University Press, Cambridge, (1932).
39. Lewis, W.K. Jr., "Rectification of Binary Mixtures," Ind. Eng. Chem. 28 (1), 399 (1936).
40. Lockett, M.J., "Distillation Tray Fundamentals", Cambridge, England, Cambridge University Press (1986).
41. Lockett, M. J., R. D. Kirkpatrick and M. S. Uddin, "*Froth Regime Point Efficiency for Gas-Film Controlled Mass Transfer on a Two Dimensional Sieve Tray*", Trans IChemE, 57, 25-34, (1979).
42. Lockett, M.J. and Plaka, T., "Effect of Non-Uniform Bubbles in the Froth on the Correlation and Prediction of Point Efficiencies", Chem. Eng. Res. Des., 61, 119-124 (1983).
43. Loon, R.E., Pinczewski, W.P., and Fell, C.J.D., "Dependence of the Froth-to-Spray Transition on Sieve Tray Design Parameters," Trans. IChemE, 51, 374-376 (1973).
44. Marshall, S.H., "Air Bubble Formation from an Orifice with Liquid Cross-flow," Ph.D. Dissertation, University of Sydney, Australia (1990).
45. MacFarland, S.A., Sigmund, P.M., and Van Winkle, M., "Predict Distillation Efficiency," Hydrocarbon Proc., 7, 111 (July 1972).
46. Nutter, D. E., "*Ammonia Stripping Efficiency Studies*", AIChE Symp. Ser., 124, 68, (1972).

47. Nutter, D. E. and Perry, D., "*Sieve Upgrade 2.0 – The MVG Tray*", Presented at the Spring 1995 AIChE Meeting, Houston, TX, (1995).
48. O'Connell, H.E., "Plate Efficiency of Fractionating Columns and Absorbers," *Trans. AIChE*, **42**, 741 (1946).
49. Porter, K.E., B. T. Davis and P. F. Y. Wong, "*Mass Transfer and Bubble Sizes in Cellular Foams and Froths*", *Trans. Inst. Chem. Eng.* **45**, T265-T273, (1967).
50. Prado, M., Johnson, K.L. and Fair, J.R., "Bubble-to-Spray Transition on Sieve Trays", *Chem. Eng. Prog.*, **83** (3), 32-40 (1987).
51. Prado, Miguel and James R. Fair, "*Fundamental Model for the Prediction of Sieve Tray Efficiency*", *Ind. Eng. Chem. Res.*, **29**, 1031-1042, (1990).
52. Raper, J.A., "Hydrodynamic Mechanisms on Industrial Sieve Trays," Ph.D. Dissertation, University of New South Wales, Australia (1979).
53. Rush, F. E. and Stirba C., "*Measured Plate Efficiencies and Values Predicted from Single-Phase Studies*", *AIChE J.*, **3**, 336, (1957).
54. Sakata, M. and Yanagi, T., "*Performance of a Commercial Sclue Sieve Tray*", *Inst. Chem. Eng. Symp. Ser.*, **56**, 3.2/21, (1979).
55. Stichlmair, J. *Die Grundlagen des Ga-Flussig-Kontaktapparates Bodenkolonne*; Verlag Chemie: Weinheim, (1978).
56. Syeda, S.R., Afacan, A., and Chuang, K.T., "Effect of Surface Tension Gradient on Froth Stabilization and Tray Efficiency," *Chem. Engr, Res.*, **82** (A6): 762-769, (2004).
57. Syeda, S.R., Afacan, A., and Chuang, K.T., "A Fundamental Model for Prediction of Sieve Tray Efficiency," *Chem. Engr, Res.*, (2007).
58. Tsuge, H., and Hibino, S., "Bubble Formation From an Orifice Submerged in Liquids," *Chem. Eng. Commun.*, **22**, 63-79 (1983).
59. Tsuge, H., Tanaka, Y., and Hibino, S., "Effect of the Physical Properties of Gas on the volume of Bubble Formed from a Submerged Orifice," *Can. J. Chem. Eng.*, **59**, 569-572 (1981a).
60. Tsuge, H., Hibino, S., and Nojima, Y., "Volume of a Bubble Formed at a Single Submerged Orifice in a Flowing Liquid." *Int. Chem. Engr.* **21** (4), 330-363 (1981b).
61. Tsuge, H., Nojima, Y. and Terasaka, K. "Behavior of Bubbles Formed from a Submerged Orifice under High System Pressure," *Chem. Eng. Sci.*, **47** (13/14), 3273-3280 (1992).
62. Valentas, K.J. and Amundson, N.R., "Breakage and Coalescence in Dispersed Phase Systems," *Ind. Engng. Chem. Fundam* **5**, 533-544, (1966).

63. Valentas, K.J. and Amundson, N.R., "Analysis of Breakage in Dispersed Phase Systems," *Ind. Engng. Chem. Fundam* **5**, (2) 271-279, (1966).
64. Wilkinson, P.M., and Dierendonck, L.L.V., "Pressure and Gas Density Effects on Bubble Break-up and Gas Hold-up in Bubble Columns," *Chem. Eng. Sci.*, **45** (8) 2309-2315 (1990).
65. Wraith, A.E., "Two Stage Growth at a Submerged Plate Orifice," *Chem. Eng. Sci.*, **26**, 1659-1671 (1971).
66. Yanagi, T. and Sakata, M., "*Performance of a Commercial Scale 14% Hole Area Sieve Tray*", *Ind. Eng. Chem. Process Des. Dev.*, **21**, 721, (1982).
67. Zuiderweg, F. J., "*Sieve Trays: A View on the State of the Art*", *Chem. Eng. Sci.*, **37**(10), 1441-1464, (1982).

APPENDIX A

NOMENCLATURE

A_A	active (bubbling) area on the tray, m^2
AA	Active area, m^2
A_H	hole area on the tray, m^2
A_f	fractional open area on tray
A_H/A_T	fractional open area on tray
A_N	net area on tray, m^2
a_i	Interfacial surface area, m^2
d_B	equivalent bubble diameter, m
$d_{B,MAX}$	maximum stable bubble size-diameter, m
C	constant defined by Bennett et al., 1983
d_{32}	Sauter mean bubble diameter, m
D_B	bubble diameter, m
$D_{B,MAX}$	maximum bubble diameter, m
D_C	Column diameter, m
D_e	liquid-phase eddy diffusivity in the gas phase, m^2/s
D_G	diffusivity in the gas phase, m^2/s
D_H	orifice diameter, m
D_H	Hole diameter, mm
D_L	diffusivity in the liquid phase, m^2/s
D_V	diffusivity in the vapor phase, m^2/s
E_{MV}	Murphree tray efficiency in vapor terms
E_{OC}	Overall column efficiency, fractional
E_{OG}	Point efficiency in gas terms, fractional
F_J	Overall tray efficiency for jetting zone.
F_J	Fraction of jetting.
F_{lv}	Flow parameter = $(L_f/G_f)(\rho_g/\rho_l)^{0.5}$, dimensionless
F_{SB}	Fraction of active holes that are issuing small bubbles

F_{SA}	Superficial F-factor based on active area, $(U_{APG}^{1/2})$, $(m/s)(kg/m^3)^{1/2}$
g	Gravitational constant, $9.8 m/s^2$
G_f or G	Vapor mass flow rate, kg/h
G_m	gas molar flow rate, $mole/s$
HA	Hole area, m^2
$H_{2\phi}$	two-phase layer height on tray (sum of liquid continuous region + vapor continuous region), m
h_f	Froth height, m
h_{fc}	effective froth height, m
h_l	clear liquid height, m
h_w	Weir height, mm
k_G	Gas-phase mass transfer coefficient, m/s
k_L	Liquid-phase mass transfer coefficient, m/s
K_{OG}	Overall gas-phase mass transfer coefficient, $mole/(s m^2 Pa)$
K_{OL}	Overall liquid-phase mass transfer coefficient, $mole/(s m^2 Pa)$
K_S	Density corrected superficial vapor velocity over active tray
L_m	liquid molar flow rate, $mole/s$
L_F	liquid path length on tray, m
L_f or L	Liquid mass flow rate, kg/h
L_T	Liquid path length on tray, mm
L_w	Weir length, mm
m	Slope of equilibrium curve, dy/dx
N_G	Number of gas-phase mass transfer units
N_L	Number of liquid-phase mass transfer units
N_{OL}	Number of overall liquid-phase mass transfer units
N_{OG}	Number of overall vapor-phase mass transfer units
N_r	Number of actual trays
N_t	Number of theoretical trays
N_v	Number of vapor-phase mass transfer units
p	hole distance (triangular pitch), m
Pe_G	Peclet number, D_{BuB}/D_G , dimensionless
Pe_L	Peclet number, D_{BuB}/D_l , dimensionless
Q_G or Q_v	Gas flow rate per orifice, m^3/s
Q_l	Liquid flow rate, m^3/s

Q_{LA}	Liquid flow rate per active area, $m^3 m^{-2} s^{-1} = m/s$
Q_L	flow rate of liquid per unit weir length (liquid loading), $m^3/m \text{ weir-s}$
Q_{LW}	flow rate of liquid per unit weir length (liquid loading), $m^3/m \text{ weir-s}$
Sc_G	Gas-phase Schmidt number, v_G/D_G dimensionless
Sc_{BG}	Effective gas-phase Schmidt number, $v_G/k D_G$ dimensionless
Sh_G	Gas-phase Sherwood number, $k_G D_B/D_G$ dimensionless
Sh_L	Liquid-phase Sherwood number, $k_G D_B/D_G$ dimensionless
TS	Tray spacing, mm
t_G	mean residence time of gas in dispersion, s
t_L	mean residence time of liquid in dispersion, s
U_{SA}	Superficial gas velocity, based on active area, $G_T/(\rho_G A_A)$, Q_V/A_A , m/s
u_B	bubble velocity, m/s
u_{LB}	Rise velocity of large bubbles, m/s
u_S	Superficial gas velocity, based on net area, m/s
We	Weber number, dimensionless
We_c	Critical Weber number, dimensionless
y	Local gas-phase concentration mole fraction, fractional
y_i	Interfacial gas-phase concentration mole fraction, fractional
y_n	Outlet gas-phase concentration mole fraction, fractional
y_{n-1}	Inlet gas-phase concentration mole fraction, fractional
y_{n-1}	Inlet gas-phase concentration mole fraction, fractional
y_n^*	Gas-phase concentration mole fraction in equilibrium with exit liquid

Greek Symbol:

ϵ	Gas volume fraction in the two-phase mixture
ϕ	Froth density, h_l/h_f
ϕ_c or α_c	effective froth density as defined by Bennett et al., 1983
η	Froth density parameter, Colwell, 1981
λ	$m(G_m/L_m)$
ν	Kinematic viscosity of the vapor, m^2/s
ρ_G	Gas or vapor density, kg/m^3

ρ_L	Liquid density, kg/m ³
ρ_L, ρ_V	Liquid and vapor densities, kg/m ³
μ_L, μ_V	Liquid and vapor viscosities, mPa s
σ	Surface tension, N/m

Subscripts:

G	Gas phase
L	Liquid-phase
MAX	Maximal
V	Vapor phase
PM-1	proposed model -1
PM-2	proposed model -2
PM-3	proposed model -3

APPENDIX B

DATA BANK FOR SIEVE TRAY EFFICIENCIES

**Table B.1.1. Sieve tray efficiencies (experimental & calculated by present models).
For acetic acid/water at atmospheric pressure. Source: Jones and Pyle, 1955.**

D_c	D_H	TS	h_w	L_w	L_T	A_A	A_N	HA/AA						
M	mm	mm	mm	mm	mm	m^2	m^2	--						
0.457	3.175	305	38.1	305	253	0.1318	0.148	8.35						
Code	ρ_L	ρ_G	μ_L	μ_G	$D_L \cdot 10^9$	$D_G \cdot 10^8$	σ	L_r	G_r	m	E_{oo} exp	E_{oo} cal	E_{oo} cal	E_{oo} cal
	kg/m^3	kg/m^3	$mPa \cdot s$	$mPa \cdot s$	m^2/s	m^2/s	mN/m	kg/hr	kg/hr	--	--	PM-1	PM-2	PM-3
AC/WA-1ATM-1	948.8	0.640	0.2890	0.0127	5.43	1.56	55.00	231.40	231.40	0.7250	69.00	50.40	49.27	52.15
AC/WA-1ATM-2	948.7	0.630	0.2890	0.0127	5.43	1.56	55.00	349.30	349.40	0.7250	68.29	52.98	51.84	56.52
AC/WA-1ATM-3	948.7	0.490	0.2890	0.0127	5.43	1.56	55.00	398.90	397.00	0.7250	66.60	52.99	53.26	58.95
AC/WA-1ATM-4	948.8	0.630	0.2890	0.0127	5.43	1.56	55.00	596.50	596.60	0.7250	64.36	55.75	54.60	61.20
AC/WA-1ATM-5	948.8	0.640	0.2890	0.0127	5.43	1.56	55.00	689.50	689.60	0.7250	62.85	56.31	55.11	62.06
AC/WA-1ATM-6	948.9	0.630	0.2890	0.0127	5.43	1.56	55.00	877.80	877.90	0.7250	59.25	56.77	55.78	63.19
AC/WA-1ATM-7	948.9	0.630	0.2890	0.0127	5.43	1.56	55.00	941.30	941.50	0.7250	58.27	56.86	55.91	63.41
AC/WA-1ATM-8	948.9	0.640	0.2890	0.0127	5.43	1.56	55.00	988.90	989.10	0.7250	62.74	57.00	55.98	63.52
AC/WA-1ATM-9	948.9	0.630	0.2890	0.0127	5.43	1.56	55.00	998.00	998.20	0.7250	61.38	56.92	56.00	63.57
AC/WA-1ATM-10	948.9	0.630	0.2890	0.0127	5.43	1.56	55.00	1016.10	1016.30	0.7250	63.29	56.93	56.03	63.61
AC/WA-1ATM-11	949.0	0.630	0.2890	0.0127	5.43	1.56	55.00	1050.20	1050.30	0.7250	72.38	56.95	56.07	63.69

**Table B.1.2. Calculations for fraction of jetting (FJ) & fraction of small bubble (FSB).
For acetic acid/water at atmospheric pressure. Source: Jones and Pyle, 1955.**

Code	U_{SA}	U_H	F_{SA}	F_J	$1-F_J$	C	α_o	Q_L	h_i	T_{GLB}	$k\Delta t$	k	$\exp(-k\Delta t)$	F_{SB}	$1-F_{SB}$
	m/s	m/s	--	--	--	--	--	m ³ /s	m	--	--	--	--	--	--
AC/WA-1ATM-1	0.762	9.128	0.610	0.395	0.605	0.5023	0.7021	0.0001	0.0404	0.0372	0.4188	11.2590	0.8578	0.0083	0.9917
AC/WA-1ATM-2	1.169	13.998	0.928	0.546	0.454	0.5023	0.5956	0.0001	0.0414	0.0211	0.3059	14.4855	0.7365	0.0057	0.9943
AC/WA-1ATM-3	1.708	20.450	1.195	0.629	0.371	0.5023	0.5207	0.0001	0.0421	0.0128	0.2164	16.8639	0.8054	0.0039	0.9961
AC/WA-1ATM-4	1.996	23.902	1.584	0.705	0.295	0.5023	0.4303	0.0002	0.0440	0.0095	0.1898	19.9689	0.8273	0.0033	0.9967
AC/WA-1ATM-5	2.271	27.196	1.817	0.734	0.266	0.5023	0.3847	0.0002	0.0452	0.0077	0.1659	21.6796	0.8472	0.0029	0.9971
AC/WA-1ATM-6	2.937	35.172	2.331	0.772	0.228	0.5023	0.3017	0.0003	0.0479	0.0049	0.1238	25.1777	0.8836	0.0021	0.9979
AC/WA-1ATM-7	3.150	37.720	2.500	0.779	0.221	0.5023	0.2788	0.0003	0.0489	0.0043	0.1136	26.2568	0.8926	0.0019	0.9981
AC/WA-1ATM-8	3.257	39.008	2.606	0.783	0.217	0.5023	0.2655	0.0003	0.0496	0.0040	0.1089	26.9179	0.8968	0.0018	0.9982
AC/WA-1ATM-9	3.339	39.992	2.651	0.785	0.215	0.5023	0.2600	0.0003	0.0499	0.0039	0.1056	27.1944	0.8998	0.0018	0.9982
AC/WA-1ATM-10	3.400	40.717	2.699	0.786	0.214	0.5023	0.2543	0.0003	0.0502	0.0038	0.1032	27.4892	0.9020	0.0017	0.9983
AC/WA-1ATM-11	3.514	42.079	2.789	0.789	0.211	0.5023	0.2440	0.0003	0.0508	0.0035	0.0989	28.0377	0.9058	0.0017	0.9983

Table B.1.3. Efficiencies for large bubble & jetting by present models.
For acetic acid/water at atmospheric pressure. Source: Jones and Pyle, 1955.

Code	PM-1				PM-2				PM-3			
	E_{LB}	E_B	E_J	E_{00} calc	E_{LB}	E_B	E_J	E_{00} calc	E_{LB}	E_B	E_J	E_{00} calc
	PM-1		PM-1	PM-1	PM-2		PM-2	PM-2	PM-3		PM-3	PM-3
AC/WA-1ATM-1	41.84	42.32	62.77	50.40	41.89	42.37	59.84	49.27	40.00	40.50	70.00	52.15
AC/WA-1ATM-2	41.51	41.84	62.27	52.98	41.89	42.22	59.84	51.84	40.00	40.34	70.00	56.52
AC/WA-1ATM-3	40.25	40.48	60.38	52.99	41.89	42.11	59.84	53.26	40.00	40.23	70.00	58.95
AC/WA-1ATM-4	41.18	41.37	61.77	55.75	41.89	42.08	59.84	54.60	40.00	40.20	70.00	61.20
AC/WA-1ATM-5	41.16	41.33	61.74	56.31	41.89	42.06	59.84	55.11	40.00	40.17	70.00	62.06
AC/WA-1ATM-6	40.94	41.06	61.41	56.77	41.89	42.01	59.84	55.78	40.00	40.13	70.00	63.19
AC/WA-1ATM-7	40.90	41.01	61.34	56.86	41.89	42.00	59.84	55.91	40.00	40.12	70.00	63.41
AC/WA-1ATM-8	40.94	41.05	61.41	57.00	41.89	42.00	59.84	55.98	40.00	40.11	70.00	63.52
AC/WA-1ATM-9	40.86	40.97	61.29	56.92	41.89	41.99	59.84	56.00	40.00	40.11	70.00	63.57
AC/WA-1ATM-10	40.85	40.95	61.27	56.93	41.89	41.99	59.84	56.03	40.00	40.10	70.00	63.61
AC/WA-1ATM-11	40.83	40.93	61.24	56.95	41.89	41.99	59.84	56.07	40.00	40.10	70.00	63.69

**Table B.2.1. Sieve tray efficiencies (experimental & calculated by present models).
For isopropanol/water at 13.3 kPa operating pressure. Source: FRI, 1966a.**

Dc	D _H	TS	h _w	L _w	L _T	A _A	A _N	HA/AA							
M	mm	mm	mm	mm	mm	m ²	m ²	--							
1.213	4.763	610	25.4	762	965	1.04052	1.096	12.7							
Code	ρ _L	ρ _G	μ _L	μ _G	D _L *10 ⁹	D _G *10 ⁵	σ	L _r	G _r	m	E _{OG} exp	E _{OG} cal	E _{OG} cal	E _{OG} cal	
	kg/m ³	kg/m ³	mPa.s	mPa.s	m ² /s	m ² /s	mN/m	kg/hr	kg/hr		--	PM-1	PM-2	PM-3	
IP/WA-13.3-1	802.6	0.270	1.5290	0.0087	5.70	6.89	20.70	4174.50	4177.60	0.8900	60.45	71.58	90.22	62.87	
IP/WA-13.3-2	802.6	0.260	1.5860	0.0087	5.50	7.26	20.80	3737.00	3742.20	0.8900	58.95	71.62	90.50	62.45	
IP/WA-13.3-3	801.0	0.260	1.5840	0.0087	5.60	7.27	20.80	3347.50	3347.50	0.9059	57.00	70.96	89.55	61.84	
IP/WA-13.3-4	802.6	0.270	1.5570	0.0087	5.60	7.07	20.80	2497.40	2494.80	0.8900	57.39	69.55	87.31	59.54	
IP/WA-13.3-5	801.0	0.270	1.5540	0.0087	5.80	7.10	20.70	1673.70	1669.20	0.9221	41.16	66.03	82.86	55.66	

**Table B.2.2. Calculations for fraction of jetting (F_J) & fraction of small bubble (F_{SB}).
For isopropanol/water at 13.3 kPa operating pressure. Source: FRI, 1966a.**

Code	U _{SA}	U _H	F _{SA}	F _J	1-F _J	C	α _o	Q _L	h _r	T _{GLB}	kΔt	k	exp (-kΔt)	F _{SB}	1-F _{SB}
	m/s	m/s	--	--	--	--	--	m ³ /s	m	--	--	--	--	--	--
IP/WA-13.3-1	4.131	32.524	2.146	0.761	0.239	0.5132	0.3013	0.0014	0.0426	0.0031	0.1082	34.8324	0.8974	0.0018	0.9982
IP/WA-13.3-2	3.842	30.255	1.959	0.747	0.253	0.5132	0.3315	0.0013	0.0404	0.0035	0.1147	32.9142	0.8917	0.0019	0.9981
IP/WA-13.3-3	3.437	27.064	1.753	0.727	0.273	0.5132	0.3685	0.0012	0.0384	0.0041	0.1266	30.7789	0.8810	0.0022	0.9978
IP/WA-13.3-4	2.467	19.423	1.282	0.649	0.351	0.5132	0.4722	0.0009	0.0344	0.0066	0.1681	25.5159	0.8452	0.0029	0.9971
IP/WA-13.3-5	1.650	12.995	0.858	0.518	0.482	0.5132	0.5939	0.0006	0.0313	0.0113	0.2264	20.0838	0.7974	0.0040	0.9960

Table B.2.3. Efficiencies for large bubble & jetting by present models.
For isopropanol/water at 13.3 kPa operating pressure. Source: FRI, 1966a.

Code	PM-1				PM-2				PM-3			
	E_{LB}	E_B	E_J	E_{∞} calc	E_{LB}	E_B	E_J	E_{∞} calc	E_{LB}	E_B	E_J	E_{∞} calc
	PM-1	--	PM-1	PM-1	PM-2		PM-2	PM-2	PM-3		PM-3	PM-3
IP/WA-13.3-1	51.83	51.92	77.75	71.58	68.01	68.07	97.16	90.22	40.00	40.11	70.00	62.87
IP/WA-13.3-2	52.12	52.21	78.18	71.62	68.54	68.60	97.91	90.50	40.00	40.12	70.00	62.45
IP/WA-13.3-3	52.03	52.13	78.04	70.96	68.27	68.34	97.53	89.55	40.00	40.13	70.00	61.84
IP/WA-13.3-4	52.46	52.60	78.69	69.55	68.27	68.36	97.53	87.31	40.00	40.18	70.00	59.54
IP/WA-13.3-5	52.38	52.57	78.56	66.03	67.76	67.89	96.80	82.86	40.00	40.24	70.00	55.66

For ortho/para xylenes at 2.13 kPa operating pressure. Source: FRI, 1966a.

Dc	D _H	TS	h _w	L _w	L _T	A _A	A _N	HA/AA						
						m ²	m ²							
1.213	4.7	610	25.4	762	965	1.04052	1.096	12.7						
Code	ρ _L	ρ _G	μ _L	μ _G	D _L *10 ⁹	D _o *10 ⁵	σ	L _r	G _r	m	E _{oo} exp	E _{oo} cal	E _{oo} cal	E _{oo} cal
	kg/m ³	kg/m ³	mPa.s	mPa.s	m ² /s	m ² /s	mN/m	kg/hr	kg/hr		--	PM-1	PM-2	PM-3
O/PX-2.13-1	839.4	0.150	0.4830	0.0067	2.68	5.95	25.70	3965.70	4485.50	0.8673	62.31	49.24	65.38	63.87
O/PX-2.13-2	841.1	0.140	0.4930	0.0067	2.61	6.41	26.00	3572.10	3827.00	0.8743	57.75	49.15	65.50	63.63
O/PX-2.13-3	844.3	0.120	0.5100	0.0066	2.50	7.26	26.40	3221.40	3250.60	0.8766	56.53	48.77	65.93	63.40
O/PX-2.13-4	845.9	0.110	0.5270	0.0066	2.41	8.23	26.70	2439.90	2328.70	0.8747	52.29	48.26	65.50	62.20
O/PX-2.13-5	847.5	0.100	0.5330	0.0066	2.37	8.65	26.80	1674.60	1545.20	0.8698	54.07	46.72	63.81	59.66
O/PX-2.13-6	849.1	0.100	0.5430	0.0065	2.32	9.18	27.00	829.20	747.40	0.8817	40.83	43.11	58.75	52.31

**Table B.3.2. Calculations for fraction of jetting (FJ) & fraction of small bubble (FSB).
For ortho/para xylenes at 2.13 kPa operating pressure. Source: FRI, 1966a.**

Code	U_{SA}	U_H	F_{SA}	F_J	$1-F_J$	C	α_s	Q_L	h_r	T_{GLB}	$k\Delta t$	k	$\exp(-k\Delta t)$	F_{SB}	$1-F_{SB}$
	m/s	m/s	--	--	--	--	--	m ³ /s	m	--	--	--	--	--	--
O/PX-2.13-1	7.983	62.859	3.092	0.795	0.205	0.5132	0.1943	0.0013	0.0470	0.0011	0.0457	39.9445	0.9553	0.0007	0.9993
O/PX-2.13-2	7.298	57.461	2.731	0.787	0.213	0.5132	0.2318	0.0012	0.0433	0.0014	0.0508	36.9102	0.9505	0.0008	0.9992
O/PX-2.13-3	7.232	56.941	2.505	0.780	0.220	0.5132	0.2595	0.0011	0.0408	0.0015	0.0511	34.8503	0.9502	0.0008	0.9992
O/PX-2.13-4	5.652	44.501	1.874	0.740	0.260	0.5132	0.3551	0.0008	0.0358	0.0022	0.0656	29.1576	0.9365	0.0011	0.9989
O/PX-2.13-5	4.125	32.481	1.304	0.654	0.346	0.5132	0.4753	0.0005	0.0320	0.0037	0.0865	23.4275	0.9172	0.0014	0.9986
O/PX-2.13-6	1.995	15.711	0.631	0.407	0.593	0.5132	0.6813	0.0003	0.0286	0.0098	0.1478	15.1097	0.8626	0.0025	0.9975

**Table B.3.3. Efficiencies for large bubble & jetting by present models.
For ortho/para xylenes at 2.13 kPa operating pressure. Source: FRI, 1966a.**

Code	PM-1				PM-2				PM-3			
	E_{LB}	E_B	E_J	E_{Oo} calc	E_{LB}	E_B	E_J	E_{Oo} calc	E_{LB}	E_B	E_J	E_{Oo} calc
	PM-1	--	PM-1	PM-1	PM-2		PM-2	PM-2	PM-3		PM-3	PM-3
O/PX-2.13-1	35.23	35.27	52.84	49.24	48.78	48.80	69.65	65.38	40.00	40.04	70.00	63.87
O/PX-2.13-2	35.26	35.32	52.89	49.15	49.04	49.08	70.05	65.59	40.00	40.05	70.00	63.63
O/PX-2.13-3	35.08	35.14	52.63	48.77	49.49	49.53	70.70	66.04	40.00	40.05	70.00	63.40
O/PX-2.13-4	35.22	35.29	52.82	48.26	49.88	49.94	71.26	65.71	40.00	40.06	70.00	62.20
O/PX-2.13-5	35.17	35.27	52.76	48.72	50.08	50.14	71.52	64.13	40.00	40.09	70.00	59.66
O/PX-2.13-6	35.74	35.90	53.61	43.11	50.29	50.42	71.85	59.15	40.00	40.15	70.00	52.31

**Table B.4.1. Sieve tray efficiencies (experimental & calculated by present models).
For ortho/para xylenes at 2.13 kPa operating pressure. Source: FRI, 1966b.**

Dc	D _H	TS	h _w	L _w	L _T	A _A	A _N	HA/AA							
						m ²	m ²								
1.22	12.7	610	25.4	762	965	1.04052	1.096	13							
Code	ρ _L	ρ _G	μ _L	μ _G	D _L ·10 ⁹	D _G ·10 ⁸	σ	L _r	G _r	m	E _{MV}	E _{OG} cal	E _{OG} cal	E _{OG} cal	
	kg/m ³	kg/m ³	mPa.s	mPa.s	m ² /s	m ² /s	mN/m	kg/hr	kg/hr			PM-1	PM-2	PM-3	
O/PX-2.13-1	844.3	0.120	0.5160	0.0066	2.47	7.81	26.50	2799.60	2961.30	0.8717	54.00	48.70	65.99	63.09	
O/PX-2.13-2	845.9	0.110	0.5220	0.0066	2.43	8.00	26.60	2535.90	2621.00	0.8710	55.00	48.29	65.83	62.78	
O/PX-2.13-3	845.9	0.110	0.5270	0.0066	2.41	8.23	26.70	2055.60	2057.40	0.8747	54.00	47.80	64.93	61.46	
O/PX-2.13-4	847.5	0.100	0.5400	0.0065	2.33	9.11	26.90	1693.80	1632.50	0.8691	51.00	47.03	64.38	60.12	
O/PX-2.13-5	849.1	0.100	0.5410	0.0065	2.33	9.13	27.00	1195.60	1133.10	0.8733	52.00	45.30	61.88	56.73	
O/PX-2.13-6	849.1	0.100	0.5430	0.0065	2.32	9.185	27.00	713.50	691.30	0.8817	23.00	42.57	58.16	51.48	

**Table B.4.2. Calculations for fraction of jetting (F_J) & fraction of small bubble (F_{SB}).
For ortho/para xylenes at 2.13 kPa operating pressure. Source: FRI, 1966b.**

Code	U _{SA}	U _H	F _{SA}	F _J	1-F _J	C	α _w	Q _L	h _r	T _{GLB}	kΔt	k	Exp (-kΔt)	F _{SB}	1-F _{SB}
	m/s	m/s	--	--	--	--	--	m ³ /s	m	--	--	--	--	--	--
O/PX-2.13-1	6.588	50.877	2.282	0.769	0.231	0.5132	0.2896	0.0009	0.0385	0.0017	0.0556	32.9049	0.9459	0.0009	0.9991
O/PX-2.13-2	6.361	48.931	2.110	0.759	0.241	0.5132	0.3157	0.0008	0.0369	0.0018	0.0575	31.3485	0.9442	0.0009	0.9991
O/PX-2.13-3	4.993	38.409	1.656	0.715	0.285	0.5132	0.3966	0.0007	0.0340	0.0027	0.0731	27.0692	0.9295	0.0012	0.9988
O/PX-2.13-4	4.358	33.524	1.378	0.670	0.330	0.5132	0.4576	0.0006	0.0322	0.0034	0.0819	24.1768	0.9214	0.0014	0.9986
O/PX-2.13-5	3.025	23.289	0.957	0.556	0.444	0.5132	0.5710	0.0004	0.0301	0.0057	0.1101	19.3948	0.8958	0.0019	0.9981
O/PX-2.13-6	1.848	14.196	0.584	0.379	0.621	0.5132	0.6995	0.0002	0.0283	0.0107	0.1548	14.4187	0.8568	0.0027	0.9973

Table B.4.3. Efficiencies for large bubble & jetting by present models.
 For ortho/para xylenes at 2.13 kPa operating pressure. Source: FRI, 1966b.

Code	PM-1				PM-2				PM-3			
	E_{LB}	E_B	E_J	E_{∞} calc	E_{LB}	E_B	E_J	E_{∞} calc	E_{LB}	E_B	E_J	E_{∞} calc
	PM-1	--	PM-1	PM-1	PM-2		PM-2	PM-2	PM-3		PM-3	PM-3
O/PX-2.13-1	35.16	35.22	52.74	48.70	49.62	49.67	70.89	65.99	40.00	40.05	70.00	63.09
O/PX-2.13-2	34.99	35.06	52.49	48.29	49.80	49.84	71.14	66.00	40.00	40.06	70.00	62.78
O/PX-2.13-3	35.20	35.28	52.80	47.80	49.88	49.95	71.26	65.18	40.00	40.07	70.00	61.46
O/PX-2.13-4	35.21	35.30	52.81	47.03	50.25	50.32	71.78	64.69	40.00	40.08	70.00	60.12
O/PX-2.13-5	35.40	35.52	53.10	45.30	50.25	50.34	71.78	62.26	40.00	40.11	70.00	56.73
O/PX-2.13-6	35.70	35.87	53.55	42.57	50.29	50.43	71.85	58.55	40.00	40.16	70.00	51.48

**Table B.5.1. Sieve tray efficiencies (experimental & calculated by present models).
For n-octanol/n-decanol at 1.3 kPa operating pressure. Source: FRI, 1966b.**

Dc	D _H	TS	h _w	L _w	L _T	A _A	A _N	HA/AA							
						m ²	m ²								
1.22	12.7	610	25.4	762	965	1.041	4.09	13							
Code	ρ _L	ρ _G	μ _L	μ _G	D _L ·10 ⁹	D _G ·10 ⁶	σ	L _r	G _r	m	E _{OG} exp	E _{OG} cal	E _{OG} cal	E _{OG} cal	
	kg/m ³	kg/m ³	mPa.s	mPa.s	m ² /s	m ² /s	mN/m	kg/hr	kg/hr		--	PM-1	PM-2	PM-3	
NO/ND-1.3-1	775.4	0.090	1.1000	0.0072	1.03	1.48	18.90	2518.30	2518.30	0.2121	51.96	55.79	79.58	63.02	
NO/ND-1.3-2	773.8	0.080	1.1130	0.0071	9.95	1.47	19.00	2267.10	2268.70	0.2121	52.66	55.47	69.59	62.84	
NO/ND-1.3-3	773.8	0.080	1.1160	0.0071	9.66	1.46	19.10	2003.50	2005.60	0.2121	51.56	55.56	68.93	62.25	
NO/ND-1.3-4	775.4	0.070	1.1950	0.0071	9.30	1.45	19.20	1549.70	1551.80	0.2121	48.55	54.60	67.87	61.08	
NO/ND-1.3-5	775.4	0.060	1.2250	0.0071	9.04	1.44	19.30	1003.80	1007.30	0.2121	49.22	52.35	65.57	58.09	
NO/ND-1.3-6	777.0	0.050	1.2700	0.0070	8.68	1.43	19.40	528.40	528.30	0.2121	22.37	48.33	62.91	52.24	

**Table B.5.2. Calculations for fraction of jetting (FJ) & fraction of small bubble (FSB).
For n-octanol/n-decanol at 1.3 kPa operating pressure. Source: FRI, 1966b.**

Code	U_{SA}	U_H	F_{SA}	F_J	$1-F_J$	C	α_o	Q_L	h_f	T_{GLB}	$k\Delta t$	k	$\exp(-k\Delta t)$	F_{SB}	$1-F_{SB}$
	m/s	m/s	--	--	--	--	--	m ³ /s	m	--	--	--	--	--	--
NO/ND-1.3-1	7.466	57.434	2.240	0.767	0.233	0.5132	0.2818	0.0009	0.0385	0.0015	0.0537	36.9328	0.9477	0.0009	0.9991
NO/ND-1.3-2	7.567	58.209	2.140	0.761	0.239	0.5132	0.2963	0.0008	0.0372	0.0015	0.0523	35.8553	0.9491	0.0009	0.9991
NO/ND-1.3-3	6.690	51.459	1.892	0.741	0.259	0.5132	0.3371	0.0007	0.0354	0.0018	0.0593	33.2294	0.9424	0.0010	0.9990
NO/ND-1.3-4	5.915	45.503	1.565	0.702	0.298	0.5132	0.4009	0.0006	0.0329	0.0022	0.0660	29.5978	0.9362	0.0011	0.9989
NO/ND-1.3-5	4.480	34.460	1.097	0.602	0.398	0.5132	0.5160	0.0004	0.0301	0.0035	0.0828	23.8689	0.9205	0.0014	0.9986
NO/ND-1.3-6	2.809	21.606	0.628	0.406	0.594	0.5132	0.6718	0.0002	0.0280	0.0067	0.1141	17.0460	0.8922	0.0019	0.9981

Table B.5.3. Efficiencies for large bubble & jetting by present models.
For n-octanol/n-decanol at 1.3 kPa operating pressure. Source: FRI, 1966b.

Code	PM-1				PM-2				PM-3		
	E_B	E_J	E_{Og} calc	E_{LB}	E_B	E_J	E_{Og} calc	E_{LB}	E_B	E_J	E_{Og} calc
	--	PM-1	PM-1	PM-2		PM-2	PM-2	PM-3		PM-3	PM-3
NO/ND-1.3-1	40.37	60.47	55.79	59.89	59.92	85.55	79.58	40.00	40.05	70.00	63.02
NO/ND-1.3-2	40.22	60.26	55.47	60.33	60.37	86.19	80.02	40.00	40.05	70.00	62.84
NO/ND-1.3-3	40.59	60.79	55.56	60.72	60.76	86.74	80.02	40.00	40.06	70.00	62.25
NO/ND-1.3-4	40.46	60.60	54.60	61.22	61.26	87.45	79.65	40.00	40.07	70.00	61.08
NO/ND-1.3-5	40.30	60.32	52.35	61.59	61.64	87.99	77.50	40.00	40.08	70.00	58.09
NO/ND-1.3-6	40.24	60.18	48.33	62.13	62.21	88.76	72.98	40.00	40.12	70.00	52.24

**Table B.6.1. Sieve tray efficiencies (experimental & calculated by present models).
For n-octanol/n-decanol at 8.0 kPa operating pressure. Source: FRI, 1966b.**

Dc	D _H	TS	h _w	L _w	L _T	A _A	A _N	HA/AA								
						m ²	m ²									
1.22	12.7	610	25.4	762	965	1.041	1.09	13								
Code	ρ _L	ρ _G	μ _L	μ _G	D _L *10 ⁹	D _G *10 ⁵	σ	L _T	G _T	m	E _{MV}	E _∞ exp	E _∞ cal	E _∞ cal	E _∞ cal	
	kg/m ³	kg/m ³	mPa.s	mPa.s	m ² /s	m ² /s	mN/m	kg/hr	kg/hr			--	PM-1	PM-2	PM-3	
NO/ND-8-1	751.3	0.320	0.6500	0.0077	1.93	2.85	16.80	5170.60	5172.70	0.2744	61.00	56.61	55.63	69.77	63.34	
NO/ND-8-2	752.9	0.310	0.6600	0.0077	1.89	2.84	16.80	4548.90	4537.50	0.2744	58.00	53.83	55.48	69.77	62.92	
NO/ND-8-3	751.3	0.320	0.6500	0.0077	1.93	2.85	16.80	4183.80	4160.90	0.2744	54.00	50.41	55.23	69.12	62.46	
NO/ND-8-4	751.3	0.320	0.6600	0.0077	1.93	2.85	16.80	3157.00	3153.50	0.2744	51.00	47.83	54.31	67.83	60.75	
NO/ND-8-5	751.3	0.310	0.6600	0.0077	1.93	2.85	16.80	2099.00	2096.30	0.2744	49.00	45.76	52.13	65.25	57.29	
NO/ND-8-6	743.3	0.490	0.6500	0.0077	1.93	2.85	16.80	1097.40	1093.50	0.2744	49.00	46.93	49.30	58.63	48.40	

Table B.6.2. Calculations for fraction of jetting (FJ) & fraction of small bubble (FSB).
For n-octanol/n-decanol at 8.0 kPa operating pressure. Source: FRI, 1966b.

Code	U_{SA}	U_H	F_{SA}	F_J	$1-F_J$	C	α_g	Q_L	h_r	T_{GLB}	$k\Delta t$	k	exp (-k Δt)	F_{SB}	$1-F_{SB}$
	m/s	m/s	--	--	--	--	--	m ³ /s	m	--	--	--	--	--	--
NO/ND-8-1	4.313	33.180	2.440	0.777	0.223	0.5132	0.2493	0.0019	0.0490	0.0028	0.1150	40.6253	0.8914	0.0019	0.9981
NO/ND-8-2	3.906	30.044	2.175	0.783	0.237	0.5132	0.2866	0.0017	0.0451	0.0033	0.1254	37.9214	0.8822	0.0021	0.9979
NO/ND-8-3	3.470	26.690	1.963	0.748	0.252	0.5132	0.3200	0.0015	0.0426	0.0039	0.1402	35.6515	0.8692	0.0024	0.9976
NO/ND-8-4	2.630	20.228	1.488	0.690	0.310	0.5132	0.4125	0.0012	0.0375	0.0059	0.1775	30.1885	0.8374	0.0031	0.9969
NO/ND-8-5	1.804	13.880	1.005	0.573	0.427	0.5132	0.5382	0.0008	0.0331	0.0099	0.2354	23.8547	0.7902	0.0042	0.9958
NO/ND-8-6	0.595	4.581	0.417	0.264	0.736	0.5132	0.7561	0.0004	0.0294	0.0373	0.5246	14.0565	0.5918	0.0109	0.9891

Table B.6.3. Efficiencies for large bubble & jetting by present models.
 For n-octanol/n-decanol at 8.0 kPa operating pressure. Source: FRI, 1966b.

Code	PM-1				PM-2				PM-3			
	E_{LB}	E_B	E_J	E_{Og} calc	E_{LB}	E_B	E_J	E_{Og} calc	E_{LB}	E_B	E_J	E_{Og} calc
	PM-1	--	PM-1	PM-1	PM-2		PM-2	PM-2	PM-3		PM-3	PM-3
NO/ND-8-1	40.04	40.16	60.07	55.63	52.32	52.42	74.75	69.77	40.00	40.12	70.00	63.34
NO/ND-8-2	40.14	40.27	60.21	55.48	52.56	52.66	75.09	69.77	40.00	40.13	70.00	62.92
NO/ND-8-3	40.18	40.32	60.26	55.23	52.32	52.44	74.75	69.12	40.00	40.14	70.00	62.46
NO/ND-8-4	40.34	40.53	60.51	54.31	52.32	52.47	74.75	67.83	40.00	40.19	70.00	60.75
NO/ND-8-5	40.44	40.69	60.66	52.13	52.32	52.53	74.75	65.25	40.00	40.25	70.00	57.29
NO/ND-8-6	43.15	43.77	64.72	49.30	52.32	52.84	74.75	58.63	40.00	40.65	70.00	48.40

**Table B.7.1. Sieve tray efficiencies (experimental & calculated by present models).
For methanol/water at 101.4 kPa. Source: Kastanek and Standart, 1967.**

D_c	D_H	TS	h_w	L_w	L_T	A_A	A_N	HA/AA							
m	mm	mm	mm	mm	Mm	m^2	m^2	--							
0.976	4	400	40	612	759	0.066	1	4.8							
Code	ρ_L	ρ_G	μ_L	$\mu_G \cdot 10^2$	$D_L \cdot 10^8$	$D_G \cdot 10^8$	σ	L_r	G_r	m	E_{OG} exp	E_{OG} calc	E_{OG} calc	E_{OG} calc	
	kg/m^3	kg/m^3	mPa.s	mPa.s	m^2/s	m^2/s	mN/m	kg/hr	kg/hr	--	--	PM-1	PM-2	PM-3	
M/W-101.4-1	940	0.830	0.380	1.10	1.00	1.70	39	780.9	100.3	1.77	78.33	45.24	42.16	49.64	
M/W-101.4-2	940	0.830	0.380	1.10	1.00	1.70	39	988.6	125.4	1.77	83.33	46.42	43.19	51.80	
M/W-101.4-3	940	0.830	0.380	1.10	1.00	1.70	39	1067.8	135.4	1.77	75.55	46.84	43.57	52.57	
M/W-101.4-4	940	0.830	0.380	1.10	1.00	1.70	39	1146.8	145.5	1.77	81.11	47.25	43.93	53.31	
M/W-101.4-5	940	0.830	0.380	1.10	1.00	1.70	39	1225.9	155.5	1.77	78.88	47.63	44.27	53.99	
M/W-101.4-6	940	0.830	0.380	1.10	1.00	1.70	39	1285.3	163.0	1.77	86.11	47.89	44.51	54.48	
M/W-101.4-7	940	0.830	0.380	1.10	1.00	1.70	39	1384.1	175.5	1.77	86.66	48.31	43.66	55.24	
M/W-101.4-8	940	0.830	0.380	1.10	1.00	1.70	39	1542.3	195.6	1.77	80.55	48.92	44.29	56.34	
M/W-101.4-9	940	0.830	0.380	1.10	1.00	1.70	39	1582.1	198.1	1.77	83.88	48.99	44.37	56.47	
M/W-101.4-10	940	0.830	0.380	1.10	1.00	1.70	39	1581.8	200.6	1.77	72.77	49.06	44.44	56.60	
M/W-101.4-11	940	0.830	0.380	1.10	1.00	1.70	39	1700.5	215.7	1.77	76.66	49.46	44.89	57.31	
M/W-101.4-12	940	0.830	0.380	1.10	1.00	1.70	39	1878.5	238.2	1.77	80.00	49.98	45.51	58.26	
M/W-101.4-13	940	0.830	0.380	1.10	1.00	1.70	39	2096.0	265.8	1.77	82.77	50.51	46.19	60.25	

**Table B.7.2. Calculations for fraction of jetting (F_J) & fraction of small bubble (F_{SB}).
For methanol/water at 101.4 kPa. Source: Kastanek and Standart, 1967.**

Code	U _{SA}	U _H	F _{SA}	F _J	1-F _J	C	α _o	Q _L	h _r	T _{GLB}	kΔt	k	exp (-kΔt)	F _{SB}	1-F _{SB}
	m/s	m/s	--	--	--	--	--	m ³ /s	m	--	--	--	--	--	--
M/W-101.4-1	0.509	10.596	0.463	0.299	0.701	0.5018	0.7583	0.0002	0.0431	0.0643	0.7035	10.948	0.495	0.016	0.984
M/W-101.4-2	0.636	13.247	0.579	0.377	0.623	0.5018	0.7124	0.0003	0.0437	0.0490	0.6136	12.518	0.541	0.013	0.987
M/W-101.4-3	0.687	14.304	0.626	0.404	0.596	0.5018	0.8952	0.0003	0.0440	0.0446	0.5841	13.108	0.558	0.013	0.987
M/W-101.4-4	0.738	15.371	0.672	0.430	0.570	0.5018	0.8783	0.0003	0.0443	0.0407	0.5571	13.686	0.573	0.012	0.988
M/W-101.4-5	0.789	16.427	0.718	0.454	0.546	0.5018	0.8821	0.0004	0.0445	0.0374	0.5328	14.243	0.587	0.011	0.989
M/W-101.4-6	0.827	17.220	0.753	0.471	0.529	0.5018	0.8502	0.0004	0.0448	0.0352	0.5158	14.651	0.597	0.011	0.989
M/W-101.4-7	0.890	18.540	0.811	0.498	0.502	0.5018	0.8310	0.0004	0.0451	0.0320	0.4897	15.315	0.613	0.010	0.990
M/W-101.4-8	0.992	20.663	0.904	0.536	0.464	0.5018	0.8016	0.0005	0.0457	0.0277	0.4526	16.345	0.636	0.009	0.991
M/W-101.4-9	1.005	20.928	0.915	0.541	0.459	0.5018	0.5981	0.0005	0.0457	0.0272	0.4484	16.470	0.639	0.009	0.991
M/W-101.4-10	1.017	21.192	0.927	0.545	0.455	0.5018	0.5945	0.0005	0.0458	0.0268	0.4442	16.594	0.641	0.009	0.991
M/W-101.4-11	1.094	22.787	0.998	0.570	0.430	0.5018	0.5738	0.0005	0.0462	0.0243	0.4204	17.333	0.657	0.008	0.992
M/W-101.4-12	1.208	25.164	1.100	0.603	0.397	0.5018	0.5445	0.0006	0.0469	0.0211	0.3889	18.396	0.678	0.008	0.992
M/W-101.4-13	1.348	28.079	1.228	0.637	0.363	0.5018	0.5108	0.0006	0.0478	0.0181	0.3556	19.647	0.701	0.007	0.993

Table B.7.3. Efficiencies for large bubble & jetting by present models.
 For methanol/water at 101.4 kPa. Source: Kastanek and Standart, 1967.

Code	PM-1				PM-2				PM-3			
	E_{LB}	E_B	E_J	E_{OG} calc	E_{LB}	E_B	E_J	E_{OG} calc	E_{LB}	E_B	E_J	E_{OG} calc
	--	--										
M/W-101.4-1	38.76	39.74	58.14	45.24	36.74	37.75	52.48	42.16	40.00	40.96	70.00	49.64
M/W-101.4-2	38.63	39.45	57.95	46.42	36.74	37.58	52.48	43.19	40.00	40.80	70.00	51.80
M/W-101.4-3	38.59	39.36	57.88	46.84	36.74	37.53	52.48	43.57	40.00	40.75	70.00	52.57
M/W-101.4-4	38.54	39.27	57.82	47.25	36.74	37.48	52.48	43.93	40.00	40.71	70.00	53.31
M/W-101.4-5	38.51	39.19	57.76	47.63	36.74	37.44	52.48	44.27	40.00	40.67	70.00	53.99
M/W-101.4-6	38.48	39.14	57.72	47.89	36.74	37.41	52.48	44.51	40.00	40.64	70.00	54.48
M/W-101.4-7	38.44	39.05	57.65	48.31	36.74	37.37	52.48	44.89	40.00	40.60	70.00	55.24
M/W-101.4-8	38.37	38.93	57.56	48.92	36.74	37.31	52.48	45.45	40.00	40.54	70.00	56.34
M/W-101.4-9	38.37	38.92	57.55	48.99	36.74	37.30	52.48	45.51	40.00	40.54	70.00	56.47
M/W-101.4-10	38.36	38.91	57.54	49.06	36.74	37.30	52.48	45.57	40.00	40.53	70.00	56.60
M/W-101.4-11	38.32	38.83	57.48	49.46	36.74	37.26	52.48	45.94	40.00	40.50	70.00	57.31
M/W-101.4-12	38.28	38.73	57.39	49.98	36.74	37.21	52.48	46.42	40.00	40.45	70.00	58.26
M/W-101.4-13	38.20	38.62	57.30	50.51	36.74	37.17	52.48	46.92	41.00	41.40	71.00	60.25

Table B.8.1. Sieve tray efficiencies (experimental & calculated by present models).

For ethylbenzenc/styrcne at 13.3 kPa operating pressure. Source: Billet et al., 1969.

Dc	D _H	TS	h _w	L _w	L _T	A _A	A _N	HA/AA						
m	mm	mm	Mm	mm	mm	m ²	m ²	--						
0.788	12.5	500	19	460	640	0.439	0.463	13.6						
Code	ρ _L	ρ _G	μ _L	μ _G	D _L	D ₀	σ	L _r	G _r	m	E _{OG} exp	E _{OG} calc	E _{OG} calc	E _{OG} calc
	kg/m ³	kg/m ³	mPa.s	mPa.s	m ² /s	m ² /s	mN/m	kg/hr	kg/hr		--	PM-1	PM-2	PM-3
EB/S-13.3-1	863.00	0.480	0.376	8.00E-03	3.23E-09	2.11E-05	25.00	715.40	708.40	9.14E-01	38.85	45.52	55.35	52.66
EB/S-13.3-2	857.00	0.490	0.377	8.00E-03	3.21E-09	2.11E-05	25.00	901.10	896.70	9.14E-01	47.16	47.08	57.02	55.06
EB/S-13.3-3	855.00	0.490	0.377	8.00E-03	3.21E-09	2.11E-05	25.00	1169.90	1167.00	9.14E-01	51.39	48.59	58.82	57.76
EB/S-13.3-4	857.00	0.490	0.377	8.00E-03	3.21E-09	2.11E-05	25.00	1264.40	1259.30	9.14E-01	53.46	48.96	59.30	58.48
EB/S-13.3-5	851.00	0.490	0.377	8.00E-03	3.21E-09	2.11E-05	25.00	1475.00	1463.70	9.14E-01	55.52	49.74	60.19	59.81
EB/S-13.3-6	849.00	0.490	0.377	8.00E-03	3.21E-09	2.11E-05	25.00	1679.60	1591.60	9.14E-01	56.45	50.12	60.64	60.49
EB/S-13.3-7	851.00	0.490	0.377	8.00E-03	3.21E-09	2.11E-05	25.00	1750.20	1709.70	9.14E-01	57.72	50.37	60.99	61.02
EB/S-13.3-8	847.00	0.490	0.377	8.00E-03	3.21E-09	2.11E-05	25.00	2140.60	2064.50	9.14E-01	58.52	51.00	61.78	62.20
EB/S-13.3-9	844.00	0.490	0.377	8.00E-03	3.21E-09	2.11E-05	25.00	2320.20	2228.80	9.14E-01	58.72	51.22	62.04	62.59
EB/S-13.3-10	844.00	0.490	0.377	8.00E-03	3.21E-09	2.11E-05	25.00	2640.00	2580.10	9.14E-01	58.92	51.48	62.44	63.19
EB/S-13.3-11	844.00	0.490	0.377	8.00E-03	3.21E-09	2.11E-05	25.00	2970.20	2811.00	9.14E-01	57.74	51.58	62.62	63.45
EB/S-13.3-12	839.00	0.480	0.376	8.00E-03	3.23E-09	2.11E-05	25.00	3637.80	3257.70	9.14E-01	52.56	51.56	62.78	63.81
EB/S-13.3-13	863.00	0.480	0.376	8.00E-03	3.23E-09	2.11E-05	25.00	735.60	727.60	9.14E-01	40.51	45.68	55.54	52.94
EB/S-13.3-14	855.00	0.490	0.377	8.00E-03	3.21E-09	2.11E-05	25.00	1123.80	1119.30	9.14E-01	57.00	48.36	58.55	57.35
EB/S-13.3-15	849.00	0.490	0.377	8.00E-03	3.21E-09	2.11E-05	25.00	1440.40	1439.10	9.14E-01	60.44	49.69	60.10	59.67
EB/S-13.3-16	849.00	0.490	0.377	8.00E-03	3.21E-09	2.11E-05	25.00	1509.60	1569.00	9.14E-01	58.43	50.06	60.57	60.38
EB/S-13.3-17	845.00	0.490	0.377	8.00E-03	3.21E-09	2.11E-05	25.00	1849.50	1823.10	9.14E-01	62.07	50.66	61.29	61.45
EB/S-13.3-18	845.00	0.490	0.377	8.00E-03	3.21E-09	2.11E-05	25.00	1864.30	1838.10	9.14E-01	61.48	50.69	61.32	61.51
EB/S-13.3-19	845.00	0.490	0.377	8.00E-03	3.21E-09	2.11E-05	25.00	2263.00	2218.80	9.14E-01	62.06	51.20	62.03	62.56
EB/S-13.3-20	844.00	0.490	0.377	8.00E-03	3.21E-09	2.11E-05	25.00	2649.50	2596.00	9.14E-01	60.98	51.49	62.46	63.21
EB/S-13.3-21	840.00	0.490	0.377	8.00E-03	3.21E-09	2.11E-05	25.00	2908.70	2823.20	9.14E-01	60.00	51.63	62.63	63.47
EB/S-13.3-22	836.00	0.480	0.376	8.00E-03	3.23E-09	2.11E-05	25.00	3567.20	3238.10	9.14E-01	56.67	51.60	62.77	63.80

Table B.8.2. Calculations for fraction of jetting (FJ) & fraction of small bubble (FSB).
For ethylbenzene/styrene at 13.3 kPa operating pressure. Source: Billet et al., 1969.

Code	U_{SA}	U_H	F_{SA}	F_J	$1-F_J$	C	α_c	Q_L	h_r	T_{GLB}	$k\Delta t$	k	exp ($-k\Delta t$)	F_{SB}	$1-F_{SB}$
	m/s	m/s	--	--	--	--	--	m ³ /s	m	--	--	--	--	--	--
EB/S-13.3-1	0.934	6.866	0.647	0.416	0.584	0.5319	0.6772	0.0002	0.0232	0.0169	0.2671	15.8440	0.7856	0.0049	0.9951
EB/S-13.3-2	1.158	8.514	0.811	0.498	0.502	0.5319	0.6188	0.0003	0.0243	0.0130	0.2353	18.1258	0.7904	0.0042	0.9958
EB/S-13.3-3	1.507	11.081	1.055	0.589	0.411	0.5319	0.5430	0.0004	0.0259	0.0093	0.1980	21.2251	0.8204	0.0035	0.9965
EB/S-13.3-4	1.626	11.957	1.138	0.614	0.386	0.5319	0.5201	0.0004	0.0265	0.0085	0.1880	22.2221	0.8286	0.0033	0.9967
EB/S-13.3-5	1.890	13.898	1.323	0.658	0.342	0.5319	0.4714	0.0005	0.0279	0.0070	0.1689	24.3038	0.8446	0.0029	0.9971
EB/S-13.3-6	2.055	15.112	1.439	0.681	0.319	0.5319	0.4437	0.0005	0.0291	0.0063	0.1605	25.5506	0.8517	0.0028	0.9972
EB/S-13.3-7	2.208	16.234	1.545	0.699	0.301	0.5319	0.4205	0.0006	0.0297	0.0057	0.1511	26.6781	0.8598	0.0026	0.9974
EB/S-13.3-8	2.668	19.603	1.866	0.739	0.261	0.5319	0.3568	0.0007	0.0328	0.0044	0.1309	29.8598	0.8773	0.0022	0.9978
EB/S-13.3-9	2.878	21.163	2.015	0.752	0.248	0.5319	0.3306	0.0008	0.0343	0.0039	0.1232	31.2526	0.8841	0.0021	0.9979
EB/S-13.3-10	3.332	24.498	2.332	0.772	0.228	0.5319	0.2824	0.0009	0.0376	0.0032	0.1087	34.1213	0.8970	0.0018	0.9982
EB/S-13.3-11	3.630	26.691	2.541	0.781	0.219	0.5319	0.2548	0.0010	0.0405	0.0028	0.1022	35.9220	0.9028	0.0017	0.9983
EB/S-13.3-12	4.294	31.576	2.975	0.793	0.207	0.5319	0.2055	0.0012	0.0476	0.0023	0.0899	39.4656	0.9140	0.0015	0.9985
EB/S-13.3-13	0.959	7.053	0.665	0.426	0.574	0.5319	0.6708	0.0002	0.0234	0.0163	0.2629	16.1003	0.7888	0.0048	0.9952
EB/S-13.3-14	1.445	10.828	1.012	0.575	0.425	0.5319	0.5555	0.0004	0.0256	0.0098	0.2037	20.7002	0.8157	0.0036	0.9964
EB/S-13.3-15	1.858	13.664	1.301	0.654	0.346	0.5319	0.4764	0.0005	0.0277	0.0071	0.1707	24.0522	0.8431	0.0030	0.9970
EB/S-13.3-16	2.026	14.898	1.418	0.677	0.323	0.5319	0.4484	0.0005	0.0283	0.0063	0.1588	25.3323	0.8531	0.0027	0.9973
EB/S-13.3-17	2.354	17.310	1.648	0.714	0.286	0.5319	0.3980	0.0006	0.0306	0.0052	0.1434	27.7065	0.8664	0.0025	0.9975
EB/S-13.3-18	2.374	17.453	1.662	0.716	0.284	0.5319	0.3952	0.0006	0.0307	0.0051	0.1425	27.8431	0.8672	0.0024	0.9976
EB/S-13.3-19	2.865	21.068	2.006	0.751	0.249	0.5319	0.3323	0.0007	0.0340	0.0039	0.1229	31.1721	0.8843	0.0021	0.9979
EB/S-13.3-20	3.352	24.649	2.347	0.773	0.227	0.5319	0.2804	0.0009	0.0377	0.0032	0.1080	34.2474	0.8976	0.0018	0.9982
EB/S-13.3-21	3.646	26.806	2.552	0.781	0.219	0.5319	0.2527	0.0010	0.0404	0.0028	0.1009	35.9984	0.9041	0.0017	0.9983
EB/S-13.3-22	4.269	31.387	2.957	0.793	0.207	0.5319	0.2067	0.0012	0.0472	0.0023	0.0898	39.3089	0.9141	0.0015	0.9985

Table B.8.3. Efficiencies for large bubble & jetting by present models.

For ethylbenzenc/styrcne at 13.3 kPa operating pressure. Source: Billet et al., 1969.

Code	PM-1				PM-2				PM-3			
	E_{LB}	E_B	E_J	E_{∞} calc	E_{LB}	E_B	E_J	E_{∞} calc	E_{LB}	E_B	E_J	E_{∞} calc
	PM-1	--	PM-1	PM-1	PM-2		PM-2	PM-2	PM-3		PM-3	PM-3
EB/S-13.3-1	37.53	37.83	56.29	45.52	46.84	47.10	66.91	55.35	40.00	40.29	70.00	52.66
EB/S-13.3-2	37.59	37.86	56.39	47.08	46.90	47.13	67.00	57.02	40.00	40.25	70.00	55.06
EB/S-13.3-3	37.46	37.68	56.19	48.59	46.90	47.09	67.00	58.82	40.00	40.21	70.00	57.76
EB/S-13.3-4	37.40	37.61	56.10	48.96	46.90	47.08	67.00	59.30	40.00	40.20	70.00	58.48
EB/S-13.3-5	37.37	37.58	56.06	49.74	46.90	47.06	67.00	60.19	40.00	40.18	70.00	59.81
EB/S-13.3-6	37.35	37.52	56.02	50.12	46.90	47.05	67.00	60.64	40.00	40.17	70.00	60.49
EB/S-13.3-7	37.29	37.45	55.93	50.37	46.90	47.04	67.00	60.99	40.00	40.16	70.00	61.02
EB/S-13.3-8	37.22	37.36	55.83	51.00	46.90	47.02	67.00	61.78	40.00	40.13	70.00	62.20
EB/S-13.3-9	37.20	37.34	55.81	51.22	46.90	47.01	67.00	62.04	40.00	40.13	70.00	62.59
EB/S-13.3-10	37.12	37.24	55.68	51.48	46.90	47.00	67.00	62.44	40.00	40.11	70.00	63.19
EB/S-13.3-11	37.08	37.18	55.61	51.58	46.90	46.99	67.00	62.62	40.00	40.10	70.00	63.45
EB/S-13.3-12	36.90	37.00	55.38	51.56	46.84	46.92	66.91	62.78	40.00	40.09	70.00	63.81
EB/S-13.3-13	37.51	37.81	56.27	45.68	46.84	47.09	66.91	55.54	40.00	40.29	70.00	52.94
EB/S-13.3-14	37.49	37.71	56.23	48.36	46.90	47.09	67.00	58.55	40.00	40.22	70.00	57.35
EB/S-13.3-15	37.40	37.59	56.10	49.69	46.90	47.06	67.00	60.10	40.00	40.18	70.00	59.67
EB/S-13.3-16	37.35	37.53	56.03	50.06	46.90	47.05	67.00	60.57	40.00	40.16	70.00	60.38
EB/S-13.3-17	37.31	37.46	55.96	50.66	46.90	47.03	67.00	61.29	40.00	40.15	70.00	61.45
EB/S-13.3-18	37.30	37.46	55.95	50.69	46.90	47.03	67.00	61.32	40.00	40.15	70.00	61.51
EB/S-13.3-19	37.20	37.33	55.80	51.20	46.90	47.01	67.00	62.03	40.00	40.13	70.00	62.56
EB/S-13.3-20	37.12	37.23	55.68	51.49	46.90	47.00	67.00	62.46	40.00	40.11	70.00	63.21
EB/S-13.3-21	37.11	37.22	55.67	51.63	46.90	46.99	67.00	62.63	40.00	40.10	70.00	63.47
EB/S-13.3-22	36.94	37.03	55.40	51.60	46.84	46.92	66.91	62.77	40.00	40.09	70.00	63.80

Table B.9.1. Sieve tray efficiencies (experimental & calculated by present models).

For cyclohexane/n-heptane at 27.6 kPa operating pressure. Source: Sakata and Yanagi,1979.

Dc	D _H	TS	h _w	L _w	L _T	A _A	A _N	HA/AA							
M	mm	mm	mm	mm	mm	m ²	m ²	--							
1.22	12.7	610	50.8	940	762	0.859	0.991	8.3							
Code	ρ _L	ρ _G	μ _L	μ _G	D _L *10 ⁹	D _G *10 ⁵	σ	L _r	G _r	m	E _o	E _{oo} exp	E _{oo} cal	E _{oo} cal	E _{oo} cal
	kg/m ³	kg/m ³	mPa.s	mPa.s	m ² /s	m ² /s	mN/m	kg/hr	kg/hr			--	PM-1	PM-2	PM-3
CH/NH-27.6-1	717.6	0.940	0.3700	0.0073	4.29	1.69	19.90	1987.00	1900.00	0.8493	44.10	39.55	54.54	52.62	53.15
CH/NH-27.6-2	716.0	0.940	0.3700	0.0072	4.24	1.68	19.80	2907.00	2770.00	0.8785	67.90	55.25	56.98	54.09	56.78
CH/NH-27.6-3	715.7	0.940	0.3700	0.0072	4.24	1.68	19.80	4295.00	4104.00	0.8790	71.30	57.56	59.16	56.31	60.25
CH/NH-27.6-4	716.9	0.940	0.3700	0.0072	4.25	1.69	19.80	5936.00	5504.00	0.8746	80.90	64.52	60.26	57.67	62.19
CH/NH-27.6-5	716.5	0.940	0.3700	0.0072	4.29	1.70	19.80	7968.00	6890.00	0.8720	77.20	64.52	60.66	58.33	63.19
CH/NH-27.6-6	715.7	0.940	0.3700	0.0072	4.35	1.71	19.80	8740.00	7286.00	0.8790	72.40	62.03	60.58	58.31	63.37
CH/NH-27.6-7	709.9	0.950	0.3700	0.0072	4.57	1.75	19.80	9946.00	7675.00	0.8924	51.50	46.94	60.10	57.82	63.51
CH/NH-27.6-8	714.0	0.940	0.3700	0.0072	4.44	1.72	19.70	9353.00	7668.00	0.8823	65.20	57.30	60.36	58.18	63.52

**Table B.9.2. Calculations for fraction of jetting (FJ) & fraction of small bubble (FSB).
For cyclohexane/n-heptane at 27.6 kPa operating pressure. Source: Sakata and Yanagi,1979.**

Code	U_A	U_H	F_{SA}	F_J	$1-F_J$	C	α_c	Q_L	h_r	T_{GLB}	$K\Delta t$	k	$\exp(-k\Delta t)$	F_{SB}	$1-F_{SB}$
	m/s	m/s	--	--	--	--	--	m ³ /s	m	--	--	--	--	--	--
CH/NH-27.6-1	0.654	7.875	0.634	0.409	0.591	0.5004	0.6596	0.0008	0.0564	0.0570	0.9588	16.8302	0.3834	0.0251	0.9749
CH/NH-27.6-2	0.953	11.481	0.924	0.544	0.456	0.5004	0.5560	0.0011	0.0590	0.0344	0.7276	21.1399	0.4831	0.0168	0.9832
CH/NH-27.6-3	1.412	17.010	1.369	0.668	0.332	0.5004	0.4319	0.0017	0.0634	0.0194	0.5190	26.7621	0.5951	0.0108	0.9892
CH/NH-27.6-4	1.893	22.813	1.836	0.736	0.264	0.5004	0.3343	0.0023	0.0694	0.0122	0.3908	31.9210	0.6765	0.0076	0.9924
CH/NH-27.6-5	2.370	28.557	2.298	0.770	0.230	0.5004	0.2606	0.0031	0.0775	0.0085	0.3113	36.5238	0.7325	0.0058	0.9942
CH/NH-27.6-6	2.506	30.199	2.430	0.777	0.223	0.5004	0.2428	0.0034	0.0806	0.0078	0.2950	37.7650	0.7446	0.0055	0.9945
CH/NH-27.6-7	2.813	31.476	2.546	0.781	0.219	0.5004	0.2271	0.0039	0.0850	0.0074	0.2879	38.9650	0.7499	0.0053	0.9947
CH/NH-27.6-8	2.638	31.782	2.558	0.782	0.218	0.5004	0.2266	0.0036	0.0835	0.0072	0.2800	39.0105	0.7558	0.0051	0.9949

**Table B.9.3. Efficiencies for large bubble & jetting by present models.
For cyclohexane/n-heptane at 27.6 kPa operating pressure. Source: Sakata and Yanagi,1979.**

Code	PM-1				PM-2				PM-3			
	E_{LB}	E_B	E_J	E_{∞} calc	E_{LB}	E_B	E_J	E_{∞} calc	E_{LB}	E_B	E_J	E_{∞} calc
	PM-1	--	PM-1	PM-1	PM-2		PM-2	PM-2	PM-3		PM-3	PM-3
CH/NH-27.6-1	44.60	45.99	66.91	54.54	44.07	45.47	62.95	52.62	40.00	41.51	70.00	53.15
CH/NH-27.6-2	44.46	45.40	66.69	56.98	44.18	45.12	63.11	54.91	40.00	41.01	70.00	56.78
CH/NH-27.6-3	44.20	44.80	66.30	59.16	44.18	44.78	63.11	57.02	40.00	40.65	70.00	60.25
CH/NH-27.6-4	43.97	44.40	65.96	60.26	44.16	44.58	63.08	58.19	40.00	40.46	70.00	62.19
CH/NH-27.6-5	43.74	44.07	65.61	60.66	44.07	44.39	62.95	58.69	40.00	40.35	70.00	63.19
CH/NH-27.6-6	43.58	43.89	65.38	60.58	43.94	44.24	62.77	58.63	40.00	40.33	70.00	63.37
CH/NH-27.6-7	43.17	43.47	64.75	60.10	43.47	43.77	62.10	58.09	40.00	40.32	70.00	63.51
CH/NH-27.6-8	43.36	43.65	65.03	60.36	43.74	44.03	62.49	58.46	40.00	40.31	70.00	63.52

**Table B.10.1. Sieve tray efficiencies (experimental & calculated by present models).
For cyclohexane/n-heptan at 165 KPa pressure. Source: Sakata and Yanagi, 1979.**

Dc	D _N	TS	h _w	L _w	L _T	A _A	A _N	H _A /A _A							
m	mm	mm	mm	mm	mm	m ²	m ²	--							
1.22	12.7	610	50.8	940	762	0.859	0.991	8.3							
Code	ρ _L	ρ _G	μ _L	μ _G	D _L *10 ⁹	D _G *10 ⁴	σ	L _r	G _r	m	E _o	E _{oo} exp	E _{oo} cal	E _{oo} cal	E _{oo} cal
	kg/m ³	kg/m ³	mPa.s	mPa.s	m ² /s	m ² /s	mN/m	kg/hr	kg/hr			--	PM-1	PM-2	PM-3
CH/NH-165-1	662.0	5.020	0.2720	0.0085	7.61	2.28	14.10	4767.00	4905.00	0.8813	74.00	58.83	60.91	51.51	58.43
CH/NH-165-2	657.7	5.050	0.2720	0.0085	7.61	2.28	13.90	6649.00	6918.00	0.9298	78.30	60.36	61.05	50.84	59.42
CH/NH-165-3	658.0	5.050	0.2720	0.0085	7.61	2.28	14.00	9087.00	9671.00	0.9306	83.10	63.20	61.99	51.25	61.21
CH/NH-165-4	658.6	5.040	0.2720	0.0085	7.61	2.28	13.90	13555.00	14369.00	0.9334	93.10	69.77	62.89	52.02	63.11
CH/NH-165-5	658.0	5.050	0.2720	0.0085	7.61	2.28	13.90	17786.00	18361.00	0.9409	94.80	72.77	63.19	52.33	63.81
CH/NH-165-6	658.0	5.050	0.2720	0.0085	7.61	2.28	13.90	20024.00	20862.00	0.9409	91.40	72.21	63.22	52.43	64.02
CH/NH-165-7	657.1	5.050	0.2720	0.0085	7.61	2.28	13.90	21038.00	21843.00	0.9465	89.40	71.59	63.24	52.45	64.08
CH/NH-165-8	651.4	5.090	0.2720	0.0085	7.61	2.28	13.70	22343.00	22867.00	0.9603	64.10	54.88	63.30	52.48	64.13

Table B.10.2. Calculations for fraction of jetting (FJ) & fraction of small bubble (FSB).
For cyclohexane/n-heptan at 165 KPa pressure. Source: Sakata and Yanagi, 1979.

Code	U_{SA}	U_H	F_{SA}	F_J	$1-F_J$	C	α_e	Q_L	h_f	T_{GLB}	$k\Delta t$	k	$\exp(-k\Delta t)$	F_{SB}	$1-F_{SB}$
	m/s	m/s	--	--	--	--	--	m ³ /s	m	--	--	--	--	--	--
CH/NH-165-1	0.316	3.807	0.708	0.449	0.551	0.5004	0.6195	0.0020	0.0620	0.1215	2.4886	20.4785	0.0830	0.1502	0.8498
CH/NH-165-2	0.443	5.337	0.995	0.570	0.430	0.5004	0.5195	0.0028	0.0666	0.0781	1.9720	25.2537	0.1392	0.0900	0.9100
CH/NH-165-3	0.619	7.481	1.392	0.672	0.328	0.5004	0.4114	0.0038	0.0735	0.0489	1.5044	30.7889	0.2221	0.0531	0.9469
CH/NH-165-4	0.922	11.108	2.070	0.756	0.244	0.5004	0.2797	0.0057	0.0893	0.0271	1.0615	39.1842	0.3459	0.0294	0.9706
CH/NH-165-5	1.176	14.165	2.842	0.785	0.215	0.5004	0.2036	0.0075	0.1080	0.0187	0.8480	45.3623	0.4283	0.0209	0.9791
CH/NH-165-6	1.336	16.095	3.002	0.794	0.206	0.5004	0.1673	0.0085	0.1214	0.0152	0.7445	48.9745	0.4750	0.0174	0.9826
CH/NH-165-7	1.399	16.852	3.143	0.796	0.204	0.5004	0.1548	0.0089	0.1277	0.0141	0.7117	50.3367	0.4908	0.0163	0.9837
CH/NH-165-8	1.453	17.503	3.278	0.798	0.202	0.5004	0.1429	0.0095	0.1358	0.0134	0.6929	51.8722	0.5001	0.0157	0.9843

Table B.10.3. Efficiencies for large bubble & jetting by present models.

For cyclohexane/n-heptan at 165 KPa pressure. Source: Sakata and Yanagi, 1979.

Code	PM-1				PM-2				PM-3			
	E_{LB}	E_B	E_J	E_{∞} calc	E_{LB}	E_B	E_J	E_{∞} calc	E_{LB}	E_B	E_J	E_{∞} calc
	PM-1	--	PM-1	PM-1	PM-2		PM-2	PM-2	PM-3		PM-3	PM-3
CH/NH-165-1	46.10	54.19	69.15	60.91	38.96	48.13	55.85	51.51	40.00	49.01	70.00	58.43
CH/NH-165-2	45.88	50.75	68.82	61.05	38.96	44.46	55.85	50.84	40.00	45.40	70.00	59.42
CH/NH-165-3	45.68	48.57	68.53	61.99	38.96	42.20	55.85	51.25	40.00	43.18	70.00	61.21
CH/NH-165-4	45.36	46.96	68.03	62.89	38.96	40.75	55.85	52.02	40.00	41.76	70.00	63.11
CH/NH-165-5	45.21	46.35	67.81	63.19	38.96	40.23	55.85	52.33	40.00	41.25	70.00	63.81
CH/NH-165-6	45.12	46.08	67.68	63.22	38.96	40.02	55.85	52.43	40.00	41.04	70.00	64.02
CH/NH-165-7	45.10	46.00	67.66	63.24	38.96	39.95	55.85	52.45	40.00	40.98	70.00	64.08
CH/NH-165-8	45.12	45.99	67.69	63.30	38.96	39.92	55.85	52.48	40.00	40.94	70.00	64.13

Table B.11.1. Sieve tray efficiencies (experimental & calculated by present models).

For iso-butane/n-butane at 1138 kPa operating pressure. Source: Sakata and Yanagi, 1979.

Dc	D _H	TS	h _w	L _w	L _T	A _A	A _N	HA/AA							
m	mm	mm	mm	mm	mm	m ²	m ²	--							
1.22	12.7	810	50.8	940	762	0.859	0.991	8.3							
Code	ρ _L	ρ _G	μ _L	μ _G	D _L *10 ⁹	D ₀ *10 ⁶	σ	L _r	G _r	m	E _{MV}	E ₀₀ exp	E ₀₀ cal	E ₀₀ cal	E ₀₀ cal
	kg/m ³	kg/m ³	mPa.s	mPa.s	m ² /s	M ² /s	mN/m	kg/hr	kg/hr			--	PM-1	PM-2	PM-3
IO/NB-1138-1	493.0	28.000	0.0900	0.0095	1.03	5.62	5.00	6424.00	6440.00	1.0562	75.10	55.80	93.70	88.24	92.63
IO/NB-1138-2	494.0	27.700	0.0900	0.0095	1.03	5.61	5.00	10428.00	10359.00	1.0562	108.20	73.42	89.15	80.29	87.62
IO/NB-1138-3	493.0	28.000	0.0900	0.0095	1.03	5.62	5.00	14100.00	14139.00	1.0562	119.20	78.88	85.97	74.80	84.11
IO/NB-1138-4	493.0	27.800	0.0900	0.0095	1.03	5.62	5.00	21378.00	21270.00	1.0562	123.70	81.77	81.15	67.24	79.01
IO/NB-1138-5	493.0	28.300	0.0900	0.0095	1.04	5.63	5.00	28200.00	28377.00	1.0562	121.60	82.29	77.71	62.21	75.38
IO/NB-1138-6	493.0	28.200	0.0900	0.0095	1.03	5.62	5.00	31670.00	31828.00	1.0562	121.20	83.22	76.32	60.27	73.80
IO/NB-1138-7	493.0	28.200	0.0900	0.0095	1.04	5.63	5.00	33351.00	33452.00	1.0562	119.00	82.22	75.60	59.39	73.17
IO/NB-1138-8	493.0	28.200	0.0900	0.0095	1.05	5.69	5.00	35028.00	35258.00	1.0562	116.40	82.13	74.83	58.45	72.49

Table B.11.2. Calculations for fraction of jetting (F_J) & fraction of small bubble (F_{SB}).
 For iso-butane/n-butane at 1138 kPa operating pressure. Source: Sakata and Yanagi, 1979.

Code	U _{SA}	U _H	F _{SA}	F _J	1-F _J	C	α _o	Q _L	h _r	T _{GLB}	kΔt	k	exp (-kΔt)	F _{SB}	1-F _{SB}
	m/s	m/s	--	--	--	--	--	m ³ /s	M	--	--	--	--	--	--
IO/NB-1138-1	0.074	0.896	0.394	0.246	0.754	0.5004	0.7201	0.0036	0.0658	0.6374	13.4904	21.1645	0.0000	0.9999	0.0001
IO/NB-1138-2	0.121	1.457	0.636	0.410	0.590	0.5004	0.6017	0.0059	0.0742	0.3693	10.4327	28.2461	0.0000	0.9982	0.0018
IO/NB-1138-3	0.163	1.967	0.864	0.521	0.479	0.5004	0.5108	0.0079	0.0829	0.2592	8.7926	33.9256	0.0002	0.9906	0.0094
IO/NB-1138-4	0.247	2.981	1.305	0.654	0.346	0.5004	0.3764	0.0120	0.1028	0.1564	6.7916	43.4382	0.0011	0.9344	0.0656
IO/NB-1138-5	0.324	3.907	1.725	0.723	0.277	0.5004	0.2835	0.0159	0.1265	0.1106	5.6792	51.3651	0.0034	0.8240	0.1760
IO/NB-1138-6	0.365	4.397	1.938	0.745	0.255	0.5004	0.2463	0.0178	0.1407	0.0949	5.2281	55.0852	0.0054	0.7489	0.2511
IO/NB-1138-7	0.384	4.622	2.037	0.754	0.246	0.5004	0.2308	0.0188	0.1480	0.0890	5.0523	56.7548	0.0064	0.7145	0.2855
IO/NB-1138-8	0.404	4.871	2.147	0.761	0.239	0.5004	0.2148	0.0197	0.1562	0.0830	4.8596	58.5719	0.0078	0.6736	0.3264

Table B.11.3. Efficiencies for large bubble & jetting by present models.

For iso-butane/n-butane at 1138 kPa operating pressure. Source: Sakata and Yanagi, 1979.

Code	PM-1				PM-2				PM-3			
	E_{LB}	E_B	E_J	E_{∞} calc	E_{LB}	E_B	E_J	E_{∞} calc	E_{LB}	E_B	E_J	E_{∞} calc
	PM-1	--	PM-1	PM-1	PM-2		PM-2	PM-2	PM-3		PM-3	PM-3
IO/NB-1138-1	49.57	100.00	74.36	93.70	36.50	99.99	52.15	88.24	40.00	99.99	70.00	92.63
IO/NB-1138-2	49.14	99.91	73.70	89.15	36.50	99.88	52.15	80.29	40.00	99.89	70.00	87.62
IO/NB-1138-3	48.99	99.52	73.48	85.97	36.50	99.40	52.15	74.80	40.00	99.44	70.00	84.11
IO/NB-1138-4	48.65	96.63	72.97	81.15	36.50	95.83	52.15	67.24	40.00	96.06	70.00	79.01
IO/NB-1138-5	48.44	90.93	72.66	77.71	36.43	88.81	52.04	62.21	40.00	89.44	70.00	75.38
IO/NB-1138-6	48.44	87.05	72.65	76.32	36.50	84.06	52.15	60.27	40.00	84.94	70.00	73.80
IO/NB-1138-7	48.30	85.24	72.45	75.60	36.43	81.85	52.04	59.39	40.00	82.87	70.00	73.17
IO/NB-1138-8	48.16	83.08	72.24	74.83	36.35	79.22	51.93	58.45	40.00	80.41	70.00	72.49

Table B.12.1. Sieve tray efficiencies (experimental & calculated by present models).
 For iso-butane/n-butane at 2068 kPa operating pressure. Source: Sakata and Yanagi, 19

Dc	D _H	TS	h _w	L _w	L _T	A _A	A _N	H _A /A _A						
m	mm	mm	mm	mm	mm	M ²	m ²	--						
1.22	12.7	610	50.8	940	762	0.859	0.991	8.3						
Code	ρ _L	ρ _G	μ _L	μ _G	D _L *10 ⁹	D _G *10 ⁶	σ	L _T	G _T	m	E _{OG} exp	E _{OG} cal	E _{OG} cal	E _{OG} cal
	kg/m ³	kg/m ³	mPa.s	mPa.s	m ² /s	m ² /s	mN/m	kg/hr	kg/hr		--	PM-1	PM-2	PM-3
IB/NB-2068-1	426.0	56.500	0.0650	0.0101	2.01	3.81	2.50	7446.00	7388.00	0.8729	71.86		90.05	94.56
IB/NB-2068-2	424.0	57.600	0.0650	0.0101	1.77	3.75	2.50	10108.00	10086.00	0.8729	79.91	91.27	87.76	91.78
IB/NB-2068-3	424.0	57.900	0.0650	0.0101	1.68	3.72	2.50	14823.00	14925.00	0.8729	76.96	87.13	81.00	87.73
IB/NB-2068-4	424.0	57.600	0.0650	0.0101	1.74	3.74	2.50	20021.00	20100.00	0.8729	78.02	83.27	75.10	84.48
IB/NB-2068-5	425.0	57.300	0.0650	0.0101	1.69	3.71	2.50	22576.00	22483.00	0.8729	77.88	82.11	73.05	83.28
IB/NB-2068-6	423.0	58.200	0.0650	0.0101	1.69	3.72	2.50	23815.00	24069.00	0.8729	76.73	81.52	71.91	82.66
IB/NB-2068-7	424.0	57.900	0.0650	0.0101	1.60	3.69	2.50	25122.00	25224.00	0.8729	58.51	81.41	71.30	82.17
IB/NB-2068-8	432.0	54.400	0.0650	0.0102	1.33	3.61	2.50	7258.00	7216.00	0.9718	66.49	94.96	92.85	94.60
IB/NB-2068-9	430.0	54.700	0.0650	0.0102	1.31	3.60	2.50	9662.00	9703.00	0.9718	75.18	92.47	88.67	91.91
IB/NB-2068-10	430.0	55.200	0.0650	0.0102	1.30	3.60	2.50	14448.00	14555.00	0.9718	76.18	88.49	81.98	87.74
IB/NB-2068-11	430.0	55.200	0.0650	0.0102	1.31	3.60	2.50	19329.00	19467.00	0.9718	73.91	85.31	76.67	84.59
IB/NB-2068-12	430.0	55.200	0.0650	0.0102	1.28	3.59	2.50	21866.00	21958.00	0.9718	73.95	84.23	74.57	83.33
IB/NB-2068-13	430.0	55.000	0.0650	0.0102	1.31	3.61	2.50	23035.00	23112.00	0.9718	73.62	83.47	73.53	82.79

Table B.12.2. Calculations for fraction of jetting (FJ) & fraction of small bubble (FSB).
For iso-butane/n-butane at 2068 kPa operating pressure. Source: Sakata and Yanagi, 1979.

Code	U_{SA}	U_H	F_{SA}	F_J	$1-F_J$	C	α_g	Q_L	h_l	T_{GLB}	$K\Delta t$	k	$\exp(-k\Delta t)$	F_{SB}	$1-F_{SB}$
	m/s	m/s	--	--	--	--	--	m ³ /s	M	--	--	--	--	--	--
IB/NB-2068-1	0.042	0.358	0.318	0.181	0.819	0.744	0.7407	0.0049	0.0775	1.3577	32.8698	24.2100	0.0000	1.0000	0.0000
IB/NB-2068-2	0.057	0.882	0.430	0.274	0.726	0.5004	0.8727	0.0066	0.0744	0.8837	25.6278	28.9997	0.0000	1.0000	0.0000
IB/NB-2068-3	0.083	1.004	0.634	0.409	0.591	0.5004	0.5682	0.0097	0.0849	0.5790	21.2082	36.6297	0.0000	1.0000	0.0000
IB/NB-2068-4	0.113	1.360	0.856	0.517	0.483	0.5004	0.4758	0.0131	0.0978	0.4125	18.0938	43.8611	0.0000	1.0000	0.0000
IB/NB-2068-5	0.127	1.529	0.960	0.557	0.443	0.5004	0.4391	0.0148	0.1045	0.3617	16.9963	46.9955	0.0000	1.0000	0.0000
IB/NB-2068-6	0.134	1.811	1.020	0.578	0.422	0.5004	0.4179	0.0156	0.1085	0.3391	16.5156	48.7061	0.0000	1.0000	0.0000
IB/NB-2068-7	0.141	1.897	1.072	0.594	0.406	0.5004	0.4020	0.0165	0.1121	0.3199	16.0534	50.1849	0.0000	1.0000	0.0000
IB/NB-2068-8	0.043	0.517	0.316	0.180	0.820	0.5004	0.7438	0.0047	0.0682	1.1834	28.6106	24.1768	0.0000	1.0000	0.0000
IB/NB-2068-9	0.057	0.891	0.424	0.270	0.730	0.5004	0.6787	0.0062	0.0733	0.8677	25.0044	28.8168	0.0000	1.0000	0.0000
IB/NB-2068-10	0.085	1.027	0.634	0.409	0.591	0.5004	0.5720	0.0093	0.0839	0.5628	20.6287	36.6542	0.0000	1.0000	0.0000
IB/NB-2068-11	0.114	1.374	0.847	0.514	0.486	0.500	0.4829	0.0125	0.0959	0.4059	17.7141	43.6411	0.0000	1.0000	0.0000
IB/NB-2068-12	0.129	1.550	0.956	0.556	0.444	0.5004	0.4439	0.0141	0.1026	0.3540	16.6050	46.9107	0.0000	1.0000	0.0000
IB/NB-2068-13	0.136	1.637	1.008	0.574	0.426	0.5004	0.4265	0.0149	0.1059	0.3323	16.0920	48.4275	0.0000	1.0000	0.0000

Table B.12.3. Efficiencies for large bubble & jetting by present models.

For iso-butane/n-butane at 2068 kPa operating pressure. Source: Sakata and Yanagi, 1979.

Code	PM-1				PM-2				PM-3			
	E_{LB}	E_B	E_J	E_{∞} calc	E_{LB}	E_B	E_J	E_{∞} calc	E_{LB}	E_B	E_J	E_{∞} calc
	PM-1	--	PM-1	PM-1	PM-2		PM-2	PM-2	PM-3		PM-3	PM-3
IB/NB-2068-1	42.72	100.00	64.08	93.48	31.62	100.00	45.17	90.05	40.00	100.00	70.00	94.56
IB/NB-2068-2	45.42	100.00	68.13	91.27	32.49	100.00	46.42	85.32	40.00	100.00	70.00	91.78
IB/NB-2068-3	45.69	100.00	68.53	87.13	32.86	100.00	46.94	78.29	40.00	100.00	70.00	87.73
IB/NB-2068-4	45.12	100.00	67.67	83.27	32.81	100.00	46.59	72.36	40.00	100.00	70.00	84.48
IB/NB-2068-5	45.27	100.00	67.91	82.11	32.82	100.00	46.88	70.39	40.00	100.00	70.00	83.28
IB/NB-2068-6	45.35	100.00	68.03	81.52	32.82	100.00	46.88	69.30	40.00	100.00	70.00	82.66
IB/NB-2068-7	45.81	100.00	68.71	81.41	33.21	100.00	47.44	68.76	40.00	100.00	70.00	82.17
IB/NB-2068-8	48.03	100.00	72.04	94.98	34.55	100.00	49.36	90.88	40.00	100.00	70.00	94.60
IB/NB-2068-9	48.05	100.00	72.07	92.47	34.66	100.00	49.52	86.38	40.00	100.00	70.00	91.91
IB/NB-2068-10	47.89	100.00	71.83	88.49	34.72	100.00	49.60	79.40	40.00	100.00	70.00	87.74
IB/NB-2068-11	47.60	100.00	71.40	85.31	34.66	100.00	49.52	74.07	40.00	100.00	70.00	84.59
IB/NB-2068-12	47.75	100.00	71.63	84.23	34.84	100.00	49.77	72.08	40.00	100.00	70.00	83.33
IB/NB-2068-13	47.46	100.00	71.19	83.47	34.66	100.00	49.52	71.03	40.00	100.00	70.00	82.79

532

Table B.13.1. Sieve tray efficiencies (experimental & calculated by present models).

For iso-butane/n-butane at 2758 kPa operating pressure. Source: Sakata and Yanagi, 1979.

Dc	D _H	TS	h _w	L _w	L _T	A _A	A _N	HA/AA							
m	mm	mm	mm	mm	mm	m ²	m ²	--							
1.22	12.7	610	50.8	940	762	0.859	0.991	8.3							
Code	ρ _L	ρ _G	μ _L	μ _G	D _L *10 ⁹	D ₀ *10 ⁵	σ	L _t	G _t	m	E _{MV}	E _{OG exp}	E _{OG cal}	E _{OG cal}	E _{OG cal}
	kg/m ³	kg/m ³	mPa.s	mPa.s	m ² /s	m ² /s	mN/m	kg/hr	kg/hr			--	PM-1	PM-2	PM-3
IB/NB-2758-1	378.0	86.200	0.0500	0.0105	2.30	3.09	1.10	7560.00	7408.00	0.9110	90.90	67.30	95.38	92.95	96.23
IB/NB-2758-2	374.0	88.500	0.0500	0.0105	2.05	3.05	1.10	11377.00	11486.00	0.9110	95.80	69.71	91.29	88.84	92.60
IB/NB-2758-3	373.0	89.100	0.0500	0.0105	2.07	3.06	1.10	15241.00	15451.00	0.9110	99.50	71.67	87.72	83.70	89.66
IB/NB-2758-4	373.0	88.800	0.0500	0.0105	2.02	3.05	1.10	17274.00	17446.00	0.9110	97.60	70.73	86.24	81.46	88.35
IB/NB-2758-5	374.0	87.700	0.0500	0.0105	2.12	3.06	1.10	18169.00	18133.00	0.9110	94.00	68.86	85.33	80.43	87.87
IB/NB-2758-6	374.0	88.300	0.0500	0.0105	2.01	3.04	1.10	19104.00	19230.00	0.9110	82.90	67.75	84.91	79.54	87.27
IB/NB-2758-7	392.0	78.700	0.0500	0.0107	1.55	2.98	1.10	5183.00	5039.00	0.9904	91.20	65.99	98.43	98.85	98.53
IB/NB-2758-8	389.0	80.500	0.0500	0.0106	1.49	2.94	1.10	6967.00	6917.00	0.9904	100.90	75.99	96.31	95.88	96.49
IB/NB-2758-9	386.0	82.600	0.0500	0.0107	1.48	2.94	1.10	10688.00	10815.00	0.9904	99.60	74.28	92.47	89.89	92.84
IB/NB-2758-10	387.0	82.200	0.0500	0.0107	1.48	2.94	1.10	14230.00	14360.00	0.9904	101.00	73.98	89.36	85.27	90.00
IB/NB-2758-11	386.0	82.200	0.0500	0.0107	1.49	2.95	1.10	15946.00	16164.00	0.9904	95.30	71.94	87.97	83.17	88.75
IB/NB-2758-12	386.0	82.200	0.0500	0.0107	1.49	2.95	1.10	16559.00	17238.00	0.9904	94.70	69.19	87.20	82.03	88.06

Table B.13.2. Calculations for fraction of jetting (F_J) & fraction of small bubble (F_{SB}).

For iso-butane/n-butane at 2758 kPa operating pressure. Source: Sakata and Yanagi, 1979.

Code	U _{SA}	U _H	F _{SA}	F _J	1-F _J	C	α _g	Q _L	h _r	T _{GLB}	KΔt	k	exp (-kΔt)	F _{SB}	1-F _{SB}
	m/s	m/s	--	--	--	--	--	M ³ /s	M	--	--	--	--	--	--
IB/NB-2758-1	0.028	0.335	0.258	0.126	0.874	0.5004	0.7585	0.0056	0.0702	1.9146	56.1263	29.3149	0.0000	1.0000	0.0000
IB/NB-2758-2	0.042	0.506	0.395	0.247	0.753	0.5004	0.6828	0.0084	0.0789	1.2454	47.0730	37.7986	0.0000	1.0000	0.0000
IB/NB-2758-3	0.056	0.676	0.529	0.345	0.655	0.5004	0.5837	0.0114	0.0880	0.9163	41.2834	45.0559	0.0000	1.0000	0.0000
IB/NB-2758-4	0.064	0.765	0.599	0.388	0.612	0.5004	0.5478	0.0129	0.0930	0.8022	38.9170	48.5104	0.0000	1.0000	0.0000
IB/NB-2758-5	0.067	0.806	0.626	0.404	0.596	0.5004	0.5354	0.0135	0.0951	0.7614	37.9537	49.8471	0.0000	1.0000	0.0000
IB/NB-2758-6	0.070	0.848	0.662	0.424	0.576	0.5004	0.5180	0.0142	0.0976	0.7181	37.0054	51.5296	0.0000	1.0000	0.0000
IB/NB-2758-7	0.021	0.249	0.184	0.049	0.951	0.5004	0.8216	0.0037	0.0647	2.5661	61.5721	23.9946	0.0000	1.0000	0.0000
IB/NB-2758-8	0.028	0.335	0.249	0.117	0.883	0.5004	0.7701	0.0050	0.0686	1.9010	54.7486	28.7990	0.0000	1.0000	0.0000
IB/NB-2758-9	0.042	0.510	0.385	0.239	0.761	0.5004	0.6766	0.0077	0.0768	1.2269	45.8090	37.3380	0.0000	1.0000	0.0000
IB/NB-2758-10	0.056	0.681	0.512	0.333	0.667	0.5004	0.6030	0.0102	0.0847	0.9045	40.1034	44.3377	0.0000	1.0000	0.0000
IB/NB-2758-11	0.064	0.766	0.577	0.375	0.625	0.5004	0.5688	0.0115	0.0890	0.7957	37.8667	47.5880	0.0000	1.0000	0.0000
IB/NB-2758-12	0.068	0.817	0.615	0.398	0.602	0.5004	0.5498	0.0119	0.0908	0.7364	36.4239	49.4607	0.0000	1.0000	0.0000

Table B.13.3. Efficiencies for large bubble & jetting by present models.

For iso-butane/n-butane at 2758 kPa operating pressure. Source: Sakata and Yanagi, 1979.

Code	PM-1				PM-2				PM-3			
	E_{LB}	E_B	E_J	E_{OG} calc	E_{LB}	E_B	E_J	E_{OG} calc	E_{LB}	E_B	E_J	E_{OG} calc
	PM-1	..	PM-1	PM-1	PM-2		PM-2	PM-2	PM-3		PM-3	PM-3
IB/NB-2758-1	42.13	100.00	63.20	95.38	30.71	100.00	43.88	92.95	40.00	100.00	70.00	96.23
IB/NB-2758-2	43.14	100.00	64.70	91.29	31.48	100.00	44.98	86.43	40.00	100.00	70.00	92.60
IB/NB-2758-3	42.91	100.00	64.37	87.72	31.42	100.00	44.88	81.00	40.00	100.00	70.00	89.66
IB/NB-2758-4	43.04	100.00	64.57	86.24	31.58	100.00	45.12	78.69	40.00	100.00	70.00	88.35
IB/NB-2758-5	42.49	100.00	63.73	85.33	31.26	100.00	44.65	77.61	40.00	100.00	70.00	87.87
IB/NB-2758-6	42.97	100.00	64.46	84.91	31.62	100.00	45.17	76.72	40.00	100.00	70.00	87.27
IB/NB-2758-7	45.30	100.00	67.94	98.43	33.43	100.00	47.76	97.44	40.00	100.00	70.00	98.53
IB/NB-2758-8	45.68	100.00	68.49	96.31	33.72	100.00	48.17	93.94	40.00	100.00	70.00	96.49
IB/NB-2758-9	45.63	100.00	68.45	92.47	33.77	100.00	48.24	87.65	40.00	100.00	70.00	92.84
IB/NB-2758-10	45.39	100.00	68.08	89.36	33.77	100.00	48.24	82.75	40.00	100.00	70.00	90.00
IB/NB-2758-11	45.27	100.00	67.90	87.97	33.72	100.00	48.17	80.57	40.00	100.00	70.00	88.75
IB/NB-2758-12	45.22	100.00	67.83	87.20	33.72	100.00	48.17	79.38	40.00	100.00	70.00	88.06

**Table B.14. 1. Sieve tray efficiencies (experimental & calculated by present models).
For cyclohexane/N-heptane 34 KPA pressure. Source: Yanagi and sakata, 1982.**

Dc	D _H	TS	h _w	L _w	L _T	A _A	A _N	HA/AA							
m	mm	mm	mm	mm	mm	m ²	m ²	--							
1.22	12.7	810	50.8	940	762	0.859	0.991	14							
Code	ρ _L	ρ _G	μ _L	μ _G	D _L ·10 ⁹	D _G ·10 ⁵	σ	L _r	G _r	M	E _{OG} exp	E _{OG} cal	E _{OG} cal	E _{OG} cal	
	kg/m ³	kg/m ³	mPa.s	mPa.s	m ² /s	m ² /s	mN/m	kg/hr	kg/hr		--	PM-1	PM-2	PM-3	
CH/NH-34-1	714.3	1.140	0.3400	0.0074	4.12	8.06	19.40	4022.00	4852.00	0.8044	52.42	57.91	57.72	60.80	
CH/NH-34-2	710.4	1.140	0.3400	0.0073	4.26	8.19	19.10	6017.00	6759.00	0.9134	56.64	58.53	58.50	62.74	
CH/NH-34-3	710.4	1.140	0.3400	0.0073	4.28	8.21	19.10	7792.00	8239.00	0.9134	59.51	58.79	58.89	63.45	
CH/NH-34-4	708.7	1.150	0.3400	0.0073	4.36	8.29	19.00	8851.00	9085.00	0.9271	55.09	58.69	58.80	63.69	
CH/NH-34-5	703.9	1.150	0.3400	0.0073	4.49	8.41	19.00	10171.00	10433.00	0.9187	36.95	58.45	58.58	63.94	

Table B.14.2. Calculations for fraction of jetting (FJ) & fraction of small bubble (FSB).
For cyclohexane/N-heptane 34 KPA pressure. Source: Yanagi and sakata, 1982.

Code	U_{SA}	U_H	F_{SA}	F_J	$1-F_J$	C	α_e	Q_L	h_r	T_{GLB}	$k\Delta t$	k	exp ($-k\Delta t$)	F_{SB}	$1-F_{SB}$
	m/s	m/s	--	--	--	--	--	m ³ /s	M	--	--	--	--	--	--
CH/NH-34-1	1.376	9.831	1.470	0.687	0.313	0.5004	0.4080	0.0016	0.0633	0.0188	0.5285	28.1498	0.5895	0.0110	0.9890
CH/NH-34-2	1.917	13.695	2.047	0.754	0.246	0.5004	0.2966	0.0024	0.0712	0.0110	0.3806	34.5400	0.6835	0.0074	0.9926
CH/NH-34-3	2.337	16.693	2.495	0.779	0.221	0.5004	0.2334	0.0030	0.0793	0.0079	0.3080	38.8971	0.7349	0.0057	0.9943
CH/NH-34-4	2.555	18.248	2.740	0.787	0.213	0.5004	0.2048	0.0035	0.0847	0.0068	0.2799	41.2153	0.7558	0.0051	0.9949
CH/NH-34-5	2.934	20.955	3.146	0.796	0.204	0.5004	0.1646	0.0040	0.0941	0.0053	0.2363	44.7521	0.7895	0.0042	0.9958

**Table B.14.3. Efficiencies for large bubble & jetting by present models.
For cyclohexane/N-heptane 34 KPA pressure. Source: Yanagi and sakata, 1982.**

Code	PM-1				PM-2				PM-3			
	E_{LB}	E_B	E_J	E_{00} calc	E_{LB}	E_B	E_J	E_{00} calc	E_{LB}	E_B	E_J	E_{00} calc
	PM-1	--	PM-1	PM-1	PM-2		PM-2	PM-2	PM-3		PM-3	PM-3
CH/NH-34-1	42.97	43.60	64.45	57.91	44.45	45.06	63.50	57.72	40.00	40.66	70.00	60.80
CH/NH-34-2	42.42	42.85	63.63	58.53	44.13	44.55	63.05	58.50	40.00	40.44	70.00	62.74
CH/NH-34-3	42.25	42.58	63.38	58.79	44.09	44.41	62.99	58.89	40.00	40.34	70.00	63.45
CH/NH-34-4	42.06	42.36	63.09	58.69	43.91	44.20	62.74	58.80	40.00	40.31	70.00	63.69
CH/NH-34-5	41.77	42.02	62.66	58.45	43.64	43.88	62.34	58.58	40.00	40.25	70.00	63.94

Table B.15.1. Sieve tray efficiencies (experimental & calculated by present models).

For cyclohexane/n-heptane at 165 kPa operating pressure. Source: Yanagi and Sakata, 1982.

Dc	D _H	TS	h _w	L _w	L _T	A _A	A _N	H _A /A _A							
m	mm	mm	mm	mm	mm	m ²	m ²	--							
1.22	12.7	610	50.8	940	762	0.859	0.991	14							
Code	ρ _L	ρ _G	μ _L	μ _G	D _L ·10 ⁹	D _G ·10 ⁵	σ	L _r	G _r	m	E _{MV}	E _{OG} exp	E _{OG} cal	E _{OG} cal	E _{OG} cal
	kg/m ³	kg/m ³	mPa.s	mPa.s	m ² /s	m ² /s	mN/m	kg/hr	kg/hr			--	PM-1	PM-2	PM-3
CH/NH-165-1	645.5	5.110	0.2500	0.0084	7.95	2.33	13.60	2433.00	2490.00	0.9299	29.00	40.00	67.14	62.40	66.23
CH/NH-165-2	645.5	5.110	0.2620	0.0084	7.55	2.27	13.60	5022.00	5124.00	0.9309	50.80	42.67	58.59	52.85	58.67
CH/NH-165-3	650.0	5.080	0.2690	0.0084	7.52	2.26	13.80	7306.00	8152.00	0.9120	72.40	56.90	58.70	51.04	60.23
CH/NH-165-4	651.0	5.080	0.2700	0.0084	7.51	2.26	13.80	9536.00	10391.00	0.9140	82.00	62.43	59.34	51.32	61.60
CH/NH-165-5	649.1	5.090	0.2600	0.0084	7.73	2.30	13.70	14305.00	14555.00	0.9312	83.80	66.39	59.70	51.67	63.15
CH/NH-165-6	652.7	5.070	0.2740	0.0084	7.44	2.25	13.90	18900.00	21196.00	O:W/O	84.50	68.82	60.43	52.59	64.03
CH/NH-165-7	650.1	5.080	0.2640	0.0084	7.64	2.29	13.80	21590.00	22867.00	0.9131	74.10	60.09	60.10	52.37	64.13
CH/NH-165-8	647.5	5.100	0.2640	0.0084	7.56	2.27	13.70	23763.00	26250.00	0.9219	57.50	49.50	60.20	52.56	64.22

Table B.15.2. Calculations for fraction of jetting (FJ) & fraction of small bubble (FSB).

For cyclohexane/n-heptane at 165 kPa operating pressure. Source: Yanagi and Sakata, 1982.

Code	U_{SA}	U_H	F_{SA}	F_J	$1-F_J$	C	α_w	Q_L	h_r	T_{GLB}	$k\Delta t$	k	$\exp(-k\Delta t)$	F_{SB}	$1-F_{SB}$
	m/s	m/s	--	--	--	--	--	m ³ /s	m	--	--	--	--	--	--
CH/NH-165-1	0.158	1.128	0.356	0.215	0.785	0.5004	0.7716	0.0010	0.0571	0.2794	3.8344	13.7245	0.0216	0.4200	0.5800
CH/NH-165-2	0.324	2.316	0.733	0.482	0.538	0.5004	0.6065	0.0022	0.0627	0.1174	2.4835	21.1612	0.0835	0.1495	0.8505
CH/NH-165-3	0.519	3.707	1.170	0.622	0.378	0.5004	0.4665	0.0031	0.0690	0.0620	1.7289	27.8655	0.1775	0.0690	0.9310
CH/NH-165-4	0.661	4.725	1.491	0.690	0.310	0.5004	0.3866	0.0041	0.0755	0.0441	1.4222	32.2381	0.2412	0.0479	0.9521
CH/NH-165-5	0.925	6.605	2.086	0.757	0.243	0.5004	0.2748	0.0061	0.0916	0.0272	1.0760	39.5424	0.3410	0.0300	0.9700
CH/NH-165-6	1.352	9.657	3.044	0.794	0.206	0.5004	0.1625	0.0080	0.1204	0.0145	0.7141	49.3450	0.4896	0.0164	0.9836
CH/NH-165-7	1.456	10.397	3.281	0.798	0.202	0.5004	0.1424	0.0092	0.1342	0.0131	0.6791	51.7417	0.5071	0.0153	0.9847
CH/NH-165-8	1.664	11.889	3.759	0.803	0.197	0.5004	0.1097	0.0102	0.1570	0.0103	0.5823	56.2820	0.5586	0.0125	0.9875

Table B.15.3. Efficiencies for large bubble & jetting by present models.

For cyclohexane/n-heptane at 165 kPa operating pressure. Source: Yanagi and Sakata, 1982.

Code	PM-1				PM-2				PM-3			
	E _{LB}	E _B	E _J	E _{oo} calc	E _{LB}	E _B	E _J	E _{oo} calc	E _{LB}	E _B	E _J	E _{oo} calc
	PM-1	--	PM-1	PM-1	PM-2		PM-2	PM-2	PM-3		PM-3	PM-3
CH/NH-165-1	43.93	67.48	65.89	67.14	38.59	64.39	55.13	62.40	40.00	65.20	70.00	66.23
CH/NH-165-2	43.94	52.32	65.91	58.59	39.02	48.14	55.75	51.65	40.00	48.97	70.00	58.67
CH/NH-165-3	43.65	47.54	65.48	58.70	39.06	43.27	55.80	51.06	40.00	44.14	70.00	60.23
CH/NH-165-4	43.49	46.20	65.24	59.34	39.07	41.99	55.81	51.53	40.00	42.88	70.00	61.60
CH/NH-165-5	43.00	44.71	64.51	59.70	38.83	40.66	55.47	51.87	40.00	41.80	70.00	63.15
CH/NH-165-6	43.12	44.05	64.68	60.43	39.15	40.15	55.93	52.68	40.00	40.98	70.00	64.03
CH/NH-165-7	42.83	43.71	64.25	60.10	38.93	39.86	55.61	52.43	40.00	40.92	70.00	64.13
CH/NH-165-8	42.86	43.58	64.29	60.20	39.01	39.77	55.73	52.58	40.00	40.75	70.00	64.22

**Table B.16.1. Sieve tray efficiencies (experimental & calculated by present models).
For iso-butane/n-butane at 1138 kPa operating pressure. Source: Yanagi and Sakata, 1982.**

Dc	D _H	TS	h _w	L _w	L _r	A _A	A _N	HA/AA							
m	mm	mm	mm	mm	mm	m ²	m ²	--							
1.22	12.7	610	50.8	940	762	0.859	0.991	14							
Code	ρ _L	ρ _G	μ _L	μ _G	D _L *10 ⁹	D _G *10 ⁵	σ	L _r	G _r	m	E _{MV}	E _{oo} _{exp}	E _{oo} _{cal}	E _{oo} _{cal}	E _{oo} _{cal}
	kg/m ³	kg/m ³	mPa.s	mPa.s	m ² /s	m ² /s	mN/m	kg/hr	kg/hr			--	PM-1	PM-2	PM-3
IB/NB-1138-1	485.0	30.200	0.0900	0.0094	1.06	5.62	5.00	6290.00	6468.00	0.9894	61.70	49.21	93.18	88.67	92.94
IB/NB-1138-2	489.0	28.800	0.0090	0.0094	1.06	5.63	5.00	10254.00	10258.00	0.9894	94.70	67.83	87.96	83.17	87.96
IB/NB-1138-3	490.0	28.800	0.0090	0.0094	1.02	5.57	5.00	14470.00	14505.00	0.9894	106.10	73.63	84.14	77.30	84.02
IB/NB-1138-4	492.0	28.500	0.0090	0.0094	1.02	5.56	5.00	21456.00	21332.00	0.9894	109.60	75.65	79.15	70.42	79.26
IB/NB-1138-5	492.0	28.700	0.0090	0.0094	1.02	5.56	5.00	27823.00	27785.00	0.9894	109.50	76.32	75.75	66.05	75.91
IB/NB-1138-6	492.0	28.700	0.0090	0.0095	1.02	5.57	5.00	32408.00	32380.00	0.9894	108.30	75.98	73.72	63.58	73.90
IB/NB-1138-7	492.0	28.800	0.0090	0.0095	1.04	5.63	5.00	35311.00	35284.00	0.9894	93.00	68.90	72.45	62.12	72.86

Table B.16.2. Calculations for fraction of jetting (FJ) & fraction of small bubble (FSB).

For iso-butane/n-butane at 1138 kPa operating pressure. Source: Yanagi and Sakata, 1982.

Code	U_{SA}	U_H	F_{SA}	F_J	$1-F_J$	C	α_o	Q_L	h_r	T_{GLB}	$k\Delta t$	k	$\exp(-k\Delta t)$	F_{SB}	$1-F_{SB}$
	m/s	m/s	--	--	--	--	--	M ³ /s	m	--	--	--	--	--	--
IB/NB-1138-1	0.089	0.495	0.381	0.235	0.765	0.5004	0.7249	0.0036	0.0657	0.6879	14.2456	20.7097	0.0000	1.0000	0.0000
IB/NB-1138-2	0.115	0.823	0.618	0.400	0.600	0.5004	0.6080	0.0058	0.0740	0.3904	10.8254	27.7262	0.0000	0.9988	0.0012
IB/NB-1138-3	0.163	1.163	0.874	0.525	0.475	0.5004	0.5059	0.0082	0.0838	0.2602	8.8825	34.1391	0.0001	0.9914	0.0086
IB/NB-1138-4	0.242	1.729	1.292	0.652	0.348	0.5004	0.3790	0.0121	0.1027	0.1609	6.9461	43.1819	0.0010	0.9432	0.0568
IB/NB-1138-5	0.313	2.236	1.677	0.718	0.282	0.5004	0.2922	0.0157	0.1244	0.1161	5.8617	50.4961	0.0028	0.8486	0.1514
IB/NB-1138-6	0.365	2.606	1.955	0.747	0.253	0.5004	0.2431	0.0183	0.1430	0.0953	5.2737	55.3525	0.0051	0.7565	0.2435
IB/NB-1138-7	0.396	2.830	2.126	0.760	0.240	0.5004	0.2172	0.0199	0.1561	0.0856	4.9821	58.2190	0.0069	0.6985	0.3015

Table B.16.3. Efficiencies for large bubble & jetting by present models.

For iso-butane/n-butane at 1138 kPa operating pressure. Source: Yanagi and Sakata, 1982.

Code	PM-1				PM-2				PM-3			
	E_{LB}	E_B	E_J	E_{∞} calc	E_{LB}	E_B	E_J	E_{∞} calc	E_{LB}	E_B	E_J	E_{∞} calc
	PM-1	--	PM-1	PM-1	PM-2		PM-2	PM-2	PM-3		PM-3	PM-3
IB/NB-1138-1	47.33	100.00	70.99	93.18	36.28	100.00	51.83	88.67	40.00	100.00	70.00	92.94
IB/NB-1138-2	46.66	99.93	69.99	87.96	36.28	99.92	51.83	80.69	40.00	99.93	70.00	87.96
IB/NB-1138-3	46.79	99.54	70.18	84.14	36.58	99.45	52.26	74.69	40.00	99.48	70.00	84.02
IB/NB-1138-4	46.42	96.96	69.63	79.15	36.58	96.40	52.26	67.63	40.00	96.59	70.00	79.26
IB/NB-1138-5	46.27	91.87	69.41	75.75	36.58	90.40	52.26	63.03	40.00	90.92	70.00	75.91
IB/NB-1138-6	46.17	86.89	69.25	73.72	36.58	84.55	52.26	60.43	40.00	85.39	70.00	73.90
IB/NB-1138-7	45.93	83.70	68.90	72.45	36.43	80.83	52.04	58.95	40.00	81.91	70.00	72.86

Table B.17.1 Sieve tray efficiencies (experimental & calculated by present models).

For methanol/water at 101.4 kPa operating pressure. Source: Korchinsky et al., 1994.

Dc	DH	TS	hw	Lw	Lt	AA	AN	HA/AA						
m	mm	mm	mm	mm	mm	m ²	m ²	--						
0.6	4.8	340	50	460	240	0.14	0.25	12.7						
Code	ρ_L	ρ_G	μ_L	μ_G	D_L	D_G	σ	L_r	G_r	m	$E_{OG\ exp}$	$E_{OG\ calc}$	$E_{OG\ calc}$	$E_{OG\ calc}$
	kg/m ³	kg/m ³	mPa.s	mPa.s	m ² /s	m ² /s	mN/m	kg/hr	kg/hr		--	PM-1	PM-2	PM-3
M/W-101.4-1	880.00	1.000	0.550	1.10E-02	1.00E-08	1.70E-05	25.00	940.6	1084.6	0.50	73.20	47.79	48.81	62.92
M/W-101.4-2	800.00	1.100	0.460	1.10E-02	1.00E-08	1.70E-05	21.00	1130.8	1196.2	0.41	73.70	48.38	48.91	63.12
M/W-101.4-3	900.00	0.970	0.510	1.10E-02	1.00E-08	1.70E-05	28.00	886.6	1076.5	0.63	71.80	48.03	48.82	62.95
M/W-101.4-4	920.00	0.940	0.450	1.10E-02	1.00E-08	1.70E-05	31.00	879.1	1094.0	0.76	73.40	48.25	48.87	63.07
M/W-101.4-5	940.00	0.840	0.340	1.10E-02	1.00E-08	1.70E-05	39.00	881.2	1099.3	1.77	62.80	48.78	48.98	63.27
M/W-101.4-6	930.00	0.900	0.420	1.10E-02	1.00E-08	1.70E-05	34.00	954.1	1198.4	1.14	69.10	48.55	49.08	63.44

Table B.17.2 Calculations for fraction of jetting (FJ) & fraction of small bubble (FSB).

For methanol/water at 101.4 kPa operating pressure. Source: Korchinsky et al., 1994.

Code	U_{SA}	U_H	F_{BA}	F_J	$1-F_J$	C	α_o	Q_L	h_f	T_{GLB}	$K\Delta t$	k	$\exp(-k\Delta t)$	F_{SB}	$1-F_{SB}$
	m/s	m/s	--	--	--	--	--	m ³ /s	m	--	--	--	--	--	--
M/W-101.4-1	2.152	16.945	2.152	0.762	0.238	0.5004	0.3155	0.0003	0.0579	0.0085	0.2772	32.65	0.758	0.005	0.995
M/W-101.4-2	2.158	16.989	2.263	0.768	0.232	0.5004	0.2833	0.0004	0.0602	0.0079	0.2827	35.74	0.754	0.005	0.995
M/W-101.4-3	2.202	17.338	2.169	0.763	0.237	0.5004	0.3167	0.0003	0.0575	0.0083	0.2597	31.42	0.771	0.005	0.995
M/W-101.4-4	2.309	18.183	2.239	0.767	0.233	0.5004	0.3098	0.0003	0.0574	0.0077	0.2374	30.81	0.789	0.004	0.996
M/W-101.4-5	2.597	20.446	2.380	0.774	0.226	0.5004	0.2933	0.0003	0.0576	0.0065	0.1901	29.22	0.827	0.003	0.997
M/W-101.4-6	2.642	20.803	2.506	0.780	0.220	0.5004	0.2747	0.0003	0.0584	0.0061	0.1933	31.81	0.824	0.003	0.997

Table B.17.3. Efficiencies for large bubble & jetting by present models.

For methanol/water at 101.4 kPa operating pressure. Source: Korchinsky et al., 1994.

Code	PM-1				PM-2				PM-3			
	E_{LB}	E_B	E_J	E_{Og} calc	E_{LB}	E_B	E_J	E_{Og} calc	E_{LB}	E_B	E_J	E_{Og} calc
	PM-1	--	PM-1	PM-1	PM-2		PM-2	PM-2	PM-3		PM-3	PM-3
M/W-101.4-1	34.55	34.88	51.83	47.79	36.74	37.06	52.48	48.81	40.00	40.31	70.00	62.92
M/W-101.4-2	34.90	35.23	52.34	48.38	36.74	37.07	52.48	48.91	40.00	40.31	70.00	63.12
M/W-101.4-3	34.72	35.03	52.08	48.03	36.74	37.04	52.48	48.82	40.00	40.28	70.00	62.95
M/W-101.4-4	34.83	35.10	52.24	48.25	36.74	37.01	52.48	48.87	40.00	40.26	70.00	63.07
M/W-101.4-5	35.13	35.35	52.70	48.78	36.74	36.95	52.48	48.98	40.00	40.20	70.00	63.27
M/W-101.4-6	34.89	35.12	52.34	48.55	36.74	36.95	52.48	49.06	40.00	40.20	70.00	63.44

Table B.18.1. Sieve tray efficiencies (experimental & calculated by present models).

For 1-propanol/water at 101.4 kPa operating pressure. Source: Korchinsky et al., 1994.

Dc	D _H	TS	h _w	L _w	L _T	A _A	A _N	HA/AA							
M	mm	mm	mm	mm	mm	m ²	m ²	--							
0.6	4.8	340	50	460	240	0.14	0.25	12.7							
Code	ρ _L	ρ _G	μ _L	μ _G	D _L *10 ⁹	D _G *10 ⁵	σ	L _r	G _r	m	E _{oo} exp	E _{oo} cal	E _{oo} cal	E _{oo} cal	
	kg/m ³	kg/m ³	mPa.s	mPa.s	m ² /s	m ² /s	mN/m	kg/hr	kg/hr		--	PM-1	PM-2	PM-3	
IP/W-101.4-1	840.0	1.160	0.3000	0.0120	5.30	1.50	22.00	637.90	900.30	0.2300	61.80	54.73	55.15	61.59	
IP/W-101.4-2	890.0	1.090	0.3000	0.0120	5.30	1.50	26.00	543.30	869.70	2.9000	65.60	54.71	52.35	61.56	
IP/W-101.4-3	870.0	1.150	0.3000	0.0120	5.30	1.50	24.00	588.50	923.30	0.7500	63.90	54.90	52.56	61.77	
IP/W-101.4-4	840.0	1.160	0.3000	0.0120	5.30	1.50	22.00	696.50	940.50	0.2300	64.00	54.86	52.66	61.86	
IP/W-101.4-5	900.0	1.000	0.3000	0.0120	5.30	1.50	35.00	576.20	869.80	4.9000	59.00	56.07	52.52	61.80	
IP/W-101.4-6	910.0	0.790	0.3000	0.0120	5.30	1.50	35.00	730.00	924.30	8.6000	55.30	55.00	53.46	62.73	

Table B.18.2. Calculations for fraction of jetting (F_J) & fraction of small bubble (F_{SB}).

For 1-propanol/water at 101.4 kPa operating pressure. Source: Korchinsky et al., 1994.

Code	U _{SA}	U _H	F _{SA}	F _J	1-F _J	C	α _o	Q _L	h _r	T _{GLB}	kΔt	k	exp (-kΔt)	F _{SB}	1-F _{SB}
	m/s	m/s	--	--	--	--	--	m ³ /s	M	--	--	--	--	--	--
IP/W-101.4-1	1.540	12.125	1.659	0.715	0.285	0.5004	0.3947	0.0002	0.0554	0.0142	0.4155	29.2550	0.6600	0.0082	0.9918
IP/W-101.4-2	1.583	12.465	1.653	0.714	0.286	0.5004	0.4055	0.0002	0.0546	0.0140	0.3840	27.4657	0.6811	0.0074	0.9926
IP/W-101.4-3	1.593	12.543	1.708	0.721	0.279	0.5004	0.3907	0.0002	0.0550	0.0135	0.3896	28.8609	0.6773	0.0076	0.9924
IP/W-101.4-4	1.609	12.667	1.733	0.724	0.276	0.5004	0.3801	0.0002	0.0559	0.0132	0.3965	30.0319	0.6727	0.0077	0.9923
IP/W-101.4-5	1.726	13.589	1.726	0.724	0.276	0.5004	0.3930	0.0002	0.0548	0.0125	0.3129	25.0551	0.7313	0.0058	0.9942
IP/W-101.4-6	2.321	18.279	2.063	0.756	0.244	0.5004	0.3351	0.0002	0.0563	0.0081	0.2268	27.9205	0.7971	0.0041	0.9959

Table B.18.3. Efficiencies for large bubble & jetting by present models.

For 1-propanol/water at 101.4 kPa operating pressure. Source: Korchinsky et al., 1994.

Code	PM-1				PM-2				PM-3			
	E_{LB}	E_B	E_J	E_{Og} calc	E_{LB}	E_B	E_J	E_{Og} calc	E_{LB}	E_B	E_J	E_{Og} calc
	PM-1	--	PM-1	PM-1	PM-2		PM-2	PM-2	PM-3		PM-3	PM-3
IP/W-101.4-1	40.21	40.70	60.31	54.73	42.11	42.58	60.16	55.15	40.00	40.49	70.00	61.59
IP/W-101.4-2	40.22	40.66	60.32	54.71	42.11	42.54	60.16	55.12	40.00	40.45	70.00	61.56
IP/W-101.4-3	40.25	40.71	60.38	54.90	42.11	42.55	60.16	55.25	40.00	40.45	70.00	61.77
IP/W-101.4-4	40.18	40.65	60.27	54.86	42.11	42.56	60.16	55.31	40.00	40.46	70.00	61.86
IP/W-101.4-5	41.10	41.45	61.66	56.07	42.11	42.45	60.16	55.26	40.00	40.35	70.00	61.80
IP/W-101.4-6	39.87	40.12	59.81	55.00	42.11	42.34	60.16	55.80	40.00	40.24	70.00	62.73

Table B.19.1. Sieve tray efficiencies (experimental & calculated by present models).

For methylcyclohexane/toluene at 101.4 kPa operating pressure. Source: Korchinsky et al., 1994.

Dc	DH	TS	hw	Lw	Lt	AA	AN	HA/AA							
m	mm	mm	mm	mm	mm	m ²	M ²	--							
0.6	4.8	340	50	460	240	0.14	0.25	12.7							
Code	ρ_L	ρ_G	μ_L	μ_G	D_L	D_G	σ	L_r	G_r	m	E_{OG} exp	E_{OG} calc	E_{OG} calc	E_{OG} calc	
	kg/m ³	kg/m ³	mPa.s	mPa.s	m ² /s	m ² /s	MN/m	kg/hr	kg/hr		--	PM-1	PM-2	PM-3	
MCH/T-101.4-1	770.0	2.970	0.250	8.70E-03	5.10E-09	3.70E-06	18.00	1628.00	1632.20	1.34	70.60	61.28	50.24	62.43	
MCH/T-101.4-2	766.0	2.990	0.250	8.70E-03	5.10E-09	3.70E-06	18.00	1709.80	1715.40	1.24	74.40	61.51	50.49	62.64	
MCH/T-101.4-3	739.0	3.080	0.270	8.40E-03	5.10E-09	3.70E-06	17.00	1769.80	1778.80	0.89	80.10	61.83	51.70	62.75	
MCH/T-101.4-4	763.0	3.010	0.260	8.60E-03	5.10E-09	3.70E-06	18.00	1791.80	1800.50	1.15	77.00	61.70	53.44	62.84	
MCH/T-101.4-5	766.0	2.980	0.250	8.70E-03	5.10E-09	3.70E-06	18.00	1786.80	1793.80	1.28	73.70	61.55	53.46	62.85	
MCH/T-101.4-6	753.0	3.040	0.260	8.50E-03	5.10E-09	3.70E-06	17.00	1825.90	1835.30	1.01	79.00	61.58	53.52	62.91	

Table B.19.2. Calculations for fraction of jetting (F_J) & fraction of small bubble (F_{SB}).

For methylcyclohexane/toluene at 101.4 kPa operating pressure. Source: Korchinsky et al., 1994.

Code	U _{SA}	U _H	F _{SA}	F _J	1-F _J	C	α _s	Q _L	h _r	T _{GLB}	KΔt	k	exp (-kΔt)	F _{SB}	1-F _{SB}
	m/s	m/s	--	--	--	--	--	m ³ /s	m	--	--	--	--	--	--
MCH/T-101.4-1	1.090	8.586	1.879	0.740	0.260	0.5004	0.3380	0.0006	0.0619	0.0192	0.6500	33.87	0.522	0.014	0.986
MCH/T-101.4-2	1.138	8.963	1.968	0.748	0.252	0.5004	0.3217	0.0006	0.0628	0.0177	0.6174	34.81	0.539	0.013	0.987
MCH/T-101.4-3	1.146	9.023	2.011	0.752	0.248	0.5004	0.3088	0.0007	0.0638	0.0172	0.6172	35.95	0.539	0.013	0.987
MCH/T-101.4-4	1.187	9.345	2.059	0.755	0.245	0.5004	0.3081	0.0007	0.0637	0.0164	0.5869	35.75	0.556	0.013	0.987
MCH/T-101.4-5	1.194	9.404	2.062	0.755	0.245	0.5004	0.3067	0.0006	0.0636	0.0163	0.5844	35.80	0.557	0.013	0.987
MCH/T-101.4-6	1.198	9.432	2.089	0.757	0.243	0.5004	0.2992	0.0007	0.0642	0.0160	0.5905	36.84	0.554	0.013	0.987

Table B.19.3 Efficiencies for large bubble & jetting by present models.

For methylcyclohexane/toluene at 101.4 kPa operating pressure. Source: Korchinsky et al., 1994.

Code	PM-1				PM-2				PM-3			
	E_{LB}	E_B	E_J	E_{og} calc	E_{LB}	E_B	E_J	E_{og} calc	E_{LB}	E_B	E_J	E_{og} calc
	PM-1	--	PM-1	PM-1	PM-2		PM-2	PM-2	PM-3		PM-3	PM-3
MCH/T-101.4-1	44.58	45.38	66.86	61.28	42.46	43.29	60.66	56.14	40.00	40.87	70.00	62.43
MCH/T-101.4-2	44.83	45.37	66.94	61.51	42.46	43.23	60.66	56.27	40.00	40.81	70.00	62.64
MCH/T-101.4-3	44.81	45.55	67.21	61.83	42.46	43.23	60.66	56.33	40.00	40.81	70.00	62.75
MCH/T-101.4-4	44.67	45.36	67.00	61.70	42.46	43.18	60.66	56.38	40.00	40.76	70.00	62.84
MCH/T-101.4-5	44.56	45.25	66.83	61.55	42.46	43.18	60.66	56.38	40.00	40.75	70.00	62.85
MCH/T-101.4-6	44.54	45.24	66.81	61.58	42.46	43.19	60.66	56.42	40.00	40.76	70.00	62.91

Table B.20.1. Sieve tray efficiencies (experimental & calculated by present models).

For cyclohexane/n-hcptanc at 101.4 kPa operating pressure. Source: Nutter and Perry, 1995.

Dc	D _H	TS	h _w	L _w	L _T	A _A	A _N	HA/AA							
M	mm	mm	mm	mm	Mm	m ²	m ²	--							
0.5	12.7	610	50.8	260	273	0.13	0.163	14							
Code	ρ _L	ρ _G	μ _L	μ _G	D _L *10 ⁹	D _G *10 ⁶	σ	L _r	G _r	m	E _{MV}	E _{OG exp}	E _{OG cal}	E _{OG cal}	E _{OG cal}
	kg/m ³	kg/m ³	mPa.s	mPa.s	m ² /s	m ² /s	mN/m	kg/hr	kg/hr			--	PM-1	PM-2	PM-3
CH/NH-101.4-1	666.0	3.040	0.3010	0.0089	6.58	3.43	15.00	571.00	570.00	0.9124	45.00	41.62	54.86	50.24	55.72
CH/NH-101.4-2	669.0	3.030	0.3100	0.0089	6.53	3.42	15.00	770.00	760.00	0.9124	72.00	61.17	55.81	50.49	57.71
CH/NH-101.4-3	667.0	3.040	0.3030	0.0089	6.56	3.43	15.00	1191.00	1178.00	0.9124	72.00	61.42	57.56	51.70	60.94
CH/NH-101.4-4	667.0	3.040	0.3040	0.0089	6.56	3.43	15.00	1751.00	2086.00	0.9124	70.00	63.55	58.84	53.44	63.58
CH/NH-101.4-5	666.0	3.050	0.3030	0.0089	6.56	3.43	15.00	2115.00	2092.00	0.9124	72.00	67.33	58.89	53.46	63.59
CH/NH-101.4-6	664.0	3.070	0.2960	0.0089	6.64	3.45	15.00	2366.00	2330.00	0.9124	78.00	74.93	58.87	53.52	63.82
CH/NH-101.4-7	662.0	3.090	0.2940	0.0089	6.60	3.44	15.00	2599.00	2601.00	0.9124	64.00	65.91	59.05	53.78	63.99

Table B.20.2. Calculations for fraction of jetting (FJ) & fraction of small bubble (FSB).
 For cyclohexane/n-heptane at 101.4 kPa operating pressure. Source: Nutter and Perry, 1995.

Code	U_{SA}	U_H	F_{SA}	F_J	$1-F_J$	C	α_g	Q_L	h_f	T_{GLB}	$K\Delta t$	k	$\exp(-k\Delta t)$	F_{SB}	$1-F_{SB}$
	m/s	m/s	--	--	--	--	--	m ³ /s	m	--	--	--	--	--	--
CH/NH-101.4-1	0.401	2.862	0.699	0.444	0.556	0.5004	0.6243	0.0002	0.0571	0.0890	1.7652	19.8304	0.1712	0.0719	0.9281
CH/NH-101.4-2	0.536	3.828	0.933	0.547	0.453	0.5004	0.5424	0.0003	0.0593	0.0600	1.4155	23.6004	0.2428	0.0475	0.9525
CH/NH-101.4-3	0.828	5.914	1.444	0.682	0.318	0.5004	0.4020	0.0005	0.0647	0.0314	0.9628	30.6590	0.3818	0.0252	0.9748
CH/NH-101.4-4	1.466	10.473	2.556	0.782	0.218	0.5004	0.2159	0.0007	0.0781	0.0115	0.4965	43.1976	0.6086	0.0102	0.9898
CH/NH-101.4-5	1.466	10.469	2.560	0.782	0.218	0.5004	0.2153	0.0009	0.0818	0.0120	0.5195	43.2231	0.5948	0.0108	0.9892
CH/NH-101.4-6	1.622	11.584	2.841	0.790	0.210	0.5004	0.1843	0.0010	0.0880	0.0100	0.4600	46.0055	0.6313	0.0093	0.9907
CH/NH-101.4-7	1.799	12.847	3.162	0.796	0.204	0.5004	0.1547	0.0011	0.0954	0.0082	0.4024	49.0347	0.6687	0.0079	0.9921

Table B.20.3 Efficiencies for large bubble & jetting by present models.

For cyclohexane/n-heptane at 101.4 kPa operating pressure. Source: Nutter and Perry, 1995.

Code	PM-1				PM-2				PM-3			
	E_{LB}	E_B	E_J	E_{Og} calc	E_{LB}	E_B	E_J	E_{Og} calc	E_{LB}	E_B	E_J	E_{Og} calc
	PM-1	-	PM-1	PM-1	PM-2		PM-2	PM-2	PM-3		PM-3	PM-3
CH/NH-101.4-1	43.03	47.12	64.54	54.86	40.20	44.50	57.42	50.24	40.00	44.31	70.00	55.72
CH/NH-101.4-2	42.85	45.57	64.28	55.81	40.26	43.10	57.52	50.99	40.00	42.85	70.00	57.71
CH/NH-101.4-3	42.58	44.03	63.86	57.56	40.22	41.73	57.46	52.46	40.00	41.51	70.00	60.94
CH/NH-101.4-4	42.21	42.80	63.32	58.84	40.22	40.83	57.46	53.83	40.00	40.81	70.00	63.58
CH/NH-101.4-5	42.24	42.86	63.36	58.89	40.22	40.87	57.46	53.84	40.00	40.65	70.00	63.59
CH/NH-101.4-6	42.12	42.66	63.18	58.87	40.12	40.67	57.31	53.82	40.00	40.56	70.00	63.82
CH/NH-101.4-7	42.16	42.62	63.25	59.05	40.17	40.64	57.38	53.98	40.00	40.47	70.00	63.99

APPENDIX C

SAMPLE CALCULATION

SAMPLE CALCULATION FOR FIRST DATA POINT OF TABLES B.1.1, B.1.2, B.1.3.

Table C.1 Flow field and physical properties of the system

D_H	TS	h_w	L_w	L_T	A_A	A_N	HA/AA	ρ_L	ρ_G	$D_L \cdot 10^9$	σ	L_r	G_r
mm	mm	mm	mm	mm	m^2	m^2	—	kg/m^3	kg/m^3	mPa.s	mN/m	kg/hr	kg/hr
3.175	305	38.1	305	253	0.1318	0.148	8.35	948.6	0.640	0.0127	55.00	231.40	231.40

Fraction of jetting, F_J

$$U_{SA} = G_r / (\rho_G \cdot A_A) = 231.40 / (0.640 \times 0.1318 \times 3600) = 0.764 \text{ m/s}$$

$$F_{SA} = U_{SA} \sqrt{\rho_G} = 0.764 \times 0.640^{0.5} = 0.610 (m/s)(kg/m^3)^{0.5}$$

$$F_J = -0.1786 + 0.9857(1 - e^{-1.43 F_{SA}}) = 0.395$$

Fraction of small bubbles, F_{SB}

$$c = 0.5 + 0.438 \exp(-13.7 h_w) = 0.5 + 0.438 \exp(-13.7 \times 0.0381) = 0.5023$$

$$\alpha_e = \exp \left[-12.55 \left(U_{SA} \left(\frac{\rho_G}{\rho_L - \rho_G} \right)^{0.5} \right)^{0.91} \right] = \exp \left[-12.55 \left(0.762 \left(\frac{0.64}{948.6 - 0.64} \right)^{0.5} \right)^{0.91} \right]$$

$$= 0.7021$$

$$h_f = h_w + c \left(\frac{Q_L}{L_w \alpha_e} \right)^{0.67} = 0.0381 + 0.5023 \left(\frac{0.001}{0.305 \times 0.7021} \right)^{0.67} = 0.0404 \text{ m}$$

$$t_{GLB} = \frac{h_f}{(Q_V/A_A)} = \frac{h_f}{U_{SA}} = \frac{0.0404}{0.762} = 0.0372 \text{ s}$$

$$k\bar{\Delta t} = 0.16 \left(\frac{3.8 \rho_L^{0.1} \rho_G^{0.3}}{\sigma^{0.4}} \right) (U_{SA} g)^{0.6} T_{GLB} = 0.16 \left(\frac{3.8}{0.055^{0.4}} \right) (0.762 \times 9.81)^{0.6} \times 0.0372$$

$$= 0.4188$$

$$F_{SB} = \frac{2(1 - e^{-k\bar{\Delta t}})}{2(1 - e^{-k\bar{\Delta t}}) + \left(\frac{d_{32L}}{d_{32s}} \right)^3 e^{-k\bar{\Delta t}}} = \frac{2(1 - e^{-0.4188})}{2(1 - e^{-0.4188}) + (5)^3 e^{-0.4188}} = 0.0083$$

Proposed model-1)

$$E_{LB} = 4.8 \left(\frac{\sigma}{\mu_L U_{SA}} \right)^{0.115} \left(\frac{\mu_L}{\rho_L D_L} \right)^{0.215} \left(\frac{h_W U_H \rho_G}{\mu_L} \right)^{0.1}$$

$$= 4.8 \left(\frac{0.055}{0.2890 \times 10^{-3} \times 0.762} \right)^{0.115} \left(\frac{0.2890 \times 10^{-3}}{948.6 \times 5.43 \times 10^{-9}} \right)^{0.215} \left(\frac{0.0381 \times 9.126 \times 0.640}{0.2890 \times 10^{-3}} \right)^{0.1}$$

$$= 41.84$$

$$E_J = 7.2 \left(\frac{0.055}{0.2890 \times 10^{-3} \times 0.762} \right)^{0.115} \left(\frac{0.2890 \times 10^{-3}}{948.6 \times 5.43 \times 10^{-9}} \right)^{0.215} \left(\frac{0.0381 \times 9.126 \times 0.640}{0.2890 \times 10^{-3}} \right)^{0.1}$$

$$= 62.77$$

$$E_B = (1 - F_{SB})E_{LB} + F_{SB}E_{SB} = 0.9917 \times 41.84 + 0.0083 \times 100 = 42.32$$

$$E_{OG} = (1 - F_J)E_B + F_J E_J = 0.605 \times 42.32 + 0.395 \times 62.77 = 50.40$$

(Proposed model-2)

$$E_{LB} = 0.7 D_L^{-0.215} = 0.7 (5.43 \times 10^{-9})^{-0.215} = 41.89$$

$$E_J = D_L^{-0.215} = (5.43 \times 10^{-9})^{-0.215} = 59.84$$

$$E_B = (1 - F_{SB})E_{LB} + F_{SB}E_{SB} = 0.9917 \times 41.89 + 0.0083 \times 100 = 42.37$$

$$E_{OG} = (1 - F_J)E_B + F_J E_J = 0.605 \times 42.37 + 0.395 \times 62.77 = 49.27$$

Proposed model-3

$$E_B = (1 - F_{SB})E_{LB} + F_{SB}E_{SB} = 0.9917 \times 40 + 0.0083 \times 100 = 40.50$$

$$E_{OG} = (1 - F_J)E_B + F_J E_J = 0.605 \times 40.50 + 0.395 \times 70 = 52.15$$

